Robust design of small hydropower plants in a changing world

Veysel Yildiz

A thesis submitted in partial fulfilment of the requirements for the degree of Doctor of Philosophy

University of Sheffield

Department of Civil and Structural Engineering

Submitted: July 15, 2024

Abstract

Hydropower, a leading renewable energy source, is cheap, reliable, and sustainable. Small hydropower plants (SHPs) under 10 MW offer an eco-friendly alternative to traditional dams, yet only 36 % of their capacity is exploited globally. This research focuses on run-of-river (RoR) plants, having (sub-daily) storage capacity, making them the predominant type of SHPs. Over 2,000 RoRs are planned or under construction in emerging economies over the next three decades despite challenges posed by climate change and socio-economic uncertainties. Traditional designs rely on cost-benefit analyses, ignore hydroclimatic variations, operational considerations and future-proofing investments. The primary goal of this thesis is to propose a robust framework for designing RoR hydropower plants, with secondary objectives to ensure computational efficiency and integration of optimized operations into design. These aims have been achieved through three core papers, all led by me. First, I developed a novel statistical generation method for generating plausible streamflow futures, enabling robust hydropower assessment without rainfall-runoff models. I used this method to represent climatic uncertainty in the rest of this thesis. I then proposed a Multi-Objective Robust Decision-Making approach to RoR design in response to the limitations of traditional approaches. This study pioneers integrating variable turbine efficiency into a framework for multi-objective hydropower design, assessing its financial viability under uncertain futures. Application to five cases challenges fundamental design assumptions, advocating for smaller designs with varying turbine capacities and high benefit-cost ratios as robust solutions across diverse plausible futures. Finally, to address the computational expense of the above framework, I developed the HYPER-FORD toolbox. It proposes approximations to slash the computational requirements associated with the robust design by over 92%, without compromising accuracy and in fact, by explicitly incorporating optimised operations into design for the first time. These contributions collectively advance RoR design, benefiting real-world decision-making and promoting effective, sustainable water resource management.

Acknowledgements

I would like to take this opportunity to express my sincere gratitude to all those who have supported me throughout my doctoral journey.

First and foremost, I am immensely thankful to my supervisors, Dr. Charles Rougé and Prof. Solomon Brown, for their invaluable guidance, unwavering support, and insightful feedback. Their expertise, encouragement, and commitment have been instrumental in shaping this research and guiding me through its challenges.

I am profoundly grateful to my beloved wife, Berivan, whose unwavering support and encouragement have been my anchor throughout this journey. To my cherished daughter, Ronya Zin, and my son, Ali Berken, your presence has illuminated my path. Your being here has transformed this journey into a stress-free and enjoyable experience, paving the way for this achievement. For this, I am forever thankful.

Furthermore, I extend my sincere thanks to the University of Sheffield Faculty of Engineering for awarding me the PhD scholarship that has made this journey possible.

I am deeply grateful to The Grantham Centre for their continued support in providing training and financial assistance. Their commitment to fostering academic growth and sustainability has been invaluable to my development.

I am also grateful to my colleagues at the DSI (General Directorate of State Hydraulic Works, Turkiye), whose collaborative spirit and intellectual exchange have enriched my academic experience. Their camaraderie and shared enthusiasm have created a stimulating environment for research and growth.

Last but certainly not least, to my friends, whose unwavering support, understanding, and encouragement have sustained me during the ups and downs of this journey, I extend my heartfelt appreciation. Your belief in me has been a constant source of motivation.

This thesis would not have been possible without the support and guidance of all these individuals and institutions. I am deeply indebted to each and every one of them for their

contribution to my academic and personal growth.

Declaration

I, the author, confirm that the Thesis is my own work except where specific reference has been made to the work of others. I am aware of the University's Guidance on the Use of Unfair Means (www.sheffield.ac.uk/ssid/unfair-means). This work has not been previously been presented for an award at this, or any other, university.

Veysel Yildiz

Date: 15^{th} of July 2024

Statement of conjoint work

The candidate affirms that the submitted work is primarily their own, except for instances where collaborative work from jointly authored publications is included. The individual contributions of the candidate and other authors to such works are explicitly outlined below. The candidate confirms that proper credit is provided within the thesis for any references to the work of others. The body of work presented in the thesis has led to the following publications or submissions for review:

- Yildiz, V. and Milton, R. and Brown, S. and Rougé, C., 2023. Technical note: Statistical generation of climate-perturbed flow duration curves. *Hydrology and Earth System Sciences*, p. 2499–2507, https://doi.org/ 10.5194/hess-27-2499-2023, 2023.

- Yildiz, V. and Brown, S. and Rougé, C., 2024. Importance of variable turbine efficiency in run-of-river hydropower design under deep uncertainty. *Water Resources Research*, https://doi.org/10.1029/2023WR035713

- Yildiz, V. and Brown, S. and Rougé, C., 2024. Robust and computationally efficient design for Run-of-River hydropower. Environmental Modelling & Software (under review)

Contents

1 Introduction **1**

1.1 The need for hydropower . . . 2

1.2 Hydropower development: controversies and challenges . . . 4

1.3 Changing conditions . . . 8

1.4 Planning under deep uncertainty . . . 9

1.5 Current state of small hydropower design . . . 11

1.5.1 Turbine system design . . . 12

1.5.2 Financial metrics . . . 13

1.5.3 Complexity and computational cost of hydropower system design . . . 15

1.6 Thesis motivation and objectives . . . 16

1.7 Thesis outline . . . 18

2 HYPER toolbox **20**

3 Statistical generation of future flows **24**

3.1 Introduction . . . 25

3.2 Methodology . . . 28

3.2.1 Kosugi model of the flow duration curve . . . 28

3.2.2 Correspondence between common flow statistics and the Kosugi model 29

3.2.3 Producing an ensemble of climate-perturbed flow duration curves . . . 31

3.3 Case study . . . 33

3.3.1 Site description . . . 33

3.3.2 Generation of climate-perturbed flow duration curves . . . 33

3.3.3 Application to infrastructure robustness . . . 36

3.4 Discussion and conclusion . . . 37

4 Revisiting small hydropower design in an uncertain world 40

4.1 Introduction . . . 41
4.2 Study sites . . . 46
4.3 Run-of-river plant design . . . 48
4.3.1 Traditional engineering design . . . 49
4.3.2 Benefits and costs . . . 51
4.3.3 HYPER and its extensions . . . 53
4.4 Methodology . . . 54
4.4.1 Generation of design alternatives . . . 55
4.4.2 Sampling Plausible Futures . . . 58
4.4.3 Metrics for financial robustness . . . 62
4.4.4 Vulnerability analysis . . . 64
4.5 Results . . . 65
4.5.1 Single-site design optimization and robustness . . . 65
4.5.2 Single-site vulnerability analysis . . . 70
4.5.3 Comparison of all cases . . . 73
4.6 Discussion . . . 76
4.7 Conclusions . . . 80

5 Computationally inexpensive robust RoR hydropower plant design 84

5.1 Introduction . . . 85
5.2 Robust design: HYPER-MORDM framework . . . 88
5.2.1 Design optimization . . . 89
5.2.2 Robustness analysis . . . 90
5.2.3 Case studies: physical characteristics and uncertainties . . . 92
5.3 HYPER-FORD toolbox . . . 95
5.3.1 Coupled design and operation optimization: HYPER$_{OP}$ module . . . 96
5.3.2 Flow duration curve discretization: approximation module . . . 98
5.4 Benchmarking the modifications to HYPER-MORDM . . . 100
5.4.1 Benchmarking of HYPER$_{OP}$ . . . 100
5.4.2 Benchmarking of FDC approximation during multi objective optimization 101

5.4.3 Benchmarking of FDC approximation during robustness analysis . . . 102
5.4.4 Benchmarking of FDC approximation across the whole analysis 103
5.5 Results . . . 105
5.5.1 HYPER$_{OP}$ validation and performance . . . 105
5.5.2 FDC sampling impact on multi-objective optimization . . . 107
5.5.3 FDC sampling impact on robustness analysis . . . 108
5.5.4 Whole-workflow impact of FDC sampling . . . 112
5.6 Summary and conclusion . . . 116

6 Conclusions and future research 119
6.1 Summary and conclusions . . . 119
6.2 Future research . . . 122
6.2.1 Statistical generation of FDCs with temporal dynamics . . . 122
6.2.2 Integrated robust design and operation of large hydropower plants . . 123
6.2.3 Optimizing turbine replacement and upgrades in hydropower . . . 123
6.2.4 Enhancing accuracy in global hydropower potential assessment . . . 124
6.2.5 Basin wide assessment of hydropower infrastructure . . . 125
6.2.6 Integrating Sustainability and Efficiency: Advancing Hydropower with LCA and EROI Metrics . . . 126

Appendices 159

A Supplementary information to Chapter 3 160
A.1 Kosugi function reminders . . . 160
A.2 "Mean" case $(M, V, L) = (\mu, \sigma, q_{low})$ . . . 161
A.2.1 Relating parameter triplets . . . 161
A.2.2 Solution strategy . . . 162
A.2.3 Simplifying $f(b)$ . . . 163
A.2.4 Unicity of the parameterisation . . . 163
A.2.5 Condition for existence . . . 164
A.3 Median, coefficient of variation and low flow quantile . . . 165
A.3.1 Relating parameter triplets . . . 165

A.3.2 Solution strategy 166
A.3.3 Range of b for which the equation for CV is defined 166
A.3.4 Unicity of the parameterisation 167
A.3.5 Condition for existence 168

List of Figures

2.1 High-level overview of HYPER with color coding for the different building blocks of the model. HYPER simulates the daily performance, investment, operation and maintenance costs, and economic profit of a RoR hydropower plant. Model inputs are highlighted in red. The design parameters (red diamond) play a key role in HYPER as they control the electricity production (gray), operational feasibility of the turbine system (green) and total costs (gray) of the RoR plant. A built-in optimization module (in blue) can be used to find optimal values of the design and/or project variables that maximize the net present value (NPV) of the plant. HYPER accommodates many other design objectives as well such as internal rate of return (IRR) and pay back time (PB). 21

2.2 Screen shot of the graphical user interface of HYPER. 23

3.1 Flowchart of the approach; (1) Kosugi model parameters are calibrated with a historical FDC, (2) a set of scenarios with modified flow statistics are determined, (3) a new set of Kosugi model coefficients are derived for each future scenario, and future scenarios are created by using these coefficients, (4) future scenarios can be used in robustness assessments. 32

3.2 Plot of the daily flow duration curves (FDC) used in the case study (red circles). Black line represents the fitted Kosugi model and the blue line is the FDC deduced from (M_h, V_h, L_h): historical median, CV and first percentile. . 34

3.3 Plot of the flow duration curves (FDCs) of the historical record (blue line) and sampled flow duration curves (grey lines) constructed by deriving the FDC parameters for the Kosugi Model shown in Table 3.1. The figure also compares 20 % mean flow reductions, obtained either with the delta change method (uniform multiplier, dashed black line) and the 12 future scenarios we generated with mean flow reductions between 19 and 21 % (orange lines). . . 36

3.4 Plot of generated flow duration curves (FDCs), with each solution colored by its Net Present Value (NPV). Gray colored lines signifies SOWs in which NPV is negative. NPV of the optimal design based on observed discharge (blue line) is 10 M$ 37

4.1 Top panel: Location of the presented five case studies on Köppen-Geiger climate classification map of Turkey (Beck et al., 2018). Bottom Panel: Presenting Flow Duration Curves (FDC) for five case studies, where normalization is applied based on the 99^{th} percentile of the flow. The FDC depicts graphically the relationship between the magnitude of the discharge (on y-axis) and its exceedance probability (on x-axis). The flow rate depicted on the y-axis is presented using a logarithmic scale. 46

4.2 Flow duration curve of the streamflows (dashed black line) and of the flows workable by a RoR hydropower plant (solid gray line). The top yellow dashed area represents the excessive flow that cannot be harnessed by the turbines, while the bottom magenta dashed area represents the flow the plant does not operate due turbine technical constraints and/or ecological flows 49

4.3 Left panel: Turbine chart (Penche, 1998). Right panel: Efficiency of the Kaplan (blue), Francis (red), and Pelton (green) turbines as function of the ratio between their flow rate and design flow respectively (Sinagra et al., 2014). . . 51

4.4 Methodological flowchart of our the design of financially robust RoR hydropower plants. Each step is associated to the sections of the paper in which it is discussed. 55

4.5 Plot of the flow duration curves (FDC) of the fitted Kosugi model (blue line) and sampled flow duration curves (gray lines) and a moderately dry future (orange colour) constructed by deriving the FDC parameters for Kosugi Model shown in Table 4.3 (panel A). Disaggregation of a moderately dry future (orange colour) to 50 time series of 49 years (panel B).The flow rate displayed on the y-axis is presented on a logarithmic scale. 63

4.6 Left panel: two-dimensional NPV and BC objective space where the alternatives of F_3 formulation (circles) are compared against the F_4 formulation (squares). Each solution colored by its robustness measure, RM_{PB}. Right panel: the alternatives of the F_3 formulation (black circles) and identical turbine solution (orange diamond) and identical turbine solution with discount (red diamond) and best NPV solution (green triangle) based on single NPV optimization. 67

4.7 The parallel plot of (1) design parameters of alternatives:large turbine design flow, O_{dS} (m^3/s), small turbine design flow O_{dL} (m^3/s), installed capacity IC (MW), average annual energy AAE (GWh), (2) two objective functions: f_{BC} (-), f_{NPV} (M$), and (3) their respective robustness measures value RM_{NPV}, RM_{PB} (%). Colour coding in lines is used for classification of results based on RM_{PB} value. 68

4.8 Operational plant efficiency (labeled as plant) and turbine efficiencies (Large turbine and Small turbine) of each selected alternatives under a the future highlighted with the orange line in Figure 4.5. Recall that the ID and ID* designs are identical. The vertical dashed lines represent the scale of probabilities. 69

4.9 The effect of the uncertain factors (x-axis) is quantified with the total-order S_{T}, sensitivity index (y-axis) based on robustness metric, RM_{PB} (first row) and RM_{NPV} (second row) and where dark gray is insensitive and white is sensitive. 71

4.10 SOWs in which the MR solution fails to meet the defined performance requirement in the two dimensional projection defined by the scaling factors on each uncertain factor. Panel plots at the first row shows analysis results of RM_{PB} and second row shows for RM_{NPV}. Blue points indicate states of the world where the MR solution satisfy to meet the performance criteria, and red points indicate states of the world where solution fails. The probability of failure as a function of these three factors is also shaded for each panel. 72

4.11 The plots of FDC in which the highest BC alternative meet the performance criteria whereas the highest NPV alternative fails(left panel), and the ID alternative fails (right panel). Orange coloured lines shows successful SOWs, gray lines represents all the SOWs.The flow rate displayed on the y-axis is presented on a logarithmic scale. 73

4.12 Robustness of the most robust (MR) alternative and the alternative with highest NPV and BC, identical turbine alternative with (ID*) and without discount (ID) of each case study where cost overrun scaling factor < 2, with full bars (all climates) and hollow bars (mean flow $< 75\%$ of historical conditions). . . 76

4.13 Robustness of the most robust (MR) alternative and the alternative with highest NPV and BC, identical turbine alternative with (ID*) and without discount (ID) of each case study where cost overrun scaling factor < 2, with full bars (all climates), hollow bars (mean flow $< 75\%$ of historical conditions) and black dots (interest rate scaling factor > 1). 77

5.1 Flowchart outlining methodological steps for developing our computationally inexpensive robust design approach. 88

5.2 Panel A: Plot of the flow duration curves (FDC) of of observed discharge (blue line), future flows (gray lines) and a random future (orange colour). Panel B: Desegregation of the selected future (orange colour) to 50 time series (orange lines). The X-axis denotes the exceedance probability, while the Y-axis logarithmically scales the flow rate. 91

5.3 The top panel displays the geographical locations of the five case studies on the Köppen-Geiger climate classification map of Turkey (Beck et al., 2018). In the bottom panel, Flow Duration Curves (FDC) for these case studies are shown, with normalization applied using the 99^{th} percentile of the flow. The flow rate values on the y-axis are presented logarithmically. 94

5.4 Top panel: The operational range of a triple Francis turbine setup featuring one small turbine (T_1, design discharge: 5 m^3/s) and two large turbines (T_2, 10 m^3/s each). The range is discretized into 1000 increments between the minimum (2 m^3/s, corresponding to 40 % of T_1's design discharge) and maximum (25 m^3/s) flow rates. Vertical black dashed lines delineate transitions between turbine operating modes. Bottom panel: Representation of the respective operational modes of the turbine(s) with their operated flows depicted based on the incremental steps outlined in the top panel. The color bar indicates turbine operation capacity, with white representing no operation and darker blue indicating higher capacity. 98

5.5 Plot of the flow duration curves (FDC) of 27 years daily discharge record comprising 9860 data points (blue line) and $N = 50$ sampled flow rates (black dots). 99

5.6 Panel A: Pareto sets derived by HYPER (white dots) and HYPER$_{OP}$ (red dots) on the two-dimensional Benefit-Cost Ratio (BC) and Net Present Value (NPV, in million dollars) objective space. Blue triangles indicate HYPER solutions within the context of HYPER$_{OP}$. Panel B: Performance comparison of HYPER and HYPER$_{OP}$ for the same Pareto solution set. The color bar illustrates the relative annual average energy (AAE) difference between the two toolboxes, with light colors indicating higher relative differences (HYPER$_{OP}$ outperforming HYPER). 106

5.7 Performance comparison of the reference Pareto front (RPF) obtained with optimization using the long-term FDC, with solutions obtained with optimization using the sampled FDC, and whose performance is re-evaluated using the long-term record. For $N = 10$ (left panel) and $N = 100$ sampled points (right panel), solutions that are non-dominated in the re-evaluated set are figured with white triangles. 109

5.8 The parallel plot of two objective functions: f_{BC} (-), f_{NPV} (M$), along with their respective robustness measures, for different sample sizes ($N = 10,\ 25,\ 50,\ 100,\ 200,$ and 500). In the top panel, the robustness measure is represented by RM_{PB}, while in the bottom panel, it is denoted as RM_{NPV}. Color coding on the lines is utilized to classify the results based on the value of f_{BC}. 111

S1 The $z(e)$ function. 161

S2 Representation of $\log(\mathcal{U}(b))$ to establish that $\mathcal{F}'(b) > 0$. Blue coloured line and dashed red line represent the derivation based on first percentile and fifth percentile of flow respectively. The dashed black line signifies e^{b^2}. 164

S3 Plot of the stationary point locus in $b-R$ space on which $\mathcal{G}'(b) = 0$, as given by Equation A.35. Blue coloured line and dashed red line represent the derivation based on first percentile and fifth percentile of flow respectively 168

List of Tables

3.1 Sampling ranges for multipliers of statistical parameters, where 1 corresponds to the values for the historical time series. 35

4.1 Hydrological and site characteristics of the RoR hydropower plant case studies. The data source for this table is provided in Section 4.7. 48

4.2 The x, y and z values in the cost function of electromechanical equipment (Equation 4.6) for the three different turbines simulated. 54

4.3 Variables and sampling ranges used for robustness analysis. SF is for scaling factor, and a SF of 1 indicates baseline conditions. 60

4.4 Design characteristics, performance metrics and robustness of the most robust (MR) alternative and the alternative with highest NPV and BC, identical turbine alternatives (ID, ID*) of given five case studies. 75

5.1 Hydrological and site characteristics of the RoR hydropower plant case studies. 93

5.2 Variables and sampling ranges used for robustness analysis. SF is for scaling factor, and a SF of 1 indicates baseline conditions. The initial four are economic parameters, while the three hydroclimatic parameters (highlighted in blue) pertain to streamflow statistics used in the construction of future streamflow time series. 95

5.3 Performance metrics for multi-Objective optimization and robustness analysis of long term discharge data and of different sample sizes ($N = 10, 25, 50, 100, 200,$ and500). 108

5.4 Design characteristics, performance metrics and robustness of the most robust (MR) alternative and the alternative with highest NPV and BC of given five case studies. 114

5.5 Optimization and robustness analysis run times for long term discharge records, $N = 100$ and $N = 50$ sampling points. 115

CHAPTER 1

Introduction

Water is essential to both society and ecosystems for maintaining an adequate food supply and a productive environment (Pimentel et al., 2004; Hussain, Muscolo, Farooq and Ahmad, 2019). There are many regions where freshwater resources are inadequate for this. Over two billion people live under water-stressed conditions, particularly in arid and semi-arid regions (UN-Water, 2023) and within a couple decades, two-thirds of the world's population may face water shortages (Cosgrove and Loucks, 2015; Mekonnen and Hoekstra, 2016; Boretti and Rosa, 2019). Because of demand growth (e.g., agriculture, population growth, economic development) and uncertainties resulting from climate change, water resources planning and management remains a problem of paramount importance (Pimentel et al., 2004; Cosgrove and Loucks, 2015; Sheffield et al., 2018). Indeed, the inability of water resource systems to meet these growing and diverse needs often reflect failures in planning, management, and decision-making (Loucks and van Beek, 2017). Planning and management of water resources needs to be resilient and sustainable to reduce water scarcity and water stress especially in vulnerable areas of the world (Loucks and van Beek, 2017; UN-Water, 2023).

The 2030 Sustainable Development Agenda and its Sustainable Development Goals (SDGs) set out a universal framework with a diverse set of goals and targets that are based on sustainable development principles (Génevaux, 2018). Although the SDGs are formulated as individual goals, they are not independent of each other. Sustainable use of water resources, for instance, is the key to attaining other goals as water is fundamentally linked to most of the SDGs' goals and targets (Bhaduri et al., 2015). There are 25 targets related to disaster risk reduction in 10 of the 17 SDGs (UNDRR, 2015). Within these, SDG 6 (Clean water and sanitation), 7 (Affordable and clean energy), 9 (industry, innovation and infrastructure)

and 13 (Climate action) (UN, 2015) put a respective emphasis on clean water, affordable and clean energy, and building resilient infrastructure. In the face of these key facts, water resources and its management, including hydropower, plays a key role in achieving the SDGs (UN, 2019; Markannen and Braeckman, 2019).

The introduction of this thesis aims to provide a comprehensive overview of the various aspects surrounding hydropower development. Section 1.1 highlights the essential role of hydropower in addressing the SDGs, emphasizing its significance in promoting sustainable energy access and combating climate change. Following that, Section 1.2 examines the current state of hydropower development, and the controversies and challenges encountered in both Reservoir-Based (RB) and small hydropower facilities. Section 1.3 then explores the changing conditions that impact hydropower development, including climate change and economic uncertainties. After that, Section 1.4 discusses the limitations of traditional hydropower design approaches and the necessity for "bottom-up" decision analytical frameworks to ensure robust design solutions. Finally, Section 1.5 provides an in-depth review of the current state of small hydropower design considerations, encompassing turbine system design, financial metrics, the complexity and computational costs associated with hydropower system design. Drawing from these discussions, the introduction outlines the motivation and objectives of the thesis in Section 1.6, aiming to address the challenges identified. Finally, it provides an overview of the thesis structure in Section 1.7, guiding the reader through the subsequent chapters.

1.1 The need for hydropower

Currently, about 10 % of the world's population, predominantly in rural areas, still lacks access to electricity (IEA, 2023a), and 2.3 billion are striving to access clean energy to meet their energy requirements (IEA, 2023b). Besides, in both developing and developed countries the need for clean and sustainable sources of energy is growing in the face of climate change (Hennig and Harlan, 2018; Deyou et al., 2019). Hydropower is often branded a renewable, clean, and environmentally benign source of energy that is also a mature, and reliable technology (Paish, 2002; Hertwich et al., 2016). It is the leading source of renewable energy across the world (Resch et al., 2008; Yah et al., 2017; Zhang et al., 2018). It has produced more than

15 % of the total electricity demand in 2022 (IHA, 2023). There is still a large potential for further development since less than 25 % of global hydropower potential is exploited to date (Zarfl et al., 2015). Therefore, considerable increases in hydropower generation capacity are needed to keep the global temperature rise to below 2 °C above pre-industrial levels (IRENA, 2020).

These days, solar and wind energy are becoming more and more competitive due to considerable cost reductions and efficiency improvements (Carlino et al., 2023; Hassan et al., 2024). They benefit from shorter installation times and lower environmental impacts during operation. Furthermore, scalable deployment is made possible by the modular design of wind and solar facilities, which can be advantageous in various settings (Hassan et al., 2023). Despite this, hydropower retains several key advantages. Hydropower plants provide valuable energy storage and contribute to grid stability, since they can immediately respond to fluctuations in the demand for electricity (Egré and Milewski, 2002; Sternberg, 2010; Zhou et al., 2015). They generally have a higher capacity factor compared to solar and wind, meaning it can produce a more consistent and reliable output of electricity. Additionally, hydropower infrastructure typically has a long operational lifespan, often exceeding 50 years, providing long-term energy security. These make hydropower an ideal complement to more intermittent sources of renewable energy such as wind and solar, which are rapidly developing and improving (Arnold et al., 2024).

Hydropower also has direct and indirect links to the SDGs since they are are designed to produce electricity for over 50 years effectively (Kishore et al., 2021). The 7^{th} SDG is to ensure access to affordable, reliable, sustainable, and modern energy for all (McCollum et al., 2017), in particular, motivate countries to invest in developing the hydropower potential. Hence, hydropower has an important role to play both in achieving this goal (Dorber et al., 2020) and in the implementation of the Paris Agreement (Markannen and Braeckman, 2019). What is more, the different targets of the SDG 7 contribute to the achievement of other SDG goals (Gielen et al., 2019).

Therefore, hydropower plants get large interest due to increasing concern regarding global warming phenomena, the increasing energy demand, grid stability, the depletion of non renewable reserves and the need to close the electricity access gap particularly in the developing

countries (Oud, 2002; Berga, 2016; Owusu and Asumadu-Sarkodie, 2016; Singh and Singal, 2017; Kuriqi et al., 2020; Miskat et al., 2021).

1.2 Hydropower development: controversies and challenges

The most common type of hydropower plant is Reservoir-Based (RB) facilities, typically a large hydropower system, uses a dam to store river water in a reservoir which is created to minimize variability in water supply. These plants are often expensive to build (Ansar et al., 2014), but can be used to meet peak electricity demand since they can immediately respond to fluctuations in the demand for electricity (Egré and Milewski, 2002; Sternberg, 2010; Zhou et al., 2015). This makes hydropower an ideal complement to more intermittent sources of renewable energy. Once commissioned, these plants have very low operation and maintenance costs (IRENA, 2012). What is more, the lake that forms behind the dam can be used for many purposes, including flood prevention, irrigation and drinking water supply, recreation and navigation (Yüksel, 2010; Tullos et al., 2009).

Despite their ability to store water for on-demand renewable energy production and for other uses, RB installations might adversely impact ecosystems around them by altering river inflow, trapping the inflow of sediments and nutrients, and impeding fish migration routes (Rosenberg et al., 2000; Chen et al., 2015; Winemiller et al., 2016; Botelho et al., 2017; Anderson et al., 2018). What is more, sediment trapping contributes to sinking deltas (Loisel et al., 2014; Kondolf et al., 2014), and collapsing fisheries could affect 10s of millions in low-income countries who rely on the fish for proteins (Schmitt et al., 2019).

Partly for these reasons, construction of large hydropower plants paused starting in the late 1960s in developed nations such as Europa and USA. In fact, suitable sites for these projects were already developed, the investment costs increased, and growing environmental and social concerns made the costs increasingly unacceptable (Moran et al., 2018). Moreover, many aged dams have been safely removed as they have filled with sediment, become unsafe or inefficient (O'Connor et al., 2015), or necessitated expensive retrofitting cost to meet regulations and growing concerns about their social and environmental impacts (Doyle et al., 2003; Kibler et al., 2011; Kornis et al., 2015).

Small hydropower plants (SHPs) are a comparably environmentally friendly and cost-

effective alternative to conventional RB plants (Tsuanyo et al., 2023). Only 36 % of small hydropower's global potential is already exploited (UNIDO, 2022), and considerable growth of SHP is expected worldwide (Couto and Olden, 2018), including in industrial countries where the best sites for large-scale hydropower are already taken. For instance, in Europe, more public subsidies are expected to become available for retrofitting or developing these plants (Kuriqi et al., 2020; Kishore et al., 2021). SHPs provide the option of decentralized power production and sustainable industrial expansion (Hennig and Harlan, 2018) in many regions. The vast majority of the SHPs worldwide are called run-of-the-river (RoR) plants (Yildiz and Vrugt, 2019), and are characterised by a negligible (sub-daily) storage capacity and by generation almost completely dependent on the quantity and variability of river flows. Although the electricity generation mechanism is identical to that of RB hydropower plants, they are quite different in design, appearance, and uses.

When compared to RoRs, RB hydropower plants generally have higher energy efficiency as they can control the flow of water and operate the turbines at optimal conditions. In contrast, RoRs have less control over water flow, making them less efficient, especially during periods of low flows (Yildiz and Vrugt, 2019). Additionally, while, the initial costs for RBs are usually higher due to the construction of dams and reservoirs, their ability to provide reliable energy during peak demand often results in a higher financial return over the long term. Conversely, RoR plants generally have lower initial costs because they do not require large-scale dams. Yet, their economic performance can be lower compared to RB plants because their power generation is less reliable, impacting long-term financial returns. Although not to the same extent as reservoir-based plants, RoR plants also offer a stable and continuous source of energy, helping to balance the intermittency of other variable renewables (Hase and Seidel, 2021). This becomes particularly significant on the grid level, where the value of reliable source of energy becomes strong as it better meets demand targets. However, deploying large-capacity reservoir-based hydropower plants instead of smaller alternatives would necessitate larger transmission capacity. The additional benefits gained through improved grid stability must be weighed against the increased costs, requiring detailed analysis beyond the scope of this study.

A common assumption is that RoRs and RB hydropower plants are not competing com-

ponents of the hydropower sector (Couto and Olden, 2018) since RoRs are, in general, smaller and located in tributary rivers. Yet due to growing concerns for the drawbacks of RB plants, RoRs have several advantages that make it an appealing alternative. The environmental footprint of RoR installations is minimal when compared to RB facilities (Kosnik, 2010; Fearnside, 2014; Kishore et al., 2021; Yildiz et al., 2021). Moreover, they have smaller socioeconomic impacts since no resettlement is required (Kumar and Katoch, 2014; Naidu, 2020) and lower environmental impact during construction. However, they are not a silver bullet since cascade RoR plants on the same river may have a significant compounding effect on river ecosystems even if their storage capacity is negligible (Jaccard et al., 2011; Finer and Jenkins, 2012; Kelly-Richards et al., 2017).

Pumped storage hydropower plants (PSHPs) are an important supplement to hydropower plants. PSHPs have the unique ability to store energy by pumping water to a higher elevation during periods of low electricity demand and then releasing it to create power during peak demand (Pérez-Díaz et al., 2015), thereby providing grid stability. While RB plants have traditionally been a cornerstone of reliable energy production, their environmental and social drawbacks have raised growing concerns about operating these plants and constructing new large hydropower projects. Utilizing an existing reservoir as the lower dam, paired with a new or existing reservoir at a higher elevation, could offer a viable and cost-effective solution for PSHPs(Kucukali, 2014; Rogeau et al., 2017). This approach would not only mitigate the drawbacks associated with RB plants but also support the transition to a more sustainable and resilient energy infrastructure. Furthermore, the integration of RoR plants with PSHPs could significantly enhance grid stability by combining the consistent, low-impact power generation of RoR systems with the flexible, rapid-response storage capabilities of PSHPs (e.g., Ceseña et al., 2019).

Despite the fact that both RoR and RB power plants have environmental impacts, major new initiatives in hydropower development are now under way in response to the energy need. Over 3,000 major power plants each with a capacity of more than 1 MW, are either planned or under construction, with RoRs accounting for more than 75% of that total (Bejarano et al., 2019), primarily in countries with emerging economies (Zarfl et al., 2015). This includes hundreds of hydropower plants being built or planned in several river basins of global

relevance, including the Amazon, Congo and Mekong (Winemiller et al., 2016; Schmitt et al., 2019). Beyond that, even locations that are currently not considered economically feasible could see expanded hydropower production in the nearby future (Kosnik, 2010; Hoes et al., 2017). These developments ensure that hydropower will remain a key energy source of global electricity supply in decades to come (Winemiller et al., 2016; Pokhrel et al., 2018; Moran et al., 2018; Gernaat et al., 2017).

Recent research has weighed in the debate RBs vs RoRs by outlining alternatives to massive reservoirs. Bertoni et al. (2019, 2020) show that a smaller size of reservoir can perform satisfactorily at lower costs if operated in a judicious way while performing well under a range of climatic and socio-economic conditions. Likewise, recent study by Wild et al. (2019) outlines how a smaller RoR installation would be an alternative to fully damming the Mekong river that better balances hydropower production with sediment and ecosystem management and emphasizes the importance of multi objective optimization of hydropower plants by considering ecological concerns.

There remains substantial room for further technological advancements in hydropower. Innovations in turbine efficiency under varying load conditions, fish-friendly designs (e.g. Olbertz, 2021), better sediment management practices, and the integration of storage capabilities, such as pumped storage, are areas where hydropower technology can continue to evolve. Additionally, optimizing existing infrastructure and integrating digital monitoring and smart grid technologies (Rehmani et al., 2018) can significantly enhance the efficiency and responsiveness of hydropower plants. Moreover, uncertainties pertaining to the integration of hydropower with other renewable energy sources in hybrid systems can impact its future deployment. A recent study by Arnold et al. (2024) have shown promising alternatives, such as a capital investment shift from planned hydropower plants in the Zambezi river basin towards fewer reservoirs and the adoption of floating photovoltaic (FPV) systems. This approach not only yields a more robust energy output, with a 12 % reduction in variability, but also proves to be robust to long-term hydrological changes. Ongoing research into hybrid systems and their optimal configuration will undoubtedly play a crucial role in shaping future energy landscapes. Because of its unique advantages, hydropower continues to be an essential part of the renewable energy mix even in the face of competition from quickly

developing renewable technologies like solar and wind (Zhou et al., 2015). Taken together, these studies suggest that sustainable and innovative solutions are possible, so hydropower development can mitigate or even eliminate negative environmental, behavioral, cultural, and socioeconomic impacts.

1.3 Changing conditions

Historically, water resources infrastructure including hydropower plants have been planned and operated under the assumption of stationarity (Milly et al., 2008; Wilks, 2011). This assumption means that the past and future of a streamflow time series will be similar statistically. However, substantial evidence suggests that streamflow records have been non-stationary due to a mix of climate change, land-cover and land-use change, the construction of large-scale infrastructure such as reservoirs and interbasin transfers, and groundwater pumping. There is substantial evidence for these changes at a range of scales (Cheng et al., 2014; Rougé and Cai, 2014; Abera et al., 2018).

Hydropower generation is closely linked to hydrological conditions in a watershed, and it is sensitive to both seasonal water availability variations (Schaeffer et al., 2012; Teotónio et al., 2017; Yildiz et al., 2022) and to droughts (Van Vliet et al., 2016). Climate change, and its widespread projected increases in dry conditions frequency and magnitude, is expected to influence the availability and stability of hydropower generation (Wasti et al., 2022). This challenges the transition to low-carbon energy generation that is necessary to avert climate catastrophe, because hydropower operation produces a renewable and largely emission-free source of energy (Hertwich et al., 2016). Hydropower plants are also ideal as a flexible complement to more variable and intermittent power sources such as solar or wind (Wang et al., 2019), so increased drought impacts could pose challenges to grid stability in many regions (Jurasz et al., 2018), further hindering the energy transition.

Water resource planners and decision makers are rightly concerned about the potential effects of future uncertainties, especially climate change, on hydropower plants because of the high investment costs, as well as social costs (in particular for RB hydropower plants which causes population displacement) and environmental costs (Ray et al., 2018). Therefore, it is key to address hydrologic non-stationarity and uncertainty and incorporate into planning

and operation of hydropower systems (Abera et al., 2018; Carvajal et al., 2019). In response, there has been a dramatic increase in research of climate change impacts on water resources and more specifically on hydropower generation (Hamududu and Killingtveit, 2012; Turner et al., 2017b).

RoR schemes are more sensitive to climate change than RB plants, because they cannot modulate flows and only operate in a predefined range (Moran et al., 2018). For these reasons, assessing climate change impacts before and during implementation of hydropower projects can result in timely responses and adaptation to climate change with a potential for considerable cost savings (Jamali et al., 2013). Therefore, new hydropower projects should consider the possible impacts of climate change during the design phase and existing schemes may need upgrading in the future if they are to continue to make the best use of available water resources.

Despite the fact that decision makers and engineers are mostly concerned about the potential effects of climate change on the future performance of hydropower investments (Ray et al., 2018), there are other economic related risk factors that need to be considered especially during planing phase (Shaktawat and Vadhera, 2021). Among these are capital cost (Ansar et al., 2014), electricity selling price (Gaudard et al., 2016), discount rate (Ray et al., 2018), currency exchange rates (Shaktawat and Vadhera, 2021) and the design lifetime of a project Moran et al. (2018). Indeed, a study carried out by Ray et al. (2018) indicates that climate change may not be the most critical future uncertainty for the performance of a hydropower investment in Nepal. This highlights the importance of considering multiple uncertainties in combination in hydropower plant design.

1.4 Planning under deep uncertainty

A conventional approach to hydropower systems planning is best summarised as a predict-then-act approach (Lempert et al., 2013), where optimisation of a design objective under the assumption of a best-estimate (i.e., most likely) future, suggests the "best" course of action. This optimal solution is generally defined based on a single objective, which lumps several conflicting and heterogeneous objectives (Lempert, 2014; Bertoni et al., 2019). If the future projections turns out to be different from the hypothesized future(s), the optimal

solution is likely to fail (Haasnoot et al., 2013; Hamarat et al., 2013). Predict-then-act is only appropriate when the uncertainty is well-characterized, i.e., decision makers know or can cover a single probability density function for each key parameter, a perfect model structure, or a single adequate objective (Singh et al., 2015). Yet, as highlighted previously in Section 1.3, hydropower production is subject to large hydroclimatic and socio-economic uncertainties. As a result, predict-then-act approaches to hydropower planning need to be replaced with better-suited paradigms.

When historical data is deemed insufficient for estimating future projections and, as a result, planners are unable to agree on or identify the full scope of possible future events, including their associated probability distributions, deep uncertainties emerge (Lempert et al., 2006; Singh et al., 2015). Deep uncertainty means that the various parties to a decision do not know or cannot agree on on the system model, its boundaries, and the prior probability distribution for uncertain inputs to the system, how likely various possible future states of the world are, and how important the various outcomes of interest are (Lempert, 2003; Kwakkel et al., 2010; Walker et al., 2013; Maier et al., 2016). Deep uncertainty also evolves out of actions taken over time in response to unpredictable evolving situations (Haasnoot et al., 2013). This implies that there are a large number of possible representations of the system, plausible futures, and relevant outcomes of interest, and different (sequences of) candidate solutions (Kwakkel et al., 2010).

Water resource planners and decision makers have increasingly recognized the inadequacies of a predict-then-act approach (Herman et al., 2015), and realized that it is no longer possible to determine a single best-guess of how future conditions might change, especially when considering longer planning horizons as a result of climatic, technological, economic and sociopolitical changes (Maier et al., 2016; McPhail et al., 2018). Accordingly, they aim to find design and operation alternatives which are robust to deeply uncertain and changing conditions (Marchau et al., 2019). A robust alternative is one for which the expected performance of the solution is insensitive to variations in the estimation of parameters which are affecting design choice (Herman et al., 2015). In other words, it works well under a range of plausible futures, instead of being "optimal" in a single future. Several “bottom-up” decision analytical frameworks have evolved to define robust alternatives by considering multiple plausible

futures, which requires uncertainties to be described with the aid of scenarios that represent coherent future pathways based on different sets of assumptions (Maier et al., 2016). Examples include Robust Decision Making (Bryant and Lempert, 2010), Decision Scaling (Brown, 2011), Info-Gap (Hipel and Ben-Haim, 1999), Robust Decision Making (Lempert, 2002), Dynamic Adaptive Policy Pathways (Haasnoot et al., 2013) and Many-Objective Robust Decision Making (Kasprzyk et al., 2013). The key steps in assessing robustness within these frameworks are (Herman et al., 2015), (1) alternative generation: this step describes the set of candidate solutions to the planning problems, and often narrows it down through optimisation, (2) sampling of states of the world: uncertain factors are identified in this step and specific combinations of them are sampled to generate an ensemble of plausible states of the World (SOWs), (3) quantification of robustness measures: this step clarifies the performance evaluation of each (or selected) alternatives across the entire ensemble of SOWs, and (4) sensitivity analysis: combinations of uncertainties that cause the candidate solutions to perform poorly are determined in this final step.

These methods are commonly contrasted with predict-then-act framework by focusing on the identification of robust rather than optimal solutions (Shortridge and Guikema, 2016), and move beyond trying to predict the most probable future(s) to discover which states of the world (SOWs) may lead to high consequence system vulnerabilities (Hadka et al., 2015).

Applications to robust design of hydropower plants proved that considering robustness as a decision criterion via a bottom up approach can dramatically change the hydropower design (Bertoni et al., 2019) and these approaches allows decision makers to characterize the most important vulnerabilities for hydropower plants (Ray et al., 2018). There is scope for building on this small set of Decision Making under Deep Uncertainty (DMDU) applications to hydropower plant design by improving hydropower system modelling in these applications.

1.5 Current state of small hydropower design

This section offers a comprehensive review of the current state of small hydropower design considerations, exploring the primary challenges they entail. It covers a range of factors, including turbine system design, financial metrics, and the complexity and computational costs associated with hydropower system design.

1.5.1 Turbine system design

The turbine system is at the heart of the power plant and converts flowing water into mechanical energy. In general, after the optimal plant size is determined, the number and type of the turbines and their respective capacities are defined with an optimization analysis of expenditures (costs) versus benefits (DSI, 2012).

The majority of the water resource literature separates design and management of hydropower plants. For instance, the majority of prior research aims to increase overall operational performance of an existing power plant that consists of several turbines while meeting several technical, physical, and strategic constraints (Siu et al., 2001; Li et al., 2013; Taktak and D'Ambrosio, 2017; Séguin et al., 2017; Onen, 2018; Cheng et al., 2021). In these studies, efficiency is often taken constant or as a function of release term (Onen, 2018) in hydropower analysis in planning phase. This is often ignored in planning analysis, leading to a mismatch of projected and real (operation) energy production. This lack of consideration of operations during hydropower plant design, combined with the current engineering practice of selecting identical turbines, becomes especially problematic with climate change. For example, new turbines at a lower elevation have had to be installed at major hydropower plants such as Hoover Dam because of the current and projected future water shortages in the Colorado River as a result of climate change (Moran et al., 2018). In the coming decades, many hydropower systems may face the necessity of redesigning their turbine configurations to enhance operational flexibility in response to dwindling river flows caused by climate change and human consumption. In parallel, similar modeling and design optimization approaches are evident in other fields, such as wind turbine design. Within wind farms, shifting from uniform layouts, where identical wind turbines are used, to a non-uniform design, incorporating various types of wind turbines with different hub heights, has shown potential to enhance financial performance (González et al., 2011; Herbert-Acero et al., 2014). Non-uniform wind farms can optimize energy production and reduce costs more effectively than their uniform counterparts, ultimately achieving higher energy efficiency and financial return (Feng and Shen, 2017).

Research in turbine system design for RoR power plants has received attention recently, since the turbine system's cost is on average around 50 % of the investment cost of a RoR

power plants (IRENA, 2012; Mamo et al., 2018; IEA, 2021). This research is much needed in an area where determining a plant's installed capacity and optimizing turbine system design are still often considered as separate steps performed in this order Yet, turbine system design still rarely considers variable turbine efficiency during plant design optimization (e.g. Voros et al., 2000; Kaldellis et al., 2005; Lazzaro and Botter, 2015). This is despite the fact the operational efficiency of the turbine(s) is crucial to linking flow variability with actual hydropower production (Okot, 2013), and therefore to determining the turbine system best suited for a particular site and river flow characteristics (Yildiz and Vrugt, 2019). Design studies also generally assume that the number of turbines considered is generally limited to two despite evidence that the use of more than one turbine improves considerably the ability of a RoR plant to respond effectively to seasonal discharge variations (Anagnostopoulos and Papantonis, 2007; Yildiz and Vrugt, 2019). Besides, when the design consists of two turbines or more, they are often assumed to be identical (Kaldellis et al., 2005; Mamo et al., 2018; Amougou et al., 2022), at the expense of added operational flexibility. The HYPER toolbox (Yildiz and Vrugt, 2019) partially addresses these limitations, as it considers variable turbine efficiency and enables to design two-turbine systems with non-identical turbines of a user-specified type – Kaplan, Pelton or Fancis. Yet, our understanding on how various climatic but also socio-economic uncertainties – such as interest rates, project cost overruns or energy prices – affect turbine design remains limited, warranting a revisiting to the design of these systems. There is scope for new advances in detailed numerical simulation and optimization to estimate the optimum capacity and turbine system design of a RoR plant for given site characteristics and record of discharge observations.

1.5.2 Financial metrics

The financial viability of a RoR hydropower investment is usually assessed by several common metrics such as the net present value (NPV), the internal rate of return (IRR), the benefit cost ratio (BC) and the levelised cost of electricity (LCOE). These metrics combine capital costs, operation and maintenance costs, and other relevant measurements (Klein and Fox, 2022). NPV is the cumulative sum of all discounted lifecycle cash inflows generated by the power plant (e.g. Hosseini et al., 2005; Bøckman et al., 2008; Santolin et al., 2011; Yildiz

and Vrugt, 2019). A project is considered feasible with a positive NPV, and a higher NPV signifies a more favorable outlook. IRR is the annual rate of return for which the NPV of lifecycle net cash flows is zero (e.g. Kaldellis et al., 2005; Basso and Botter, 2012). An IRR value exceeding the discount rate signals project feasibility with a higher value implying a more attractive investment opportunity. Unlike NPV, the IRR does not provide the return on the initial investment in nominal terms; rather, it expresses the profitability of an investment as a percentage rate of return. BC is the ratio of NPV lifecycle benefits to the lifecycle costs (e.g. Anagnostopoulos and Papantonis, 2007; Forouzbakhsh et al., 2007; Nedaei and Walsh, 2022), requiring a value greater than 1 for a project to be deemed feasible, with a higher BC indicating a more favorable scenario. It is a metric that helps in prioritizing projects based on their economic efficiency. LCOE is the average cost per unit electricity production to recover the cost of investment (e.g. Zhang et al., 2012; Ceran et al., 2020). It serves as a frequently employed indicator for technology comparison, with a lower LCOE relative to the selling price of electricity indicating the project's attractiveness and viability as an investment. LCOE does not provide a comprehensive assessment of a project's economic or technical viability as NPV and BC do, as it often overlooks revenue streams (Klein and Fox, 2022). Of all these metrics, the NPV is the most frequently used in the hydropower literature to asses the economical performance of RoR hydroelectric plants (Yildiz and Vrugt, 2019). It focuses on the expected profit, whereas the IRR, BC and LCOE focus on the risk of the projects (Anagnostopoulos and Papantonis, 2007; Basso and Botter, 2012). Thus, maximizing the NPV leads to a design that offers the highest return, whereas maximizing the IRR, BC, or minimising LCOE would result in design with lower risk and investment costs.

Despite recognition that there is a trade-off between financial viability metrics for RoR plant design (Basso and Botter, 2012), there remains opportunities for systematic approaches to exploring these possible trade-offs, especially in the context of climate change. In the rest of this work, we choose BC as a metric because of its preponderance in the RoR literature (USBR, 2011; Klein and Fox, 2022). Despite literature cautioning that BC can be easily manipulated in multi-objective cases, where the conversion of a non-monetary objective (e.g., reliability or vulnerability) into a benefit or cost will arbitrarily impact the benefit cost ratio (Lund, 1992), these concerns are not relevant in the majority of RoR plant feasibility studies,

as other water uses are treated as constraints that the design will need to meet, rather than given a monetary value.

1.5.3 Complexity and computational cost of hydropower system design

Design and operations of RoR hydropower plants are often considered separately, even though it has been proved that design (generally understood in the literature as size) and operations are critically dependent on each other (Tian et al., 2018; Bertoni et al., 2020). This is particularly the case in situations where there is a need (1) to better address hydro-climatic variability, climate change and unintended consequences of development, and (2) to avoid overdesign in a context where a 1 % reduction in the size of planned dams could save $300 billion worldwide (Bertoni et al., 2019). Careful exploration of the planning and operation search space (Bertoni et al., 2019, 2020) yields designs that outperform the larger alternatives designed using traditional sizing methods. These smaller solutions would be less costly and could perform well under a range of climatic and socio-economic conditions. Additionally, to achieve future-proof planning where investments remain financially resilient to perturbations, design and operations should be robust, i.e., able to withstand deviations from design conditions (Herman et al., 2015).

In water resource systems that include complex interactions between design variables and operation restrictions, both optimization including multi-objective optimization and robustness analysis typically demand a substantial amount of computing time and resources, as both steps involve extensive simulation ensembles. These computational requirements become even more pronounced when conducting exploratory studies involving both steps (e.g., Quinn et al., 2018; Bertoni et al., 2019). This is in part because optimisation of large-scale water infrastructure involving hydropower plants is a complex and dynamic process which often necessitates re-analysis based on evolving conditions and the larger number of alternative strategies available. They then create a need for large-scale computing solutions – High-Performance Computing (HPC) or cloud-based computing, and contributes significantly to the increasing need for large-scale computing solutions, including supercomputers and data centers (Hussain, Wahid, Shah, Akhunzada, Khan, Amin, Arshad and Ali, 2019; Lannelongue et al., 2021). In turn, this quest for enhanced processing capacity raises environmental con-

cerns (Hernandez et al., 2018; Katal et al., 2023), because the electricity that needs to be mobilized for the continuous use of computational facilities contributes to climate change, resource depletion, and strain on local power infrastructures (Bharany et al., 2022). Thus, scientific and large-scale technical computing presently account for 0.3 % of global carbon emissions, and this share is likely to increase in the future (Jones, 2018; Cao et al., 2022*a*; Katal et al., 2022), creating an additional, considerable challenge to global climate change mitigation measures.

As the need for large-scale computing grows, finding innovative technical solutions that balance these computing demands with energy economy and environmental responsibility becomes critical. These solutions will also remove barriers to application of these methods beyond actors in industrialised nations – academia and corporations – that often lack the human and physical infrastructure to use the most largest computing facilities.

1.6 Thesis motivation and objectives

Traditional assessments of hydropower plants usually rely on historical flows and set conditions of use by ignoring impacts of climate change and economic related other future uncertainties. These plants are optimised under these arbitrary conditions based on cost - benefit analysis by focusing on identification of optimal solution rather than robust alternatives which perform well under a range of uncertain conditions. Moreover, design and operation of these plants are considered separately without taking into account turbine system design. In regards to the gaps identified, there is a need for developing a new integrated framework to reconsider hydropower development with its planning and decision-making process.

Expanding upon the identified research challenges and opportunities in hydropower plant design and operation, the aim of this thesis is to address these shortcomings to contribute to scientific and technical advances in hydropower plant design. These contributions aim to directly inform and benefit real-world decision-making processes, thereby facilitating more effective and sustainable water resource management practices. To achieve the research aim, I formulated the following research questions and worked to answer them by fulfilling the corresponding research objectives:

- 1) How can plausible future streamflows, informed by climate studies, be defined effec-

tively to assess the robustness of a hydropower plants's performance?

– The first objective is to parameterise flow duration curves (FDCs), the cumulative frequency curve that shows the percentage of time specified discharges were equaled or exceeded during a given period, and to perturb these parameters using available climatic information to simulate a range of future flow scenarios.

- 2) Is current RoR design based on NPV maximisation and itendical turbine setup the most robust to climate change and changing economic conditions? How can we identify design solutions that exhibit robust performance across a spectrum of uncertain future scenarios?

  – The second objective is to develop a new framework that couples the Many Objective Robust Decision Making (MORDM) approach with the the HYPER toolbox to illuminate the trade-offs between the conflicting objectives to determine which design including turbine configuration and plant operation is most robust and reliable for given site conditions and river stream characteristics.

- 3) Are climate or economic uncertainties more crucial to the success of hydropower investments?

  – The third objective is to conduct global sensitivity analysis and scenario discovery, within the HYPER-MORDM framework, to identify and analyse the key factors influencing the robustness of these plants.

- 4) How can design and operation optimization be effectively integrated for RoRs to maximize efficiency, considering the interactions between turbine configuration and varying water flow dynamics?

  – The fourth objective is to develop a new toolbox for integrated design and operation optimization. This toolbox incorporates optimized turbine operations directly into the design phase, ensuring the optimal allocation of flow to turbines during simulation, thereby enhancing overall efficiency.

- 5) How can optimisation and robustness analysis be performed for RoRs by using far less computational resources (time, processing power and memory)?

– The fifth objective is to approximate FDCs of long term observed and/or synthetic stream flow data using a limited number of points to minimise computing hours and resources. Together with this, develop a new toolbox that integrates design and operation optimization using this sampled data for both robustness analysis and optimization purposes.

1.7 Thesis outline

My starting point for this work is the HYPER toolbox, published based on previous work (Yildiz and Vrugt, 2019) and introduced in Chapter 2 for the reader's information. HYPER is a state-of-the-art toolbox that identifies optimal design parameters that maximize either the power production or net economic profit of run-of-river (RoR) hydropower plants. This toolbox serves as the backbone of the methodologies presented here, as it is used to generate RoR design alternatives.

In Chapter 3, I present the first statistical generation method based on a near-universal parameterisation of FDCs, and perturbation of these parameters to simulate a range of futures. These future flow scenarios can then be used for stress-testing and robustness analyses. The findings indicate that unlike methods that uniformly adjust streamflow statistics across a time series using multipliers, this approach seamlessly represents a large range of futures with increased frequencies of both high and low flows. This aligns with anticipated climate change impacts in the region of interest, and supports analyses of the financial robustness of a proposed RoR infrastructure to climate change.

The content of this chapter is adapted from Yildiz et al. (2023a).

In Chapter 4, I put forward a novel framework that couples the MORDM approach with the the HYPER toolbox for robust design and operations of RoR hydropower plants. The framework draws on the principles of decision-making under deep uncertainty (DMDU), that is centered around stress-testing to navigate hard-to-quantify uncertainties. Applying the HYPER-MORDM approach to five proposed hydropower plants in Turkey challenges two fundamental design assumptions: the use of net present value as the sole design objective and the deployment of identical turbines. Instead, optimizing the benefit-cost ratio leads to plants with enhanced financial viability across a spectrum of potential futures. These

optimized designs often feature smaller capacity and incorporate a smaller turbine that is well-adapted to low-flow periods. Additionally, analysis results reveal that socio-economic uncertainties can have an equal or greater impact on the robustness of hydropower projects compared to climate conditions. Consequently, these uncertainties have the potential to make many small hydropower projects too risky for implementation.

The content of this chapter is adapted from Yildiz et al. (2024a).

In Chapter 5, I introduce the HYPER-FORD toolbox comprising two innovations in RoR hydropower plant design. First, the HYPER$_{OP}$ module builds operational tables that integrate optimized operations to design. Second, the approximation of the FDC with a regular sampling of the FDC builds upon HYPER$_{OP}$ to enhance computational efficiency through strategic reduction of data inputs. The findings show HYPER$_{OP}$ is able to increase electricity generation by about 2% compared with traditional operational rules. The results also demonstrate the capability of the HYPER$_{OP}$ to find design solutions not traditionally considered in engineering design of RoR hydropower plants, showing how optimized operations can expand design options. Furthermore, despite potential loss of discharge information from sampling datasets, the impact on design optimization and robustness analysis remains negligible. This new toolbox aims to facilitate the discovery of optimal and robust designs while reducing the computational costs typically associated with analyzing complex systems such as hydropower plants, thus decreasing dependence on high-performance computing or data centers.

The content of this chapter is adapted from Yildiz et al. (Under Review, 2024c).

Finally, I present concluding remarks and recommendations for further work in Chapter 6. While each chapter discusses specific findings and limitations, I also provide a broader discussion on the implications of these findings. This includes insights into the wider applicability of our methods and their potential impact on the field of hydropower research and water resource management.

CHAPTER 2

HYPER toolbox

HYPER (Yildiz and Vrugt, 2019) is a state-of-the-art toolbox for the optimal design of a RoR plant. This toolbox has undergone rigorous testing and validation during its development, ensuring its reliability and accuracy. To my knowledge, this is the only generic toolbox that incorporates turbine system design into design optimization by considering variable turbine efficiency, marking the first instance of such an approach in hydropower literature. It's crucial to acknowledge that while the HYPER toolbox forms the backbone of this study, its introduction in this context is not the thesis's original contribution.

The HYPER toolbox constitutes the first numerical model that takes into explicit consideration the turbine design flow, penstock diameter, penstock thickness, specific speed, rotational speed, and admissible suction head (to combat cavitation) in evaluating the technical performance, energy production, management and operational costs, and economic profit of a RoR plant. HYPER considers the possibility of using turbines of different sizes for increased flexibility across the full range of flows. Moreover, a built-in evolutionary algorithm allows optimization of the design and project parameters, including turbine selection and configuration. It (a) uses the specific speed as guiding principle to determine the most appropriate turbine(s) for given site characteristics and record of river discharge values, (b) simulates the Pelton, Francis, Kaplan and Crossflow turbines, and (c) accommodates single and dual, side-by-side turbine systems.

Figure 2.1 presents a high-level overview of the modeling framework. Color coding is used to distinguish between the different building blocks of HYPER. Model inputs are highlighted in red and include the turbine chart, and the flow duration curve, project variables and design parameters (discussed in detail in Yildiz (2015); Yildiz and Vrugt (2019)) of the

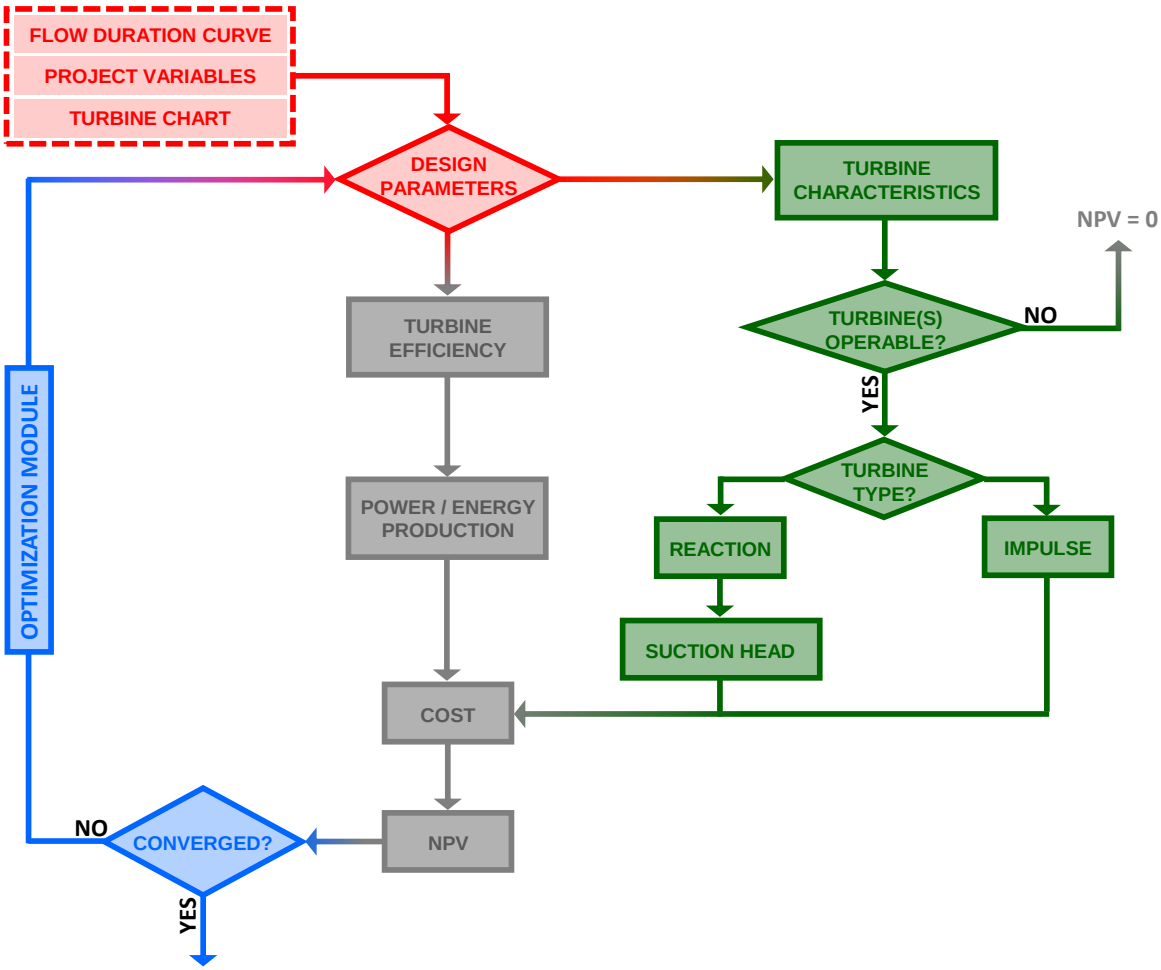

Figure 2.1: *High-level overview of HYPER with color coding for the different building blocks of the model. HYPER simulates the daily performance, investment, operation and maintenance costs, and economic profit of a RoR hydropower plant. Model inputs are highlighted in red. The design parameters (red diamond) play a key role in HYPER as they control the electricity production (gray), operational feasibility of the turbine system (green) and total costs (gray) of the RoR plant. A built-in optimization module (in blue) can be used to find optimal values of the design and/or project variables that maximize the net present value (NPV) of the plant. HYPER accommodates many other design objectives as well such as internal rate of return (IRR) and pay back time (PB).*

installation site. The design parameters (in gray diamond) not only govern the plant's electricity production and investment, operation and maintenance costs (grey track), but also control the technical characteristics (e.g. rotational speed and suction head) of the turbines. These characteristics must satisfy manufacturer guidelines, otherwise the turbine system is deficient and cannot operate. The design parameters and project variables can be specified by the user or their values can be determined via a built-in optimization module (in blue). This module implements an evolutionary search algorithm and allows users to maximize (or minimize, if appropriate) a suite of different design objectives. The present chart returns the net present value, or NPV, of the plant. This metric measures the net difference between all revenues received from the produced hydroelectric energy and the life time costs of the plant.

HYPER is easy to execute and allows users to handpick and optimize relevant project and decision variables. It includes a graphical user interface (see 2.2) to simplify model setup, numerical simulation, and selection and optimization of the decision variables. The left panel (in cyan) provides a list with project variables that be changed by the user depending on the properties of the local installation site, and anticipated design and economic variables of the RoR plant. The user can select whether to operate the RoR plant with a single turbine or two turbines configured in parallel. The settings of optimisation algorithm (Differential Evaluation, DE) is defined in the purple box in the bottom right corner. This box allows the user to specify values for the population size and number of generations in the DE algorithm, and the feasible ranges of the most important design parameters considered in the literature in optimization analysis of RoR plants. The search is conducted using a population size of $I = 100$ individuals and $J = 1000$ generations, which is generally sufficient for most cases. However, it is recommended to run the algorithm multiple times separately to ensure convergence and reliability of the results. The user-specified algorithm parameters, such as population size and number of generations, allow for fine-tuning, ensuring a balance between exploration and exploitation and enhancing the overall reliability and efficiency of the optimization process. The brown box labeled "Objective Function" allows the user to select which objective function to maximize, and is currently limited to the power production, net profit, internal rate of return (IRR) and pay-back (PB) of the plant. Finally, the user has the option to specify their own efficiency curves for the Kaplan, Francis, Crossflow, and Pelton

turbines.

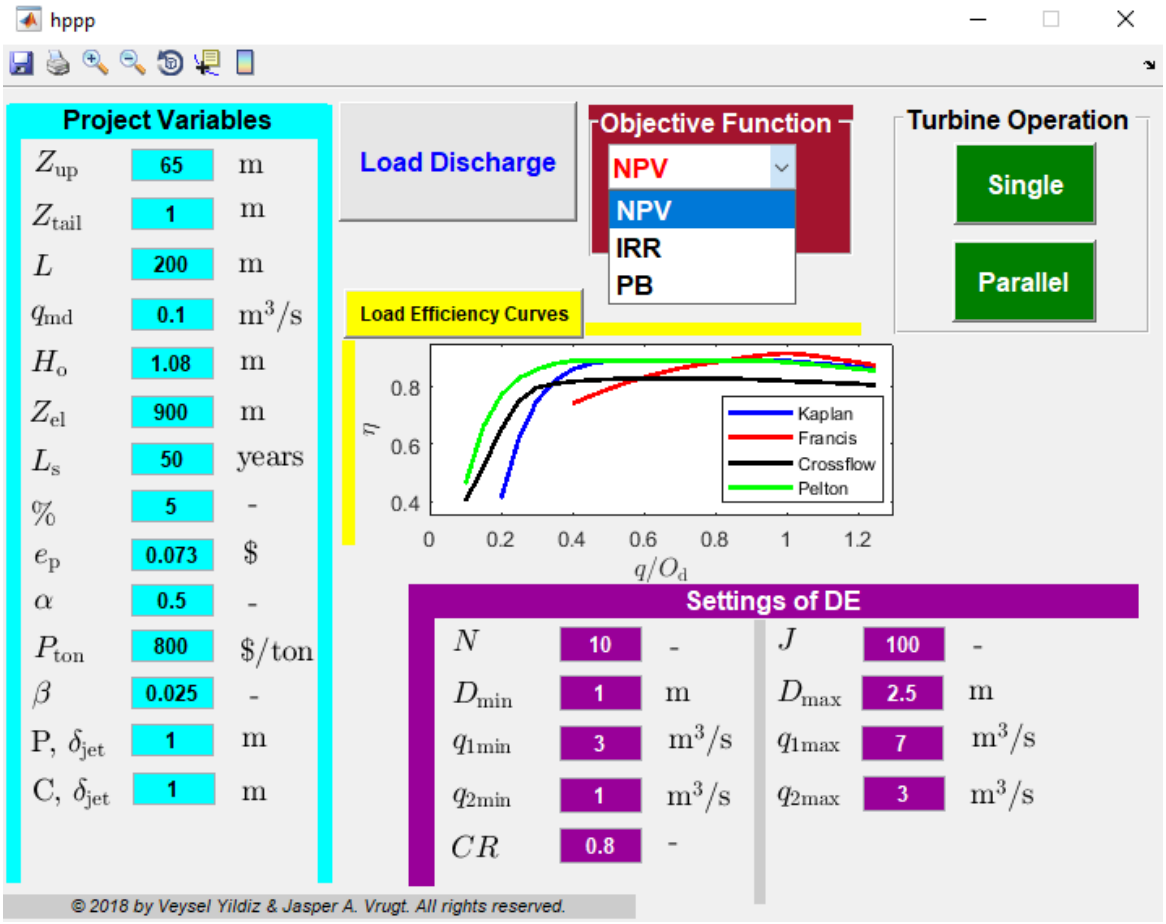

Figure 2.2: *Screen shot of the graphical user interface of HYPER.*

CHAPTER 3

Statistical generation of future flows

Abstract[1]

Assessing the robustness of a water resource system's performance under climate change involves exploring a wide range of streamflow conditions. This is often achieved through rainfall-runoff models, but these are commonly validated under historical conditions with no guarantee that calibrated parameters would still be valid in a different climate. In this note, we introduce a new method for the statistical generation of plausible streamflow futures. It flexibly combines changes in average flows with changes in the frequency and magnitude of high and low flows. It relies on a three-parameter analytical representation of the flow duration curve (FDC) that has been proved to perform well across a range of basins in different climates. We rigorously prove that for common sets of streamflow statistics mirroring average behavior, variability, and low flows, the parameterisation of the FDC under this representation is unique. We also show that conditions on these statistics for a solution to exist are commonly met in practice. These analytical results imply that streamflow futures can be explored by sampling wide ranges of three key flow statistics, and by deriving the corresponding FDC to model basin response across the full spectrum of flow conditions. We illustrate this method by exploring in which hydro-climatic futures a proposed run-of-river hydropower plant in eastern Turkey is financially viable. Results show that contrary to approaches that modify streamflow statistics using multipliers applied uniformly throughout a time series, our approach seamlessly represents a large range of futures with increased

[1] Yildiz, V. and Milton, R. and Brown, S. and Rougé, C., 2022. Technical note: Statistical generation of climate-perturbed flow duration curves. Hydrology and Earth System Sciences

frequencies of both high and low flows. This matches expected impacts of climate change in the region, and supports analyses of the financial robustness of the proposed infrastructure to climate change. We conclude by highlighting how refinements to the approach could further support rigorous explorations of hydro-climatic futures without the help of rainfall-runoff models.

3.1 Introduction

Projections of climate change and its impact on water resources are inherently uncertain, and this is likely to increase as a result of climatic, technological, economic and sociopolitical changes (Maier et al., 2016; McPhail et al., 2018). Water resource planners and decision makers are rightly concerned about the potential effects of future uncertainties, with the upfront cost of action to be weighed against the high potential social and environmental costs of inaction over time (Singh, 2018; Ray et al., 2018). Conventional engineering approaches to water systems planning have been summarised as "predict-then-act" (Lempert et al., 2013), with optimisation of a design objective under the assumption of a best-estimate (i.e., most likely) prediction of the future suggesting the "best" course of action. To produce future streamflow in this framework, rainfall-runoff models are routinely forced by rainfall and temperature projections of dynamically downscaled global climate models (GCMs; Peel and Blöschl, 2011; Chen et al., 2019). There are, however, two categories of issues with this type of approach.

First, "predict-then-act" is not compatible with hard-to-quantify uncertainties, as it works best when a known single probability density function is available for each key parameter (Singh et al., 2015). If the future turns out to be different from the hypothesized projection(s), the optimal solution could fail, sometimes catastrophically (Haasnoot et al., 2013; Hamarat et al., 2013). To avoid this, several emerging decision-making frameworks (Lempert, 2002; Bryant and Lempert, 2010; Brown et al., 2012; Haasnoot et al., 2013; Kasprzyk et al., 2013) strive to find adaptation solutions that are robust to uncertain and changing conditions. In the climate adaptation context, a robust alternative maintains satisfactory expected performance under a range of plausible futures (Maier et al., 2016; McPhail et al., 2018; Marchau et al., 2019), instead of being "optimal" in a single future. Therefore, to identify robust alternatives, uncertainties have to be described with the aid of scenarios that represent co-

herent future pathways based on different sets of assumptions (Maier et al., 2016). In water resource applications, this entails defining specific ranges for future uncertainties including streamflow, then sampling them to generate an ensemble of plausible future conditions.

The second category of issues is with the use of rainfall-runoff models to generate future flow conditions. Indeed, these models have generally been calibrated and validated under historical conditions, with no assurance that these parameters would still be valid under different hydro-climatic conditions (Peel and Blöschl, 2011). There is evidence that rainfall-runoff models' predictive skill decreases with changed climatic conditions (Saft et al., 2016; Seibert et al., 2016; Fowler et al., 2020). In fact, a study of the Rhine-Meuse basin from 1901 to 2010 shows that optimal calibration evolves with climate variability, and land use and river structure change (Ruijsch et al., 2021). To compound these calibration issues, the significant resources and modelling skill needed for calibration and validation mean that is costly for water resource assessments based on rainfall-runoff models to explore the full uncertainty space associated with climate change, with far-reaching consequences for planning. However, it's worth noting that using model-related uncertainties could potentially expand the search to encompass a broader range of future scenarios. Despite this potential, it still demands substantial time and computational resources for comprehensive water resource evaluations.

For these reasons, approaches aimed at finding climate-robust adaptation solutions have often relied on multipliers applied uniformly along a time series also known as the "delta change" approach (Brown et al., 2012). Examples of this affect streamflow either directly through multiplication (e.g., Herman et al., 2014, 2015) or indirectly by applying to climate variables such as temperature and precipitation, before using regression to deduce annual runoff (e.g. Ray et al., 2018). More sophisticated versions of this exist, e.g., Quinn et al. (2018) distinguished several multipliers to isolate changes to the mean, to variance, and to monsoonal dynamics in the Red River basin in Vietnam. However, to our knowledge there is no approach that seeks to describe catchment response under changing climate in a coherent way across the full range of hydrological conditions.

As the representation of the empirical cumulative distribution function (CDF) of streamflow (Vogel and Fennessey, 1994), a flow duration curve (FDC) precisely represents the full

range of hydrological conditions. The FDC is unique to each catchment, and it is influenced by various factors including climate, topography, physiography, vegetation cover, land use (Castellarin et al., 2013; Brown et al., 2013; Sadegh et al., 2016). It has become a popular tool used in modern hydrology for various water resources applications (Leong and Yokoo, 2021), since it provides concise and valuable information about river streamflow variability and catchment response (Blöschl et al., 2013; Boscarello et al., 2016). For example, slope steepness in the middle part of a FDC is characteristic of a catchment's precipitation retention properties (Yilmaz et al., 2008).

This remark has led Sadegh et al. (2016) to adapt a set of soil retention functions such as those proposed by van Genuchten (1980) and Kosugi (1996) to mimic the empirical FDCs of catchments. These models are used in soil physics and hydrology to characterise water flow in unsaturated soils and to estimate soil water retention properties. This analogy is based on the idea that both watersheds and soils are governed by similar hydroclimatologic forcing, and are able to store and dispel precipitation in response to similar gradients (Vrugt and Sadegh, 2013; Sadegh et al., 2016). Fitting FDCs to a set of 430 catchments of the MOPEX dataset (Duan et al., 2006), Sadegh et al. (2016) found that the three-parameter Kosugi model they proposed offered the best quality of fit across a broad range of climate zones, under a goodness-of-fit criterion that weighs high and low flows equally. It is based on a lognormal distribution with three parameters (Kosugi, 1994, 1996) that are determined by calibration against the empirical FDC of a watershed. However, while it fits well across diverse climate zones, its applicability globally remains uncertain and needs to be evaluated to ensure it meets the requirements for use in other hydroclimatic conditions. This paper leverages the existence of high-performing parameterisations of the FDC across a range of climates to statistically generate plausible streamflow futures. We directly link parameter triplets of the Kosugi model with three streamflow statistics that are relevant to the management of water resources: central tendency, variability, and low-flow indicator. This one-on-one correspondence enables us to (1) sample hydro-climatic futures according to plausible ranges for streamflows statistics, and (2) convert these into ensembles of FDCs that represent the differentiated impacts of climate change across flow quantiles. The latter is consistent with studies of historically observed streamflow change (e.g. Pumo et al., 2016).

3.2 Methodology

This section demonstrates the technique that is the core of this paper, and introduces its workflow. First, Section A.1 will introduce the Kosugi model of the flow duration curve (FDC). Then Section 3.2.2 will give results on how to parameterise the FDC with the Kosugi model to reproduce desired streamflow statistics. These are the key results that enable us to build the methodological workflow to produce an ensemble of climate-perturbed flow duration curves, which we present in Section 3.2.3.

3.2.1 Kosugi model of the flow duration curve

The flow duration curve (FDC) is a cumulative frequency curve that ranks the observed record of n discharge values in descending order $\{q_1, q_2, \ldots, q_n\}$. The ranking of each value directly gives its empirical probability of exceedance u. In this work, we represent the FDC with the three-parameter Kosugi model, which has been shown to provide an excellent approximation to FDCs under a wide range of climates (Sadegh et al., 2016), and is given by:

$$q(u) = c + (a - c)\ z(u)^b, \text{ with } \ z(u) = \exp\left[\sqrt{2}\ \text{erfc}^{-1}\ (2\ u)\right] \tag{3.1}$$

where q is the streamflow value for a given value of the exceedance probability $u \in [0, 1]$, (a, b, c) are the three coefficients of the Kosugi model, and erfc is the complementary error function. Given a discharge record, the Kosugi model is fitted by minimising the root mean square srror (RMSE). Minimising the RMSE on $q(u)$ would lead to weigh errors in the high flows more than those on the low flows. For this reason, we minimise the RMSE in the exceedance probability space, i.e., the error on $\mathcal{U}$, the inverse of the $q(u)$ function defined in equation (A.1):

$$RMSE(x) = \left[\frac{1}{n}\ \sum_{i=1}^{n} [u_i - \mathcal{U}(q_i|a, b, c)]^2 \quad \right]^{0.5} \text{where} \quad \mathcal{U}(q|a, b, c) = \frac{1}{2}\ \text{erfc}\left[\frac{1}{\sqrt{2}\ b}\ \ln\left(\frac{q - c}{a - c}\right)\right] \tag{3.2}$$

To fit the Kosugi model and capture flow variability within the FDC, it is necessary to have daily discharge measurements over a sufficient period of time, e.g., more than 20 years.

3.2.2 Correspondence between common flow statistics and the Kosugi model

In this paragraph, we directly relate the three parameters of the Kosugi FDC model with sets of three streamflow statistics that are of interest to water resource management. This is key to relating a hydro-climatic future (described with different flow statistics) to a well-defined FDC. The central tendency, and the spread or the degree of variation are the two key aspects to describing a distribution (Weisberg, 1992; McCluskey and Lalkhen, 2007). Low flows are also of interests where water scarcity and availability are issues. With this we construct a triplet of streamflow statistics (M, V, L) where M is the central tendency (mean or median), V is variability (standard deviation or coefficient of variation), and L can be given by a low flow quantile (first or fifth percentile of flow distribution).

We can entirely define the flow distribution associated to a hydro-climatic future defined by (M, V, L), if we can find a relationship relating it to parameters (a, b, c) of the Kosugi model defined in equation (A.1):

$$(a, b, c) = \mathcal{F}\,(M, V, L) \tag{3.3}$$

This correspondence needs to be unique: if there is more than one (a, b, c) for a future defined by (M, V, L), a method based on the Kosugi model cannot define future flows unambiguously. In this paper we focus on two sets of (M, V, L). On the one hand, using M as the mean, V as the standard deviation and L as a low flow percentile corresponds to a very common statistical description of a flow distribution. We will refer to this as the "mean" case hereafter. On the other hand, there are cases where using the median, coefficient of variation and low flow quantile as (M, V, L) is of interest. This is the case e.g., in appraisals of run-of-river hydropower, see Section 3.3. We will refer to this as the "median" case hereafter.

Step by step derivation of these equations, along with proof of the uniqueness of a parameterisation, and conditions on the existence of solutions are provided in the Supplementary Information (SI) to this paper. In this section, we provide the main results for both the "mean" and "median" cases.

"Mean" case

In the "mean case", we know $(M, V, L) = (\mu, \sigma, q_{low})$ where where μ is the mean, σ is the standard deviation and q_{low} is the 1^{st} or 5^{th} percentile of flow. To parameterise the Kosugi equation in this case, one needs to first find b that is solution of:

$$\frac{\sigma}{\mu - q_{low}} = \frac{\sqrt{e^{b^2} - 1}}{1 - e^{-b^2/2}\varepsilon^b} \tag{3.4}$$

where ε is the value of $z(u)$ at q_{low}. For instance $\varepsilon = z(0.99) \approx 0.0976$ if q_{low} is the first percentile, and $\varepsilon = z(0.95) \approx 0.1930$ if q_{low} is the fifth percentile. There is at most one solution to this equation, and it exists if:

$$\frac{\sigma}{\mu - q_{low}} > \frac{-1}{\ln(\varepsilon)} \tag{3.5}$$

where $\varepsilon < 1$ so $\ln(\varepsilon) < 0$ and $-1/\ln(\varepsilon) \approx 0.43$ if q_{low} is the first percentile; 0.61 if q_{low} is the fifth percentile. Then one can deduce a and c using the following equations:

$$\begin{cases} a = \dfrac{q_{low}\ (1 - e^{-b^2/2}) + \mu\, e^{-b^2/2}(1 - \varepsilon^b)}{1 - e^{-b^2/2}\varepsilon^b} \\ c = \dfrac{q_{low} - \mu\ e^{-b^2/2}\ \varepsilon^b}{1 - e^{-b^2/2}\varepsilon^b} \end{cases} \tag{3.6}$$

"Median" case

In the "median" case, we know $(M, V, L) = (m, CV, q_{low})$, where m is the median, $CV = \mu/\sigma$ is the coefficient of variation, and q_{low} continues being a low flow percentile. One parameter of the Kosugi equation is easy to obtain:

$$a = m \tag{3.7}$$

To find the other parameters it is necessary to find the b that is the solution of:

$$CV = (1 - R)\frac{\sqrt{e^{b^2} - 1}}{1 - R + (R - \varepsilon^b)e^{-b^2/2}} \tag{3.8}$$

where $R = q_{low}/m$. b is unique, and exists provided a similar existence condition as in the "mean" case:

$$\frac{CV}{1 - R} > \frac{-1}{\ln(\varepsilon)} \tag{3.9}$$

Then the final parameter c is obtained through:

$$c = \frac{q_{low} - m\varepsilon^b}{1 - \varepsilon^b} \tag{3.10}$$

Domain of validity of existence conditions

In this paragraph, we explain what the conditions for the existence and uniqueness provided imply – see equations 3.5 and 3.9 for "mean" case and "median" case respectively. Both equations are equivalent to:

$$CV > \frac{-(1-R)}{\ln(\varepsilon)} \tag{3.11}$$

where $0 < R < 1$ is a ratio of the low flows by the mean or median; recall that $-1/\ln(\varepsilon) \approx 0.43$ if the low flow parameter is the first percentile, or 0.61 if it is the fifth percentile.

From equation 3.11, it is sufficient to have $CV > -1/\ln(\varepsilon)$ for both existence conditions to be verified. This condition has been verified for a large majority of the catchments over a large dataset of 6807 gages in the continental US (see Ye et al. (2021)). Yet for the existence condition to not be met the multiplier of $(1 - R)$ must also be close to 1. In other words, low flows must be extremely low relative to the mean (for the "mean" case) or median (for the "median" case), but this may be incompatible with a low value of CV. In fact, in Figure 10 from Ye et al. (2021), all time series with zero flow days in the sample have a CV value close or equal to 1. Together, these remarks suggest that the existence condition should be realised in most cases where flows are not strongly regulated. However, we would like to point out that whether the conditions of equations 3.5 or 3.9 are met for historical flows is of limited relevance. They need to be verified for each plausible future flow for which a FDC is generated. For this reason, we consider that checking these conditions across large databases of historical flows would be of limited interest within the scope of this work.

3.2.3 Producing an ensemble of climate-perturbed flow duration curves

Figure 3.1 illustrates our four-step methodology. In step (1), we fit the Kosugi FDC model to the available discharge record by finding the parameters (a_h, b_h, c_h) for the historical record, using equation (3.3) and the chosen historical flow statistics (M_h, V_h, L_h). We need to verify that this fit is close in performance to the best-fit model (a^*, b^*, c^*) obtained through RMSE minimisation as described by equation (3.2). It is essential to prove that the FDC model provides a good representation of historical observations, otherwise a perturbation of the model would be a poor representation of a perturbation of the historical flow regime. We then check the method by deriving the FDC parameters based on three key statistics of

historical flow. The method can be used if both curves adequately fit the functional shape of the empirical FDC.

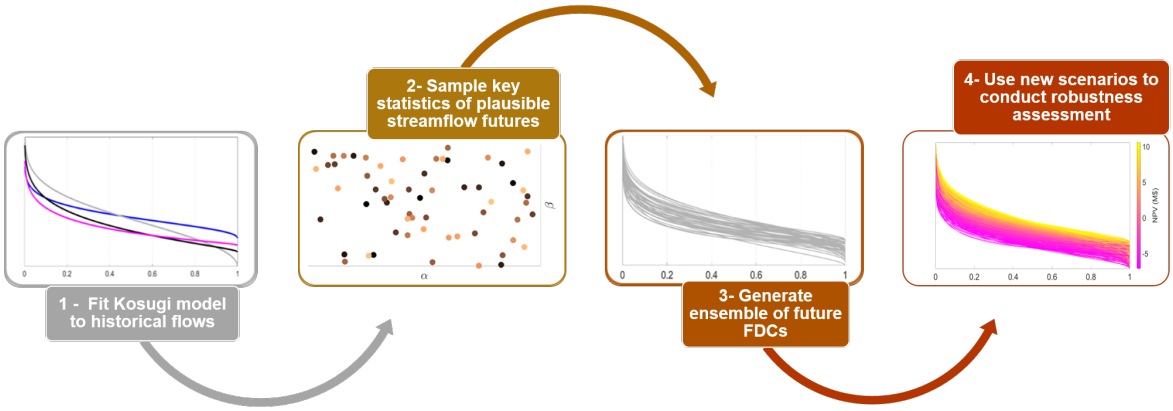

Figure 3.1: *Flowchart of the approach; (1) Kosugi model parameters are calibrated with a historical FDC, (2) a set of scenarios with modified flow statistics are determined, (3) a new set of Kosugi model coefficients are derived for each future scenario, and future scenarios are created by using these coefficients, (4) future scenarios can be used in robustness assessments.*

To generate future flows, one needs to sample a set of futures in step (2). This corresponds to sampling the chosen parameters (M, V, L) to construct an ensemble $\{(M_i, V_i, L_i)_{1 \leq i \leq N}\}$ of N alternative futures, reflecting a broad range of plausible future conditions. Then in step (3), we find the unique set of parameters (a_i, b_i, c_i) for each triplet (M_i, V_i, L_i) and construct the corresponding FDC. Finally in step (4), we use the resulting ensemble of FDCs to support robustness assessments in a changing climate, by evaluating the performance of a decision adaptation(s) across future scenarios.

Note that the first three steps of this workflow can be replicated for any site using the Zenodo repository (Yildiz et al., 2023b) that accompanies this paper. The fourth step depends on the specificities of each robustness assessment, e.g., what infrastructure is considered, what performance measures, etc.

3.3 Case study

This section demonstrates the fitness of our method for robustness assessments.

3.3.1 Site description

The case study involves the climate change impact analysis of a proposed RoR hydropower plant at the Besik site on the Mukus River in Van province located in the Eastern Anatolia region of Turkey (Lat: 38.15°N; Lon: 42.80°E). Summers are dry and hot with temperatures above 30 °C. Spring and autumn are generally mild, but during both seasons sudden hot and cold spells frequently occur. 27 years of daily discharge observation are available. The discharge fluctuates considerably between values of 2 and 38 m^3/s, with median flow of 4.79 m^3/s, first percentile flow of 2.23 m^3/s and coefficient of variation of 0.60. The design of the run-of-river hydropower project was optimised using the HYPER toolbox (Yildiz and Vrugt, 2019). The resulting design has an installed capacity of 8.73 MW, a penstock length of 208 m with a diameter of 1.60 m, and two side-by-side Francis turbines whose design discharge are 4.80 and 2.87 m^3/s respectively.

3.3.2 Generation of climate-perturbed flow duration curves

Contrary to reservoir-based hydropower plants, RoR schemes have virtually no storage, so they are vulnerable to changes in flow as they cannot modulate flows and only operate in a predefined range. Extreme low flows are insufficient to activate the turbines, and equally, flows above the design discharge do not produce additional energy. Because of this focus on the mid-range flows, the median is a more important indicator of performance than the mean flow, which can be skewed by high discharges. For this reason, this application will relate median, coefficient of variation and first percentile flows to Kosugi parameters (the "median" case).

In step (1) of our approach, we fit the three-parameter Kosugi model to the daily discharge data. Figure 3.2 shows the historical records (red circles), the fitted Kosugi Model (black line) and the derived FDC based on the three statistical parameters of historical records (FDC from (M_h, V_h, L_h)). Both fitted curves offer close fits across the entire spectrum of flow

conditions described by the FDC of historical records. In particular, the quality of the fit for middle and low flows shows the consistency of the proposed approach, as their estimation is vital in assessing and managing water resources such as hydropower plants.

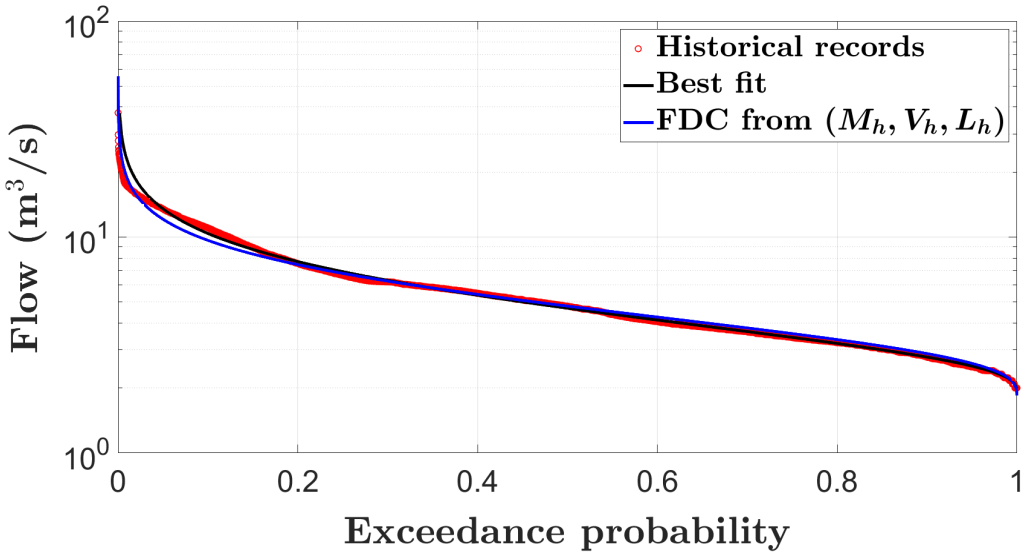

Figure 3.2: *Plot of the daily flow duration curves (FDC) used in the case study (red circles). Black line represents the fitted Kosugi model and the blue line is the FDC deduced from (M_h, V_h, L_h): historical median, CV and first percentile.*

In step (2), we determine plausible ranges for the three statistical parameters over the operational life of the proposed plant. In Turkey, hydropower projects are licensed to generate electricity for a period of 49 years. Projections from three global climate models—HadGEM2-ES, MPI-ESM-MR, and CNRM-5.1—selected from the CMIP5 database under the RCP 4.5 and RCP 8.5 scenarios were incorporated into hydrological models such as SWAT and WEAP to assess the potential impacts of climate change. These projections indicate a potential decrease in mean discharge values by up to 60 % for the period from 2041 to 2070 (SYGM, 2016). An increasing intensity of drought conditions is expected for the period of 2040 - 2071 in the region of the presented case study (Demircan et al., 2017; Turkes et al., 2020; Yildiz et al., 2022). In parallel, precipitation variability is widely forecast to increase (GCMs; Pendergrass et al., 2017), with the coefficient of variation of precipitation projected to almost double by 2060 in various neighboring regions such as the Mediterranean (Giorgi and Lionello, 2008) or Iran (Zarrin and Dadashi-Roudbari, 2021). To reflect these various results while

Table 3.1: Sampling ranges for multipliers of statistical parameters, where 1 corresponds to the values for the historical time series.

Sampling Parameter	**Lower Bound Multiplier**	**Upper Bound Multiplier**
Median, m	0.3	1
Coefficient of Variation, CV	1	2
1st percentile, q_{low}	0.3	1

reflecting the uncertainties that surround them, we chose wide ranges for the scaling factors of our three parameters. These sampling ranges are summarised in Table 3.1 and reflect the concurrent tendencies for severe drying and an increase in variability. Recall these ranges represent plausible rather than probable values. We then sampled $N = 500$ alternative future streamflow conditions using Latin hypercube sampling.

Next, in step (3), we primarily check if the samples satisfy the condition for existence; the smallest and largest measured value of $\frac{CV}{1-R}$ across the sample are 0.75 and 5.15 respectively. All values are significantly larger than the existence condition for the parameterisation ($-1/\ln(\varepsilon) \approx 0.43$, see equation 3.9). Therefore we can derive the distribution parameters of Kosugi model by using equations (3.7) to (3.10) for each sampled future. Thereafter, we generate future scenarios by using these distribution parameters. Figure 3.3 showcases the versatility of our method and compares to the lack of flexibility provided by a uniform multiplier across the FDC of historical flows. For instance, a uniform 20 % reduction across the flow distribution (dotted black lines) provides a single possible future. For comparison, there are 12 scenarios from our ensemble generated with mean flow reductions ranging from 19 % to 21 % (orange lines), and they display a wide range of low and median flow behaviours, generally lower than the dotted black line, combined with higher high flows. Clearly, our method can provide a suitable range of hydroclimatic conditions, with increased frequency of high flows and low flows. This aligns with the anticipated impacts of climate change in the region, which include more arid conditions and a rising trend of extreme hydrological events. This versatility can be compared to the lack of flexibility offered by a uniform multiplier across the FDC of historical flows, also shown on Figure 3.3 with the examples of ±20% across the flow distribution (dotted red and black lines).

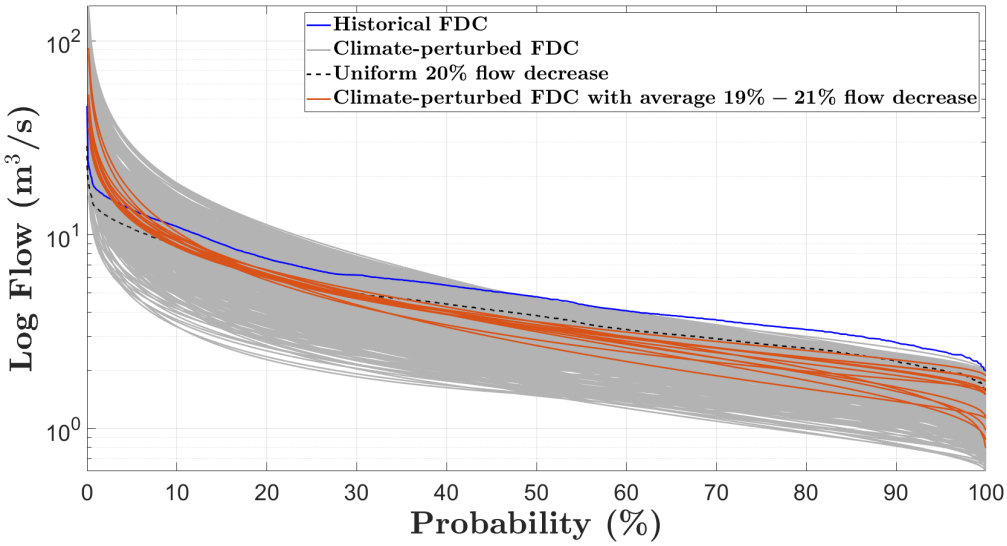

Figure 3.3: *Plot of the flow duration curves (FDCs) of the historical record (blue line) and sampled flow duration curves (grey lines) constructed by deriving the FDC parameters for the Kosugi Model shown in Table 3.1. The figure also compares 20 % mean flow reductions, obtained either with the delta change method (uniform multiplier, dashed black line) and the 12 future scenarios we generated with mean flow reductions between 19 and 21 % (orange lines).*

3.3.3 Application to infrastructure robustness

Finally, in step (4), we evaluate the performance of a design under generated future flows. We input each ensemble member into state-of-the-art software to compute technical performance, energy production and economic profit of a design at a given site characteristics (HYPER; Yildiz and Vrugt, 2019). This enables us to quantify the Net Present Value (NPV) of the optimal design of the run-of-river hydropower project under a range of changing climate conditions. The inputs of the HYPER model are daily discharge records, ecological flow requirements, and project-based parameters such as gross head, penstock length, interest rate, energy price, project life time and site factor for civil works, maintenance and operation cost factor, fixed costs such as transmission line, expropriation costs. Recall that the NPV is the value of projected cash flows, discounted to the present. We assess that the investment is robust to a future climate if NPV is greater than zero. Future FDCs with their respective

robustness measure are presented in Figure 3.4. The Figure shows that although the NPV of current design based on historical records (blue line) is around 10 M$, it decreases dramatically and even becomes negative (gray lines) under dry futures characterised in particular by a median m under 2.3 m^3/s; or a m under 2.6 m^3/s accompanied by q_{low} under 1.10 m^3/s and CV below 0.8. The project is unfeasible under such conditions.

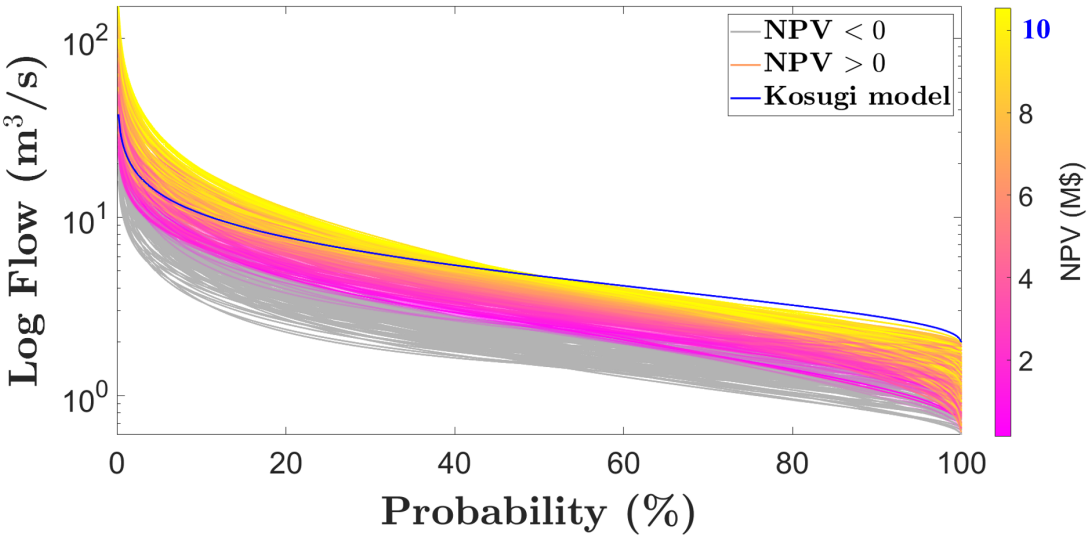

Figure 3.4: *Plot of generated flow duration curves (FDCs), with each solution colored by its Net Present Value (NPV). Gray colored lines signifies SOWs in which NPV is negative. NPV of the optimal design based on observed discharge (blue line) is 10 M$*

3.4 Discussion and conclusion

In this technical note, we present an effective, practical and novel approach based on a near-universal parameterisation of flow duration curves (FDCs), and perturbation of these parameters to simulate a range of futures in a way that is hydrologically consistent across the spectrum of hydrological conditions. Our application to a run-of-river hydropower project in Eastern Turkey showcases the ability of our method to provide a large range of climate-modified catchment responses, including increased frequency of both high flows and low flows to mimic the future projections for the area (i.e. more arid conditions with increased trend

of extreme hydrological events). It compares favorably with existing statistical methods to perturb flows such as the delta change approach. This then supports robustness analyses for rivers for which no detailed hydrological model is available: applied here to assess the financial viability of run-of-river hydropower design in a changing climate. The ease of application of the method illustrates its wide applicability in support of robustness assessments of infrastructure for which streamflow variability impacts performance. We now conclude with some remarks on how this novel approach could be extended to further support such assessments.

Even though the three-parameter Kosugi model has been shown to fit FDCs well across a wide range of catchment characteristics (Sadegh et al., 2016), this does not a guarantee that it would be a good fit in all cases. Sadegh et al. (2016) proposed other functional forms such as the 2-parameter Kosugi model, and 2-parameter and 3-parameter van Genuchten models for the FDC. Despite the superior fit of the 3-parameter Kosugi model across a range of climate zones, these models could also be perturbed to generate future flows. Moreover, future studies can validate generated scenarios using climatic projections from rainfall-runoff models across diverse locations with varying hydrologic properties.

Our method focuses on catchments free of major flow regulation (reservoir, effluent discharge). Yet, those catchments do not have to be pristine, and can for example experience significant human interference in land use change. Indeed, the MOPEX dataset (Duan et al., 2006), which was used to assess the quality of the three parameter Kosugi model (Sadegh et al., 2016), has been found to be affected by significant human interference (Wang and Hejazi, 2011).

We also identified two current limitations to this method that we believe can be addressed by future developments. First, recent studies reveal that there is an increasing trend of the number of zero-flow days in many regions such as the Mediterranean (e.g., Tramblay et al., 2021). Yet, the number of zero-flow days remains constant in this approach. Preliminary results show that our proposed method supports time series with a large number of zero-flow days, by keeping the number of no-flow days constant and perturbing the FDC when flows are positive. Admittedly, this approximation ignores the fact that a change in climate regime could affect the number of no-flow days. Future work needs to examine the possibility of using

the proportion of no-flow days as the low-flow indicator L, instead of a low flow quantile. Derivations for the existence and unicity of a parameterisation should then also be extended to that case.

Our approach only considers the FDC, and says nothing of the seasonality, frequency and duration of dry and wet spells. The shifting seasonality of flows in a changing climate can easily be captured by combining our approach with methods such as the log-space rescaling of stationary flows (Quinn et al., 2018) or the reconstruction annual flow hydrographs (Nazemi et al., 2013). Beyond changes in seasonality, there is mounting evidence that climate change is bound to cause hydrological intensification, i.e., it will make dry periods longer and more severe and wet periods more intense (Ficklin et al., 2022). Information on hydrological intensification scenarios comes from outputs from large-scale climate models, and integrating that information requires turning the climate information into streamflow. One way to do it without the help of a rainfall-runoff model is to control the parameters of a daily streamflow model with a monthly climate model (Stagge and Moglen, 2013). The generation of a FDC for every climate the daily streamflow model simulates could then be used to improve results, e.g., by providing a quantile-by-quantile adjustment of the synthetic streamflow generator outputs. A similar procedure could combine hydrological model simulations with statistical generation of FDCs. The latter could correct outputs from the former, if they were obtained with a calibration that reflects historical conditions.

Code data availability

The climate-perturbed FDC generation model has been developed in Python 3.10.4. and is provided with an environment file. It is accessible from the Zenodo open-access repository at https://doi.org/10.5281/zenodo.7662679, with a link to the GitHub source codes of the latest release, including a detailed “run guide” and input files to statistically generate plausible streamflow futures.

CHAPTER 4

Revisiting small hydropower design in an uncertain world

Abstract[1]

When less water is available, hydropower turbines are less efficient, or have to stop altogether. This reality is often neglected in recent work on the planning and operations of hydropower systems, despite widespread expected increases in drought intensity, frequency and duration. This paper is the first to integrate variable-efficiency turbines into a hydropower plant design framework that accounts for design optimization as well as deep uncertainty in climatic and socio-economic variables. Specifically, this framework focuses on leveraging multi-objective robust decision making for the financially robust design of run-of-river hydropower plants, whose output is highly sensitive to flow variability. Application to five plants in Turkey challenges two key design assumptions, use of NPV as a design objective and use of identical turbines. Instead, maximising the BC yields plants with better financial viability over a range of plausible futures. They tend to have smaller capacity, and feature a small turbine that is well-adapted to low-flow periods. Another key insight is that socio-economic uncertainties have as much or even more impact on robustness than climate conditions. In fact, these uncertainties have the potential to make many small hydropower projects too risky to build. Our findings are of considerable practical relevance at a time where 140 GW of unexploited small hydropower potential could help power the energy transition. They also highlight the

[1] Yildiz, V. and Brown, S. and Rougé, C., 2024. Importance of Variable Turbine Efficiency in Run-Of-River Hydropower Design Under Deep Uncertainty, Water Resources Research

need for similar research in reservoir-based plants, considering over 3,000 such plants planned or in construction worldwide.

4.1 Introduction

Droughts are among the most damaging natural disasters globally, with dramatic impacts on ecosystems, agriculture, water supply, and socioeconomic systems (Dai, 2011; Field et al., 2012). Observations from the Global Precipitation Climatology Center (GPCC) have revealed positive trends in the frequency, length, and intensity of meteorological droughts in many regions including Mediterranean, Central Africa, Amazonia, North-Eastern China, and Southern Australia between 1951 and 2010 (Spinoni et al., 2014). In addition, numerous scientific studies and reports show that due to global heating, droughts are expected to be more frequent, severe, and long-lasting in the future than in prior decades globally (Field et al., 2012; Spinoni et al., 2018; Ault, 2020; Sreeparvathy and Srinivas, 2022; Fang et al., 2022). This is part of a phenomenon called hydrological intensification, whereby global heating is expected to translate into increased variability globally at a range of timescales, and posing serious challenges to water management (Ficklin et al., 2022).

Hydropower generation is closely linked to hydrological conditions in a watershed, and it is sensitive to both seasonal water availability variations (Schaeffer et al., 2012; Teotónio et al., 2017) and to droughts (Van Vliet et al., 2016). This is why climate change, and its widespread projected increases in dry conditions frequency and magnitude, is expected to influence the availability and stability of hydropower generation (Wasti et al., 2022). This challenges the transition to low-carbon energy generation that is necessary to avert climate catastrophe, because hydropower is a mature and reliable technology whose operation produces a renewable and largely emission-free source of energy (Paish, 2002; Hertwich et al., 2016), and it is currently responsible for around 15% of global electricity generation (IEA, 2022). We are in the middle of a hydropower construction boom (Zarfl et al., 2015) with thousands of TWh/year of untapped potential (Gernaat et al., 2017), it is expected to keep playing a role in the global electricity supply in decades to come (Winemiller et al., 2016; Pokhrel et al., 2018; Moran et al., 2018). Hydropower plants are also ideal as a flexible complement to more variable and intermittent power sources such as solar or wind (Wang et al.,

2019), so increased drought impacts could pose challenges to grid stability in many regions (Jurasz et al., 2018), further hindering the energy transition.

Longer drought periods and hydrological intensification are not only expected to affect the amount of water available to hydropower, but also the efficiency at which water flows can be converted into kinetic energy by turbines. Indeed, hydropower turbines are designed based on specific head and discharge characteristics, leading deviations from these conditions to reduce plants' overall operational efficiency (Diaz et al., 2010). In some cases, efficiency can decrease to a point where turbines can no longer work. For instance, the threat of hydropower failure looms large in the Colorado River basin as large reservoirs get depleted (Wang and Rosenberg, 2023). In spite of these high-profile cases underlining the urgency of accounting for variable turbine efficiency when designing hydropower plants in a changing climate, there is a gap in research and engineering know-how on this topic. Variable turbine efficiencies are routinely accounted for in studies aiming to increase overall operational performance of an existing plant while meeting several technical, physical, and strategic constraints (Siu et al., 2001; Li et al., 2013; Taktak and D'Ambrosio, 2017; Séguin et al., 2017; Cheng et al., 2021). Yet, time-invariant turbine efficiencies remain the norm during the plannning phase, including in recent research evaluating the ability of planned hydropower infrastructure to withstand various climatic and socio-economic stressors (e.g., Taner et al., 2017; Ray et al., 2018; Bertoni et al., 2019; Hurford et al., 2020; Bertoni et al., 2021). This ability to withstand deviations from design conditions is called robustness (Herman et al., 2015), and it is an important element of future-proof planning. Several analytical frameworks have been proposed to evaluate and foster robustness in water systems (Lempert, 2002; Bryant and Lempert, 2010; Brown et al., 2012; Haasnoot et al., 2013; Kasprzyk et al., 2013). They are meant to resolve design and operational problems in conditions where uncertainty is so pervasive that it becomes challenging to form a consensus on how to even represent and tackle it (Kwakkel et al., 2016), a situation known as deep uncertainty.

This paper is the first study to address this gap by proposing an approach to integrate variable-efficiency turbine design into a decision making under deep uncertainty (DMDU) framework that both optimizes hydropower plant design and tests its financial viability under a range of climatic and socio-economic conditions. It focuses on run-of-river (RoR)

hydropower plants where turbine system costs are about half of a plant's construction costs (Mamo et al., 2018; IEA, 2021). This cost distribution makes RoR plants an ideal entry point to exploring the interactions between climate change and detailed plant and turbine design. Our approach relies on, and further develops, a state-of-the-art toolbox for run-of-river hydropower design (Yildiz and Vrugt, 2019). It integrates HYPER into a multi-objective robust decision making framework (MORDM; Kasprzyk et al., 2013) to define and evaluate a plant design's financial robustness. The rest of this section provides a detailed overview to small hydropower, including the shortcomings of current planning practices.

Small hydropower plants (SHPs) are generally defined as having an installed capacity of less than 10 MW (Manzano-Agugliaro et al., 2017; UNIDO, 2022), corresponding to an annual production potential under 87.6GWh. They are a comparably environmentally friendly and less costly alternative to conventional dam-based plants (Tsuanyo et al., 2023). Only 36 % of the global potential of small hydropower ($\leq$ 10 MW) is currently exploited, leaving a substantial untapped capacity of 140 GW, (UNIDO, 2022). As a result, a considerable growth of SHP is expected worldwide (Couto and Olden, 2018), including in industrial countries where the best sites for large-scale hydropower are already taken. This is the case for instance in Europe as more public subsidies become available for retrofitting or developing these plants (Kuriqi et al., 2020; Kishore et al., 2021). SHPs provide the option of decentralized power production and sustainable industrial expansion (Hennig and Harlan, 2018) in many areas, including locations that were considered marginal for hydropower production until recently (Kosnik, 2010; Hoes et al., 2017). Yet, integrating SHPs to the grid in remote or rural locations may necessitate significant investment in transmission infrastructure, thereby reducing their financial viability. Therefore, addressing grid connection concerns is critical for increasing their attractiveness and assuring their viability in cooperative financial structures. This study focuses on run-of-river plants (RoR), the most common type of small hydropower plants (Yildiz and Vrugt, 2019). They are characterised by a negligible (sub-daily) storage capacity and by generation almost completely dependent on the quantity and variability of river flows. RoRs accounts for more than 75% of the 3,000 sites (installed capacity over 1MW) concerned by the current hydropower boom at total (Zarfl et al., 2015; Bejarano et al., 2019). These plants have an important role to play in achieving the seventh SDG goal (Dorber

et al., 2020), of ensuring access to affordable, reliable, sustainable, and modern energy for all (McCollum et al., 2017), and in contributing to the achievement of other SDG goals (Gielen et al., 2019).

Yet, ultimately, decisions of whether to build a RoR hydropower plant often depends on its forecast financial viability, calculated with metrics that combine capital costs, operation and maintenance costs, and other relevant measurements (Klein and Fox, 2022). The most common metric to assess is the NPV, the cumulative sum of all discounted lifecycle cash inflows generated by the power plant (e.g., Hosseini et al., 2005; Bøckman et al., 2008; Santolin et al., 2011; Yildiz and Vrugt, 2019). A project is considered feasible with a positive NPV, and a higher NPV signifies a more favorable outlook. Yet, with its focus on expected profit, NPV is best complemented by metrics that can quantify project risk, such as the the internal rate of return (IRR; Kaldellis et al., 2005; Basso and Botter, 2012) , the BC (e.g., Anagnostopoulos and Papantonis, 2007; Forouzbakhsh et al., 2007; Nedaei and Walsh, 2022) and the levelized cost of electricity (LCOE; Zhang et al., 2012; Ceran et al., 2020). Whereas maximizing the NPV leads to a design that offers the highest return, optimizing based on a risk-based metric would result in design with lower risk and investment costs. Despite recognition that there is a trade-off between financial viability metrics for RoR plant design (Basso and Botter, 2012), there remains opportunities for systematic approaches to exploring these possible trade-offs, especially in the context of climate change. In the rest of this work, we choose BC as a metric because of its preponderance in the RoR literature (USBR, 2011; Klein and Fox, 2022). BC is the ratio of discounted lifecycle benefits to the discounted lifecycle costs; maximizing it often results in alternatives that keep costs and risks low (e.g., Anagnostopoulos and Papantonis, 2007; Forouzbakhsh et al., 2007; Nedaei and Walsh, 2022). A value greater than 1 is needed for a project to be deemed feasible, with a higher BC indicating a more favorable scenario, and a lower risk of insolvency. Despite literature cautioning that BC can be easily manipulated in multi-objective cases, where the conversion of a non-monetary objective (e.g., reliability or vulnerability) into a benefit or cost will arbitrarily impact the benefit cost ratio (Lund, 1992), these concerns are not relevant in the majority of RoR plant feasibility studies, as other water uses are treated as constraints that the design will need to meet, rather than given a monetary value.

Research in turbine system design for RoR power plants has received attention recently – recall that the turbine system's cost is on average around 50 % of the investment cost of a RoR power plants (IRENA, 2012; Mamo et al., 2018; IEA, 2021). This research is much needed in an area where determining a plant's installed capacity and optimizing turbine system design are still often considered as separate steps performed in this order (DSI, 2012). Yet, turbine system design still rarely considers variable turbine efficiency during plant design optimization (e.g., Voros et al., 2000; Kaldellis et al., 2005; Lazzaro and Botter, 2015). This is despite the fact the operational efficiency of the turbine(s) is crucial to linking flow variability with actual hydropower production (Okot, 2013), and therefore to determining the turbine system best suited for a particular site and river flow characteristics (Yildiz and Vrugt, 2019). Design studies also generally assume that the number of turbines considered is limited to two despite evidence that the use of more than one turbine improves considerably the ability of a RoR plant to respond effectively to seasonal discharge variations (Anagnostopoulos and Papantonis, 2007; Yildiz and Vrugt, 2019). Besides, when the design consists of two turbines or more, they are often assumed to be identical (Kaldellis et al., 2005; Mamo et al., 2018; Amougou et al., 2022),at the expense of added operational flexibility. The HYPER toolbox (Yildiz and Vrugt, 2019) partially addresses these limitations, as it considers variable turbine efficiency and enables to design two-turbine systems with non-identical turbines of a user-specified type – Kaplan, Pelton or Francis. Yet, our understanding on how various climatic but also socio-economic uncertainties – such as interest rates, project cost overruns or energy prices – affect turbine design remains limited, warranting a revisiting to the design of these systems.

The remainder of this study is organized as follows. Section 4.2 introduces the five case-study sites located in a range of hydro-climatic regions of Turkey. In Section 4.3, we discuss traditional RoR hydropower design, cost and benefit analysis. This is followed in Section 4.4, where we explain the fundamentals of the methodology, including alternatives generation, sampling plausible futures, quantification of robustness and vulnerability analysis. In Section 4.5 we demonstrate the analysis of the proposed approach with illustrative case studies. The penultimate section of this paper (Section 4.6) discusses how to have the wider implications of our results and opportunities for future research. Finally, Section 4.7 concludes this paper

with a summary of our main findings.

4.2 Study sites

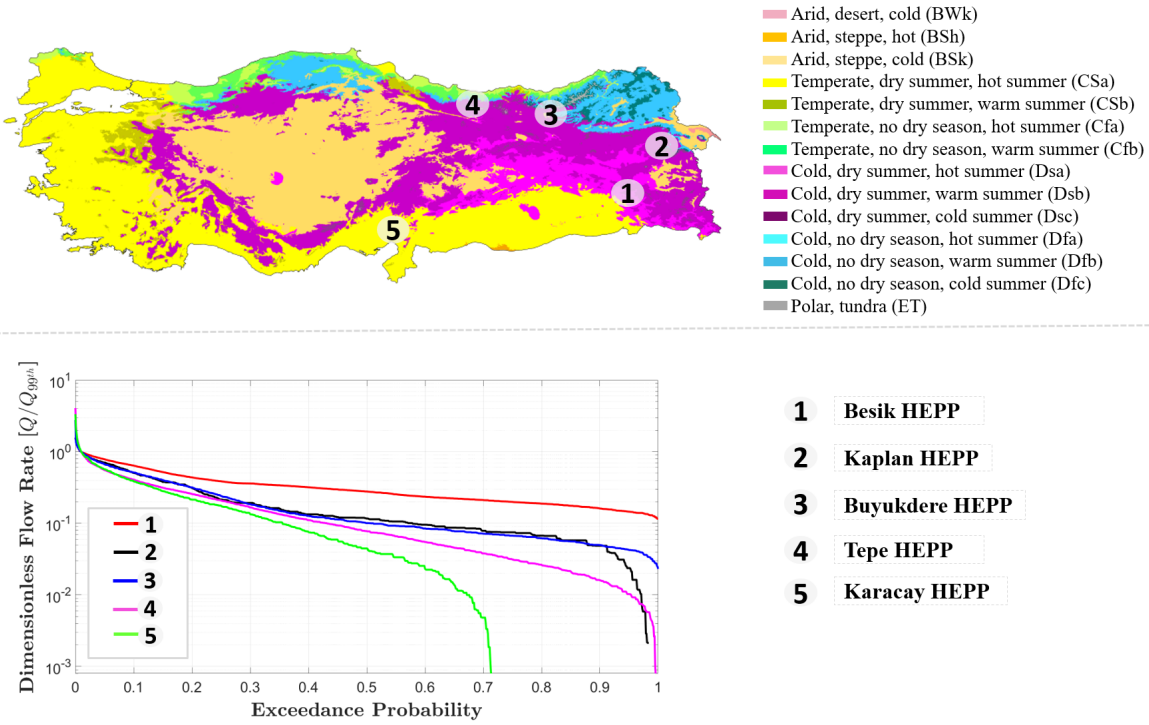

Figure 4.1: *Top panel: Location of the presented five case studies on Köppen-Geiger climate classification map of Turkey (Beck et al., 2018). Bottom Panel: Presenting Flow Duration Curves (FDC) for five case studies, where normalization is applied based on the* 99^{th} *percentile of the flow. The FDC depicts graphically the relationship between the magnitude of the discharge (on y-axis) and its exceedance probability (on x-axis). The flow rate depicted on the y-axis is presented using a logarithmic scale.*

The framework developed in this paper will be applied to five proposed RoR hydropower plants in Turkey. The map displayed in the top panel of Figure 4.1 shows they are set in a range of hydro-climatic regions, according to the Köppen-Geiger climate classification derived from an ensemble of four high-resolution climatic maps for the period of 1980–2016 (Beck

et al., 2018). This is confirmed by the fact that they exhibit markedly different daily flow duration curves (FDCs; bottom panel of Figure 4.1). Besik and Kaplan hydroelectric power plants (HEPPs) have a mediterranean-influenced humid continental climate with snowy winters and warm, dry summers. Buyukdere HEPP has a humid continental climate with very cold, snowy winters and warm, dry summers. Tepe HEPP has a humid subtropical climate with warm and humid summers and wet winters. Karacay HEPP is under Mediterranean climate with wet winters and very hot, humid summers. Most precipitation forms as snow during winters for Besik, Kaplan and Buyukdere hydro sites. Snowpack at these sites act as a natural reservoir, providing water throughout the drier summer months which results in less variability in low-flow ranges when compared to the other two sites. These catchments' ability to store precipitation characteristically translates into a gentle slope in the middle part of the FDC (Yilmaz et al., 2008), contrary to the Tepe and Karacay sites whose slopes are steeper. What is more, precipitation is rare with short duration in Karacay site, which leads to zero-flow days (green line in bottom panel of Figure 4.1).

Table 4.1 summarises the site and streamflow characteristics of the five different case-studies. Section 4.7 provides information on the source of the data used in this study which is obtained from the feasibility reports of DSI. All the sites have sufficient amount of streamflow record with a minimum of 19 years daily discharge data for Tepe HEPP. Drainage areas at all sites are close to each other except Tepe site whose area 405 km^2. The coefficient of variation (CV) is the ratio of the mean by the standard deviation of the daily streamflow time series, and differences reflect the different hydro-climatic regimes in the diverse catchments. As showcased in the bottom panel of the Figure 4.1, where FDC is presented for five case studies with normalization based on the 99^{th} percentile of the flow, variations in precipitation patterns and drainage areas are driving distinct hydrological characteristics. This distinction is also evident in Table 4.1,indicating a range of 1 to 6 in mean flows and and reveals a threefold difference between the highest and smallest values of CV across the sites. The table also shows the portion of river discharge allocated to minimum environmental flow by state authorities. This quantity should be transported by the river network at all times to sustain ecosystem health, and does not go through the turbines. Finally, the table shows the gross hydraulic head available at each site, and the gross potential annual

average energy (GAAE) of each site, computed by taking into consideration the available gross head or water pressure, and average long-term discharge. Note that this calculation neglects hydraulic losses, impacts of flow variability on turbine efficiency, and the fact that flows exceeding design plant discharged do not produce hydropower. The different features of these sites will lead to unique hydropower plant designs to best harness available energy. For instance, Besik, Tepe and Buyukdere HEPPs exhibit higher potential compared to other sites, with Besik and Buyukdere having similar hydropower potential. This variation is attributed to significant differences in streamflow and site characteristics, which necessitate distinct hydropower design. Likewise, Karacay and Kaplan HEPPs are located completely different climate zones, yet they have similar hydropower potential despite very distinct site and streamflow characteristics.

Table 4.1: Hydrological and site characteristics of the RoR hydropower plant case studies. The data source for this table is provided in Section 4.7.

Case Study	Length [Daily]	Drainage Area [km^2]	Mean [m^3/s]	Coefficient of Variation [-]	Environmental flow [m^3/s]	Gross Head [m]	Potential GAAE [GWh]
Besik	27 years	75.1	5.8	0.59	0.63	117	58.31
Buyukdere	36 years	78.7	1.88	1.09	0.156	394	63.65
Tepe	19 years	405	6.22	1.39	0.662	56	29.93
Karacay	34 years	106.2	1.47	1.69	0.18	134	16.92
Kaplan	24 years	100	1.07	1.08	0.12	190	17.47

4.3 Run-of-river plant design

First, Section 4.3.1 explains the key features and assumptions in traditional engineering design of RoR plants. Following this, Section 4.3.2 details benefit and cost calculations that are key in evaluating project feasibility. It is essential to emphasize that the financial assessment of Run-of-River projects in this study is conducted at the project level, rather than at the grid level. Lastly, Section 4.3.3 cover the HYPER model, and in particular the novelties introduced from the original toolbox (Yildiz and Vrugt, 2019).

4.3.1 Traditional engineering design

In traditional hydropower plant design, the determination of the design discharge capacity, which is key to determining the installed capacity, is typically addressed separately from the design of the turbine system. The initial step involves determining the design discharge capacity, which is governed by site hydrology and financial constraints. Assuming a long enough record of daily discharge measurements is available, flow duration curves are commonly used to determine this design discharge capacity when over a sufficient period of time are available to construct the curve (Kao, 2013). Figure 4.2 demonstrates FDC with operating flow boundaries of a typical RoR hydropower plant. The flow rate that is exceeded for 30 % of the time (Q_{30}, dashed blue line in Figure 4.2) is an USBR standard for estimating the optimal installed capacity of hydropower plants (USBR, 2011).

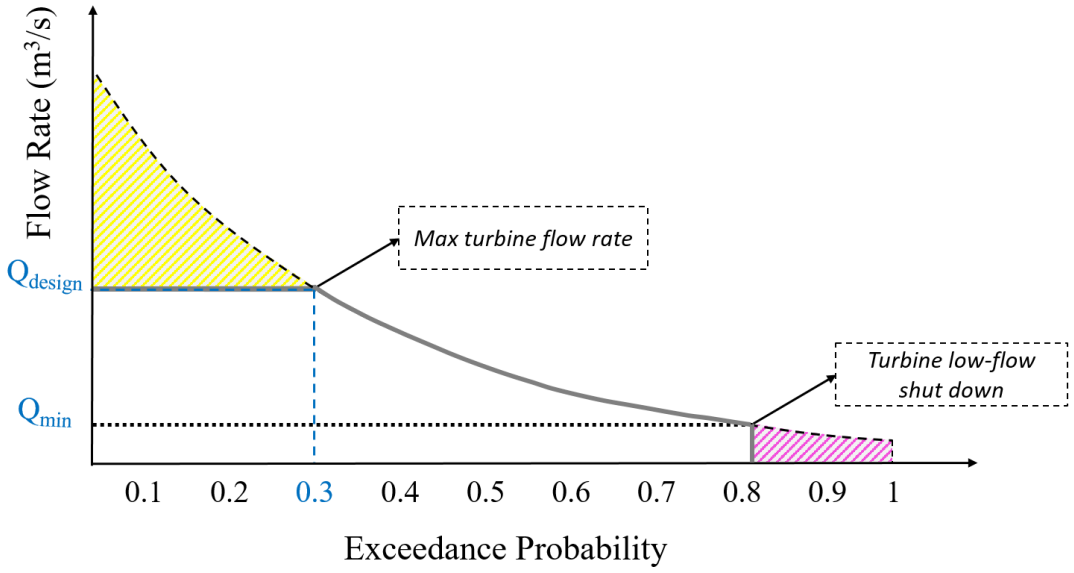

Figure 4.2: *Flow duration curve of the streamflows (dashed black line) and of the flows workable by a RoR hydropower plant (solid gray line). The top yellow dashed area represents the excessive flow that cannot be harnessed by the turbines, while the bottom magenta dashed area represents the flow the plant does not operate due turbine technical constraints and/or ecological flows*

Subsequently, the appropriate type and number turbines are determined based on the chosen design flow and net water head of hydro site. The selection chart shown in left panel of Figure 4.3 shows three major types of turbines and their manufacturer-recommended ranges for of head and flow (Penche, 1998).

Note that available zones overlap, which means that in some cases there is more than one turbine type that is well-suited to the site. The graph is meant to highlight that turbines have technical flow constraints and can only operate effectively within certain flow ranges. The efficiency curve shown for all three turbine types on the right panel of Figure 4.3 and adapted from Sinagra et al. (2014) further illuminates why different turbine types are best for different sites. The curve introduced illustrates the correlation between the ratio of flow rate to design flow (q/O_{d}) and efficiency (η). Francis and Pelton turbines are designed for operating with (much) larger heads than Kaplan turbines. Although Francis turbines are highly efficient, they can only operate efficiently over a limited flow range, whereas Pelton turbines maintain a high efficiency even running below design. On the other hand, thanks to its high efficiency at low flows, the Kaplan turbine can be an appropriate alternative to the Francis turbine. The final choice of which turbine(s) to select for a RoR plant warrants a detailed cost benefit analysis along with turbine technical constraints. In most cases, hydropower plants have identical units in the case of more than two turbines installation to make maintenance easier and slightly cheaper (DSI, 2012).

These factors collectively define the operational boundaries of a hydropower plant. For instance, the yellow and magenta shaded areas in Figure 4.2 represent unexploited hydropower potential due to design limitations and environmental constraints. The Figure highlights that only a portion of the flow can be harnessed as hydropower. Typically, these plants have an average annual capacity factor that falls within the range of 30 to 60 % (IEA, 2021). Therefore, the expected yearly energy generation of a typical RoR hydropower plant is generally below 60 % of its gross potential (GAAE in Table 4.1 when design capacity is around Q_{30} and capacity factor less than % 60). Factoring in that turbines work have a flow-dependent efficiency, the lack of integration of design discharge determination and turbine system design, coupled with the use of identical turbines, can lead to designs that are inefficient in practice. This can ultimately affect a project's financial feasibility.

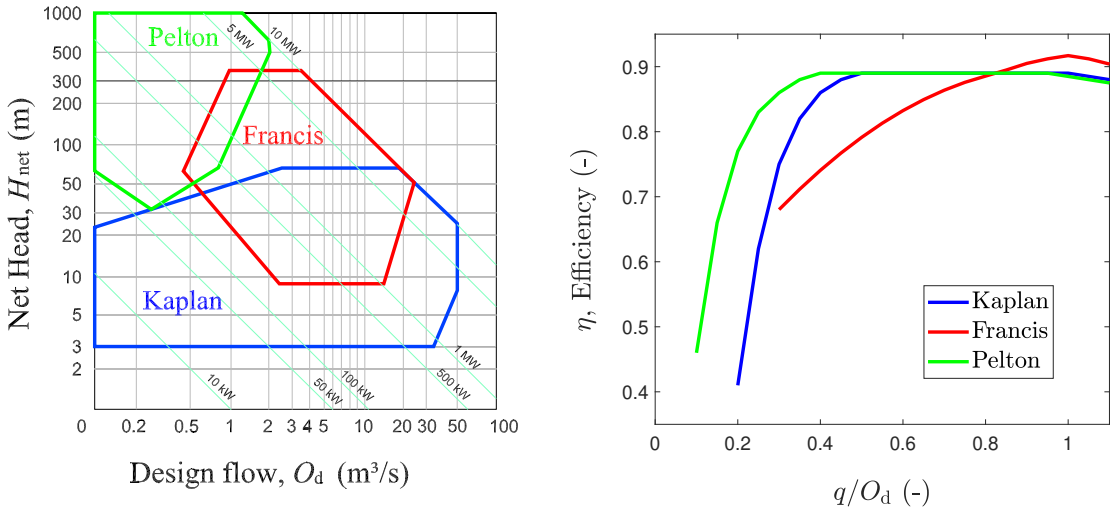

Figure 4.3: *Left panel: Turbine chart (Penche, 1998). Right panel: Efficiency of the Kaplan (blue), Francis (red), and Pelton (green) turbines as function of the ratio between their flow rate and design flow respectively (Sinagra et al., 2014).*

4.3.2 Benefits and costs

A comprehensive benefit and cost analysis is crucial to evaluating the feasibility and viability of Run-of-River (RoR) hydropower projects. The main elements of a cost-benefit analysis, detailed in Yildiz and Vrugt (2019) are presented here because they have a key role in the optimization and financial robustness analysis presented in Section 4.4.

Evaluating the installed capacity of the hydropower project is the first step in the analysis. It also entails assessing the expected generation of energy over the project's lifetime. The installed capacity of a hydropower plant, P is commonly expressed in megawatt (MW):

$$P = \frac{1}{10^3}\,\eta_g\,\rho_w\,g\,H_{net}(D, O_d)\sum_{j=1}^{N} O_{dj}\eta_j, \tag{4.1}$$

where the multiplication factor converts the units of P from Watt to kW, η_g (-) is the generator efficiency, ρ_w (kg/m^3) is the density of water, g (m/s^2) signifies the gravitational constant, H_{net} (m) is the net head or water pressure at the bottom of the penstock, O_d (m^3/s) signifies the system design flow, D (m) denotes the penstock diameter, O_{dj} (m^3/s) and η_j (-) characterize design flow and efficiency of the jth turbine, respectively.

The amount of energy E that a N-turbine hydropower plant ($N \in 1, 2, 3$) can produce over a time period, Δt (days), is calculated in kilowatt hours (kWh) via:

$$E(t) = 24 \sum_{t}^{t+\Delta t} \sum_{j=1}^{N} P_j(t) \ [q_j(t) \ H_{\text{net}}(t) \ \eta_j(t)] \,, \tag{4.2}$$

where the multiplication factor converts the units of day to hour, t (days) denotes time, P_j is the power produced by the jth turbine, q (m^3/s) represents the inflow to the turbine system, and q_j is the volumetric water flux, (m^3/s) of the jth turbine. Note that H_{net} and η_j are time dependent and vary as function of turbine inflow, penstock diameter and/or design flow, respectively.

The expected cumulative revenues from hydropower production through the lifecycle of the project are computed through:

$$\text{R} = \frac{R_1}{1 + r(1)} + \frac{R_2}{\left(1 + r(2)\right)^2} + \ldots + \frac{R_{L_\text{s}}}{\left(1 + r(L_\text{s})\right)^{L_\text{s}}} \tag{4.3}$$

where L_s is the project's lifetime, typically 50 years, and $\mathbf{R} = \{R_1 \ldots, R_{L_\text{s}}\}$ and $\mathbf{r} = \{r(1), \ldots, r(L_\text{s})\}$ are L_s-vectors with the annual plant revenues in US dollars assuming an average hydropower production throughout the year ($) and the annual interest (discount) rate in %, respectively.

The final stage of a cost-benefit analysis involves estimating the investment cost of a RoR hydropower plant design, which significantly depends on site-specific factors. The investment cost associated with the design can be expressed as:

$$C_{\text{Tp}} = C_{\text{em}}(P, H_{\text{net}}) + C_{\text{p}}(D) + C_{\text{cw}}(C_{\text{em}}, C_{\text{p}}) + C_{\text{PH}}(C_{\text{em}}) + C_{\text{ss}} \tag{4.4}$$

where C_{em} is the cost of the electromechanical equipment, C_{p} represents penstock costs, C_{cw} is the cost of civil works, C_{PH} is the cost to build the power house, C_{ss} represent site-specific costs, either fixed such as access roads, or variables such as when previous landowners need to be compensated. Computing total project costs involves adding maintenance costs to these construction costs. These include yearly maintenance and operation cost on the total cost, but also the need to replace the electro-mechanical equipment at the end of its design life, typically 25 years. Hence, the total net present cost of a project is given by:

$$\text{C} = C_{\text{Tp}} + \frac{C_{\text{om}}}{1 + r} + \frac{C_{\text{om}}}{\left(1 + r\right)^2} + \ldots + \frac{C_{\text{om}} + C_{\text{Rem}}}{\left(1 + r\right)^{25}} + \ldots + \frac{C_{\text{om}}}{\left(1 + r\right)^{L_\text{s}}} \tag{4.5}$$

where, C_{Rem} is the the renovation and reconstruction cost of electro-mechanic equipment at year 25 and C_{om} is the yearly maintenance and operation cost. Each component of benefit and cost equations is discussed in detail in Yildiz and Vrugt (2019).

4.3.3 HYPER and its extensions

HYPER (Yildiz and Vrugt, 2019) is a state-of-the-art toolbox for the optimal design of a RoR plant. It provides a fast computation of technical performance (energy production and economic profit), as well as maintenance and operational costs of a RoR plant in response given project characteristics (e.g., head, daily streamflow record). This enables the optimization of design variables through simulation-optimization. Design parameters include turbine type, configuration and design flow, along with penstock diameter and thickness. HYPER considers the possibility of using turbines of different sizes for increased flexibility across the full range of flows. Yet, in Yildiz and Vrugt (2019) the number of turbines in HYPER is limited to two, and the user needs to pre-specify the type and number of turbines.

This work extends the existing HYPER toolbox in three main ways, to improve HYPER's flexibility across a range of cases. First, now it adds the possibility to leave choices of turbine number and type to design optimization. In other words, instead of using selection charts similar to the left panel of Figure 4.3, it uses turbine- and site-specific constraints to determine which turbine types are eligible for the search (Penche, 2004). Second, it is the first RoR design to consider three-turbine designs, leading to maximal flexibility designs. For this, it extends the existing module simulating plant operations to the more complex three-turbine case. Note that the two larger turbines are considered identical in this study in the case of a three turbine installation. Besides, dual- and triple-turbine designs are assumed to be manufactured from the same makers. Third, this new version enables to run HYPER in pure simulation, whereas previously, simulation was always embedded in a simulation-optimization setup.

Besides, built-in parameters are regularly updated in light of recent advances; for instance, the cost function of electro-mechanical equipment was updated here (AlZohbi, 2018) compared with the original HYPER toolbox. The electromechanical equipment (turbine, generator, and power transformer) are most cost intensive (IEA, 2021). Recently AlZohbi (2018)

Table 4.2: The x, y and z values in the cost function of electromechanical equipment (Equation 4.6) for the three different turbines simulated.

Turbine	x	y	z
Pelton	1.984	1.427	−0.4808
Francis	2.927	1.174	−0.4933
Kaplan	2.76	0.5774	−0.1193

introduced several empirical cost equations for C_{em} (M$), the electromechanical equipment. Accordingly, C_{em} eguation is updated in HYPER as follows,

$$C_{\text{em}} = x\xi \left(P\right)^{(y)} \left(H_{\text{d}}\right)^{z}, \tag{4.6}$$

where ξ signifies the exchange rate of Euro (€) to US dollar ($), P (MW) is the installed capacity of the RoR hydropower plant (see Equation 4.1), and x, y, and z are coefficients whose values are reported in Table 4.2 for three turbines simulated in this study. Note that (AlZohbi, 2018) do not specify an equation for the cost of the electromechanical equipment of the Crossflow turbine. Moreover, this kind of turbine is not well-studied in the literature when compared to other well know turbine types such as Francis, Kaplan and Pelton turbine and this turbine, in general, is not preferred for small hydro power plants. This is why the Crossflow turbine is not considered in this study.

4.4 Methodology

In this paper we first explore the impact of using alternative financial objectives for design, then evaluate the financial robustness of design solutions in a changing world. These modeling choices, along with the taxonomy for robustness frameworks introduced by Herman et al. (2015), informed our use of an analysis framework adapted from Many-Objective Robust Decision-Making (MORDM; Kasprzyk et al., 2013), in which we incorporate for the first time turbine design considerations thanks to the improved HYPER toolbox (Section 4.3). We outline the four main steps of our analysis in Figure 4.4, each of which is detailed in a separate sub-section.

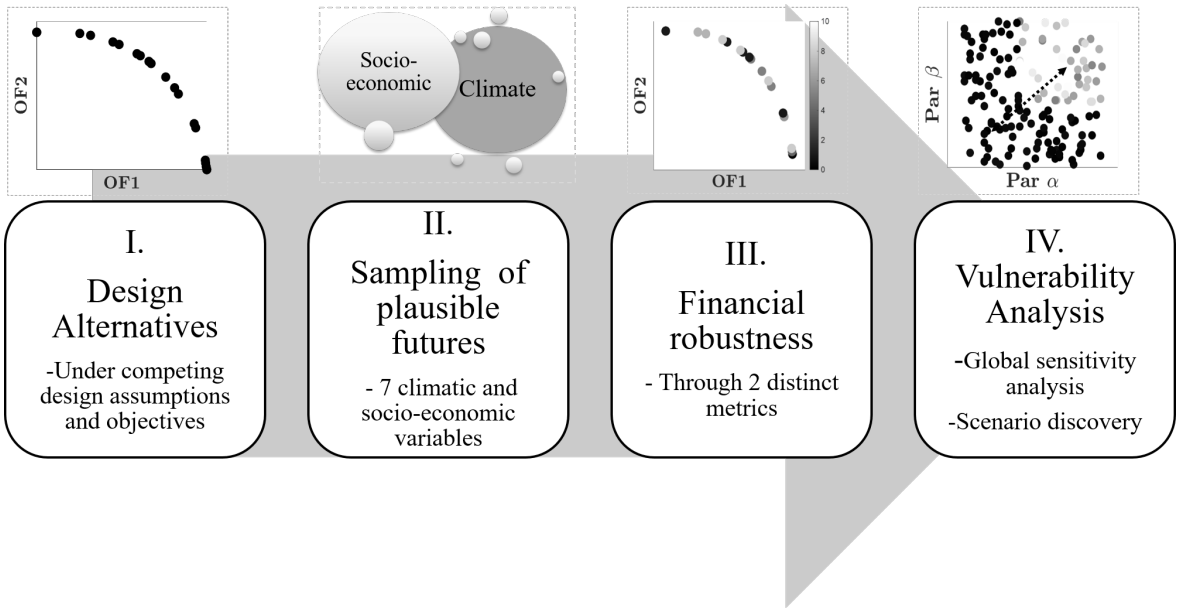

Figure 4.4: *Methodological flowchart of our the design of financially robust RoR hydropower plants. Each step is associated to the sections of the paper in which it is discussed.*

In step (I), we formulate a set of single- and multi-objective design problems to be solved by coupling of a multi-objective evolutionary algorithm (MOEA) with HYPER and using a statistically robust representation of flow variability (Section 4.4.1). This is a prerequisite to evaluating the consequences of design assumption on robustness. Step (II) features the sampling of deeply uncertain factors to analyse robustness to uncertain climatic and financial futures, along with careful justifications for the chosen ranges (Section 4.4.2). In step (III) we define and two quantify financial robustness metrics (Section 4.4.3), and in step (IV) we discover and analyse the main factors that influence robustness (Section 4.4.4).

4.4.1 Generation of design alternatives

In this section we present the experimental design to explore different financial design objectives. These objectives are evaluated through daily streamflow time series, so the method for daily streamflow generation (Section 4.4.1) is presented before the objective themselves (Section 4.4.1). Then, Section 4.4.1 details the experimental design for RoR optimization.

Synthetic streamflow generation

RoR plant performance is evaluated through 20 time series of 50 years of daily streamflows generated by synthetic time series generation. In this study, we used the Kirsch-Nowak streamflow generator for synthetic streamflow generation already used in several existing robustness assessments (Giuliani et al., 2014; Quinn et al., 2018) for its ability to reproduce the statistical characteristics of the historical record. By generating these flows during a longer period of time than the period of record, we also provide a more accurate picture of variability and extremes associated with the historical streamflow regime.

Objective Functions (OFs)

Since we are investigating financial robustness, objectives we consider have to do with the total lifetime expected revenue R and cost C as defined in equations (4.3) and (4.5) respectively. We first define expected total discounted revenue and cost as objectives in their own right:

$$\begin{cases} f_{\text{revenue}} = \text{R} \\ f_{\text{cost}} = \text{C} \end{cases} \tag{4.7}$$

The most common design objective is the maximisation of the net present value (NPV), defined as the value of projected cash flows discounted to the present (Santolin et al., 2011):

$$f_{\text{NPV}} = R - C \tag{4.8}$$

As discussed in the introduction, there exist alternative metrics to NPV that help to find less risky designs. In this work, we selected the cost-benefit ratio (BC) because it is the most easily interpretable in relation to NPV. BC is defined as present value of net positive cash flow divided by net negative cash flow, and reads:

$$f_{\text{BC}} = \frac{R}{C} \tag{4.9}$$

Finally, we defined as an objective the worst first percentile annual energy production from our 1,000 year synthetic time series to account for energy production during droughts. This is because incorporating risk-averse objective in multi-objective optimization is a common practice where decision-makers need to make robust and reliable decisions in the face of uncertainty (e.g., Giuliani et al., 2017). This approach is much less sensitive to the time series

used than would be using the single worst year Quinn et al. (2017). Worst first percentile energy production rate is expressed as:

$$f_{\text{dry}} = percentile(E_{\text{a}}(k), 1) \qquad (k = 1, 2, \ldots, K_{\text{s}}), \tag{4.10}$$

where $E_{\text{a}}(k)$ is equal to the sum of the daily values of $E(t)$ in Equation 4.2 computed by HYPER for year k, and K_{s}, is the number of flow years used for energy production of the power plant.

Design of experiments

We consider four design formulations. For all four formulations below the search aims to generate design alternatives. A design consists of turbine configurations (single, dual and triple), turbine type (Francis, Kaplan, Pelton) and related design parameters (penstock diameter, turbine(s) design flow) of the RoR hydropower plant. HYPER is used to simulate all proposed design during the searches, and it is coupled in a simulation-optimization setup with the Amalgam MOEA (Multiobjective Evolutionary Algorithm) introduced by Vrugt and Robinson (2007). Amalgam MOEA is a self-adaptive multi-method search which employs four sub-algorithms simultaneously within its structure, including NSGA-II, adaptive metropolis search, particle swarm optimization and differential evolution (Vrugt and Robinson, 2007). Amalgam MOEA was benchmarked against another state of the art algorithm, Borg MOEA (Hadka and Reed, 2013) as a check of its appropriateness for RoR design optimization (see SI). It can be used both in single- and multi-objective settings. With all four formulations, the search was conducted using a population size of $I = 100$ individuals and running Amalgam for $J = 1000$ generation.

Our first formulation corresponds most closely to a traditional RoR design: identical turbine design (ID) with NPV maximisation, with NPV defined in equation 4.8. This corresponds most closely to a traditional RoR design. In this case, we have considered two different configurations; (1) ID alternative; identical turbines with the same cost assumptions as other alternatives, (2) ID* alternative; the cost of electromechanical equipment (see SI) is reduced by 10 % which is then propagated through equation 4.5.

Second, we propose a single-objective NPV maximisation where turbines are allowed to be different. This mirrors the previously published iteration of HYPER (Yildiz and Vrugt,

2019). This is our benchmark. In the two multi-objective formulations below, turbines are allowed to be of different design flow and installed capacity as well.

Third, we explore the possible trade-off between NPC and BC as design objectives, with the following two-objective problem:

$$F_3(x) = \max[\ f_{\text{NPV}},\ f_{\text{BC}}] \tag{4.11}$$

where x is the vector of decision variables including all the key design parameters. This enables us to compare the robustness of solutions with how they trade-off the most commonly used traditional design objective with another financial objective assumed to be more focused on project risks.

Finally, we present an explicit three-objective formulation where we explicitly use the two components of f_{NPV} and f_{BC}, discounted lifetime revenue and cost, as standalone revenue and cost objectives f_{revenue} and f_{cost}. We add the dry year revenue objective f_{dry} defined in equation (4.10) as our third objective, in order to explore possible tradeoff between these two key financial objectives and hydropower revenue during dry periods. This formulation aims to verify that the two-objective search does not ignore obvious financially robust solutions. Formally, this problem is expressed as:

$$F_4(x) = \min[\ -f_{\text{revenue}},\ f_{\text{cost}},\ -f_{\text{dry}}] \tag{4.12}$$

4.4.2 Sampling Plausible Futures

The second element of the approach described in Figure 4.4 is to evaluate the performance of the alternatives identified under competing design assumptions across a set of uncertain future states of the world (SOWs). For this we first assigned a range to multipliers for each of these 7 variables (Table 4.3). The 4 economic multipliers in this analysis are interest rate r, cost overruns C_{or} during construction, and two energy prices, reflecting Turkey's energy regulations. A first price e_{Pf} is fixed for the first 10 year by the Turkish government, including subsidies (EMRA, 2022), with a different energy price for the remainder of the project's lifetime e_{Pr}. The 3 hydroclimatic parameters are streamflow statistics: its median, coefficient of variation and 1st percentile. Following Section explains how ranges were chosen to reflect projections involving climates with greater aridity and trend towards an increase in

hydrological extremes. Note that multiplier ranges in Table 4.3 represent plausible rather than probable values. They provide a mechanism for understanding how wrong our baseline model assumptions can be before significant vulnerabilities to deep uncertainties occur (Herman et al., 2014). After determining ranges for the variables, we constructed a 7-dimensional Latin Hypercube Sample of 500 future states of the world (SOWs) to reflect the deep uncertainties across socio-economic and hydroclimatic futures. After preliminary results showed the key role of the cost overruns scaling factor, our final sampling uses Progressive Latin Hypercube Sampling strategy introduced by Sheikholeslami and Razavi (2017) so cost overruns scaling factors sampled in the 1-2 and 2-3 ranges are both a latin hypercube sampling with 250 future SOWs.

Socio-economic Factors

The first four deeply uncertain factors factors in Table 4.3 are socio-economic. First, and as illustrated by the definition of NPV in equation (4.8), key financial viability indicators can be very sensitive to the interest rate used. The higher the interest rate, the faster the future values of cash flows are discounted, resulting a lower NPV. This makes r a crucial piece of information for decision makers and investors in determining the fair value or market price for projects (Thornton and Pipeline, 2018). Selection of an appropriate interest rate to evaluate investments in the energy sector is therefore a contentious topic (Zhuang et al., 2007; Saługa and Kamiński, 2018; Steffen, 2020), with significant country-to-country variations, as developed countries apply lower discount rates (3% – 7%) than developing countries (8% – 15%) (Steinbach and Staniaszek, 2015; Ray et al., 2018). To reflect this uncertainty and explore the impact of r on financial viability of a plant, this parameter ranges from 3% to 15% in this analysis.

As indicated in Equation 4.4, construction-stage costs are a key component of total project costs. Cost , C_{cw}, are difficult to anticipate as they depend on several interacting factors, including extreme high-discharge events during construction, topography and underlying geology of the site supporting the structure of the intake weir, forebay tank and conveyance line, and its distance to existing infrastructure and transmission lines (Mishra et al., 2011; Yildiz and Vrugt, 2019). Construction delays arising from any mix of these factors can lead to

Table 4.3: Variables and sampling ranges used for robustness analysis. SF is for scaling factor, and a SF of 1 indicates baseline conditions.

Uncertain Factor	**Current Value**	**Lower Bound**	**Upper Bound**	**Comments**
r, Interest (discount) rate (-)	0.095	0.03	0.15	significant variations in applications
e_{Pf}, Energy price, first 10 years (¢/kWh)	5.5	5	6.5	feed-in tariffs mechanism
e_{Pr}, Energy price, rest of the years (¢/kWh)	5.5	3	6.5	relatively high variability in market prices
C_{or}, Cost overrun SF (-)	1	1	3	elevated likelihood of construction delays
$\tilde{m}$, Median SF (-)	1	0.3	1	expected rise in drought conditions
CV, Coefficient of Variation SF (-)	1	1	2	expected increased variability in flow
$P_{1\mathrm{st}}$, 1st percentile SF (-)	1	0.3	1	expected rise in drought conditions

large cost overruns, as commonly observed in hydropower projects around the world (Plummer Braeckman and Guthrie, 2015; Ray et al., 2018; Azam et al., 2020). In fact, overruns can double construction costs on average (Ansar et al., 2014; Callegari et al., 2018). This uncertainty is represented in the model by a scaling factor that ranges from 1 (no cost overruns) to 3 (200% cost overruns). Note that, contrary to, e.g., Ray et al. 2018, this range does not include the cost of turbine and generator pieces, since these costs are more predictable and are not affected by unknown site specific factors.

The main source of income for investment in hydropower plants is revenue from the sales of electricity (e_{P}) to the power grid. Several financial support schemes such as feed-in tariff

policies have been adopted worldwide (Pyrgou et al., 2016) to promote the evolution of the Renewable Energy Sources (RES). The main principle of feed-in tariff policies is to offer long term guaranteed prices for fixed periods of time for electricity produced from RES (Klein, 2008) to significantly reducing perceived risks in investing in renewable energy technologies (Lipp, 2007). This is meant to attract investor interest (Couture and Gagnon, 2010; Alizamir et al., 2016), despite concern on the durability of generous tariffs of various schemes offered to clean energy producers (Lütkenhorst and Pegels, 2014; Pyrgou et al., 2016). The support mechanism in Turkey, initiated in 2011 and updated in 2021, is offering purchase guarantee by feed-in tariffs for electricity generated from renewable resources for 10 years (EMRA, 2022). Based on the 2021 framework, the selling price range selected for the first 10 years of RoR operation is between 5.5 ¢/kWh and 6.5 ¢/kWh.

However, potential depreciating in Turkish Lira (TL) against the USD and Euro remains a big concern after the end of support mechanism. Therefore, electricity prices are subjected to a higher degree of uncertainty for the rest of the prject's lifetime. Although annual average electricity selling price increase from 14.9 krs/kWh (8.33 ¢ in 2012) to 27 Krs/kWh (4 ¢ in 2020) and 50.8 Krs/kWh (5.7 ¢ in 2021) (EXIST, 2022), there is a sharp decline when the values are converted to USD. Due to the trend of potential depreciating in Turkish Lira (TL) against the USD and historical market prices, we chose a range for electricity selling price from 3 ¢/kWh to 6.4 ¢/kWh for the operation time after 10 years.

Hydroclimatic Factors

The observed drying and warming patterns are compatible with regional climate models projections indicating that the region is likely to become hotter and dryer in the future (Kelley et al., 2015). Further analyses indicate a decrease in the mean discharge values that could reach up to 60% (SYGM, 2016). An increasing intensity of drought conditions is expected for the period of 2040 - 2071 in the regions of the presented case study (Demircan et al., 2017; Turkes et al., 2020; Yildiz et al., 2022). In parallel, precipitation variability is widely forecast to increase (e.g. Pendergrass et al. (2017)), with the coefficient variation of precipitation projected to almost double by 2060 in various neighboring regions such as the Mediterranean (Giorgi and Lionello, 2008) or Iran (Zarrin and Dadashi-Roudbari, 2021). To

reflect these various results while reflecting the uncertainties that surround them, we chose wide ranges for the scaling factors of our three climate parameters. These sampling ranges are summarised in Table 4.3 and reflect the concurrent tendencies for severe drying and an increase in variability. We chose to model the median rather than the mean flow because for RoR design, the flow distribution matters more than the average (Figure 4.2), which is often skewed by high flows that the turbine cannot fully use. Also recall that these ranges represent plausible rather than probable values. Note that we only consider scenarios in which the median is 20 % or more above the first percentile of flow, to avoid modelling unrealistic futures. This reduces our number of sampled states (456 out of 500) only for the Besik site.

These ranges are then converted into flow duration curves (FDCs) using a novel approach (Yildiz et al., 2023a). In this approach, streamflow statistics that are of interest to water resource management; median, standard deviation and first percentile flows are related to the three parameters of a statistical representation of the FDC. New FDCs are then generated to represent full flow distributions that mirror these parameters, and they can be used in our subsequent robustness analysis. Panel A of Figure 4.5 demonstrates how the FDC samples differs from the baseline and the wide range of flow conditions considered. Clearly, our method can provide a suitable range of hydroclimatic conditions, with increased frequency of high flows and low flows, matching expected impacts of climate change in the region. Each sampled FDC consists of 50 time series of 49 years daily discharge values which are created by combining the statistical generation of climate-perturbed FDCs (Yildiz et al., 2023a) with the Kirsch-Nowak streamflow generator. Decomposition of a fairly arid future (orange colour) into 50 time series of 49 years is shown in panel B of Figure 4.5.

4.4.3 Metrics for financial robustness

The third element of our approach in Figure 4.4 is to evaluate financial robustness of selected (or all) alternatives across a set of uncertain states of the world, using two distinct but complementary financial feasibility metrics. Using more than one robustness metrics makes conclusion more solid because metric choices usually affect our evaluation of the robustness of competing options (Herman et al., 2015; Giuliani and Castelletti, 2016; McPhail et al., 2018).

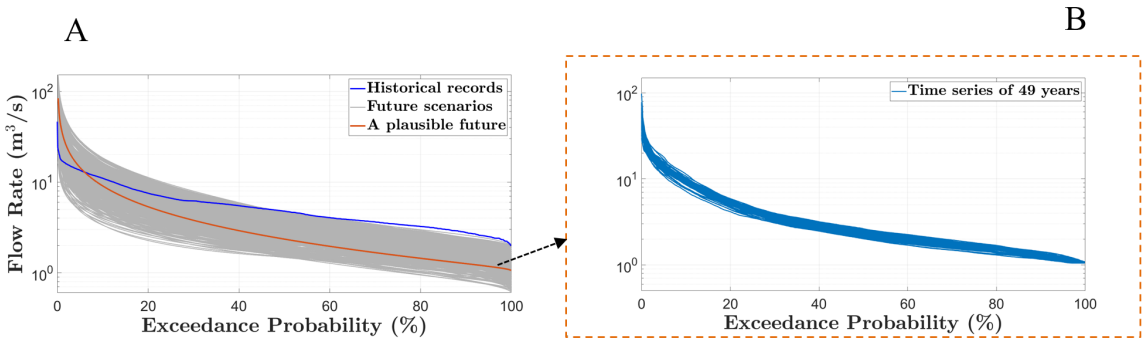

Figure 4.5: *Plot of the flow duration curves (FDC) of the fitted Kosugi model (blue line) and sampled flow duration curves (gray lines) and a moderately dry future (orange colour) constructed by deriving the FDC parameters for Kosugi Model shown in Table 4.3 (panel A). Disaggregation of a moderately dry future (orange colour) to 50 time series of 49 years (panel B).The flow rate displayed on the y-axis is presented on a logarithmic scale.*

Two financial feasibility metrics

The payback period (PB) is a metric that shows the length of time required to recover capital investments. It is computed as;

$$PB = \frac{C_{Tp}}{\overline{R} - C_{om}} \tag{4.13}$$

where C_{Tp} it the investment cost defined in equation (4.5), and the denominator is the expected amount of net cash inflow that the project generates each year. The desirability of an investment of high initial cost such as hydropower plants is directly related to its PB (Lin, 2010). A shorter PB indicates a high net cash flow compared with the initial investment, and therefore a project that will pay for itself (and repay annual instalments on any loan) more easily. In addition to its simplicity, the PB formula also serves as a straightforward risk analysis tool (Yard, 2000).

Yet, PB does not account for the long-term profitability of the investment since it ignores any returns generated beyond the payback period (Lefley, 1996). Besides, it does not take the time value of money into account. To account for these we also complement PB with NPV to asses robustness. Whereas PB evaluates the attractiveness of an investment in absolute

terms, NPV assesses the relative value of investing vs. not investing.

Robustness metric construction

The payback period (PB) which is a metric that shows the length of time required to recover capital investments and NPV are transformed into robustness metrics based on satisficing criteria (Herman et al., 2015) i.e., by comparing these values to a desirability threshold.

In general, small hydropower projects are considered feasible if the PB is less than 15 years (Alonso-Tristán et al., 2011; Girma, 2016; Ak et al., 2017). Therefore, for each of the 49-year time series we define robustness based on PB as a binary variable:

$$\mathrm{RM}_k = \begin{cases} 0, & \mathrm{PB} > 15 \text{ years} \\ 1, & \mathrm{PB} \leq 15 \text{ years} \end{cases}$$

These binary variables are aggregated over all 50 time series for each plausible future to form an average robustness score RM_{PB} over all 500 futures – or less excluding the futures where the flow median is lower than or close to the first percentile. For each of the plausible futures, we also assigned success if at least 75% of the time series (38 of 50 or more) verify $RM_k = 1$.

We calculate the robustness metric based on NPV, RM_{NPV}, using the same approach as RM_{PB}. For each of the 49-year time series we define robustness as a binary variable:

$$\mathrm{RM}_k = \begin{cases} 0, & \mathrm{NPV} > 0 \text{ \$} \\ 1, & \mathrm{NPV} \leq 0 \text{ \$} \end{cases}$$

Then, we aggregate over all 50 time series over all futures to compute RM_{NPV}. Alternatively, we define a future as success or failure depending on whether $NPV > 0$ over 75% of the time.

4.4.4 Vulnerability analysis

Finally, we carry out a vulnerability analysis in two steps. First, a global sensitivity analysis (Sobol, 2001; Saltelli et al., 2008) of robustness metrics through the method of Sobol' will aim to find the uncertainties financial robustness is most sensitive to. We then use scenario discovery to understand what combinations of uncertainties might lead to critical system

failures. We then conducted scenario discovery analysis to identify the thresholds of deeply uncertain factors responsible for critical system failures by using a logistic regression method to separate success regions from failure regions. The model evaluations were performed using the ShARC high-performance cluster (HPC) at the University of Sheffield.

4.5 Results

In this section, we first illustrate analysis results using the case of the Besik hydropower project, which is expected to be the most profitable based on conventional assessments of RoR plants. We start by presenting design alternatives determined by various sets of objective functions, and by quantifying their robustness across the plausible futures we sampled (Section 4.5.1). We then investigate how the deeply uncertain hydrologic and economic factors affect the performance of these alternatives (Section 4.5.2). The result of this analysis is then compared with the other four case studies in Section 4.5.3.

4.5.1 Single-site design optimization and robustness

Results of the four competing design optimizations introduced in Section 4.4.1 are presented for the Besik site in Figure 4.6 in the space of design objectives NPV (x-axis) and BC (y-axis). Recall that in this work, design optimization uses historical flows. f_{NPV} denotes single-objective NPV optimization, F_3 involves two objectives—NPV and BC optimization, and F_4 represents the three objectives of revenue, cost, and dry year revenue optimization. Identical turbine solutions (ID) are identified through a single-objective NPV optimization. We differentiate between raw solution results (ID solution), with the same design for which a 10% discount is applied to the cost of electro-mechanical equipment and propagated through equation 4.5 (ID* solution). This latter solution is used to check the solidity of our results under the possibility that turbine manufacturers may be able to lower the cost of electromechanical equipment when turbines are identical. The Francis and Pelton turbines are the most suitable options for this project. The efficiency of Francis turbines makes them a superior choice over Pelton turbines to reflect the relative lack of streamflow variability at this site. This is because Francis turbines are highly efficient under steady or moderate flow conditions. Besides, while the F_3 formulation only includes a configuration with dual Francis turbines,

the F_4 formulation offers a wider range of alternatives including a single Pelton turbine, a single Francis turbine, dual Pelton and dual Francis designs, and even a triple Francis turbine configuration to satisfy different objectives. Indeed, triple Francis operations have the highest energy revenue with the largest design parameters (e.g. discharge design capacity, penstock diameter). Yet, these designs are costly, so the NPV is low when compared to dual configurations. The left panel compares the F_3- and F_4 formulations, and each alternative is also colored by its robustness measure, RM_{PB}, value. This enables us to verify that despite the presence of a dry-year production objective in the F_4 formulation, it does not find more robust solutions than the design alternatives found in the F_3 formulation. The F_4 optimization also offers many solutions that are far from the more profitable region in terms of costs and benefits. For these reasons, alternatives from the F_4 formulation will not be analysed further, and we will focus on comparing results from the F_3 with "traditional" designs using NPV as a single objective, with or without identical turbines. The right panel zooms in on the region of the NPV-BC space where the solutions from these f_{NPV} and F_3 formulations are all present, including the best NPV solution with different-size turbines (green triangle), as well as identical turbine solutions (red and orange diamonds).

All designs found across these three competing optimization formulations consist of two Francis turbines. The absence of three-turbine solutions demonstrate that the dual Francis option is sufficient to operate in the historical flow range for the site. Each line in the parallel plot of Figure 4.7 represents a design alternative with (i) its design parameters: design flows of the large and small turbine, installed capacity, average annual energy production, (ii) the values of the BC and NPV design objectives (regardless of whether BC was used as an objective in design determinations), and (iii) the two financial robustness measures introduced in Section 4.4.3. Across the alternatives, we highlighted a few remarkable solutions, noted MR (most robust based on RM_{PB}), best NPV (based on single objective NPV optimization), the best BC solution from the two-objective optimization, ID and ID* (identical turbines NPV maximisation). The color of each line represents RM_{PB}, the average probability of timely payback across all futures. It is apparent that RM_{PB} correlates favourably with f_{BC} and smaller design alternatives with less turbines design discharge and installed capacity. It additionally exhibits a negative correlation with f_{NPV} and annual energy capacity due

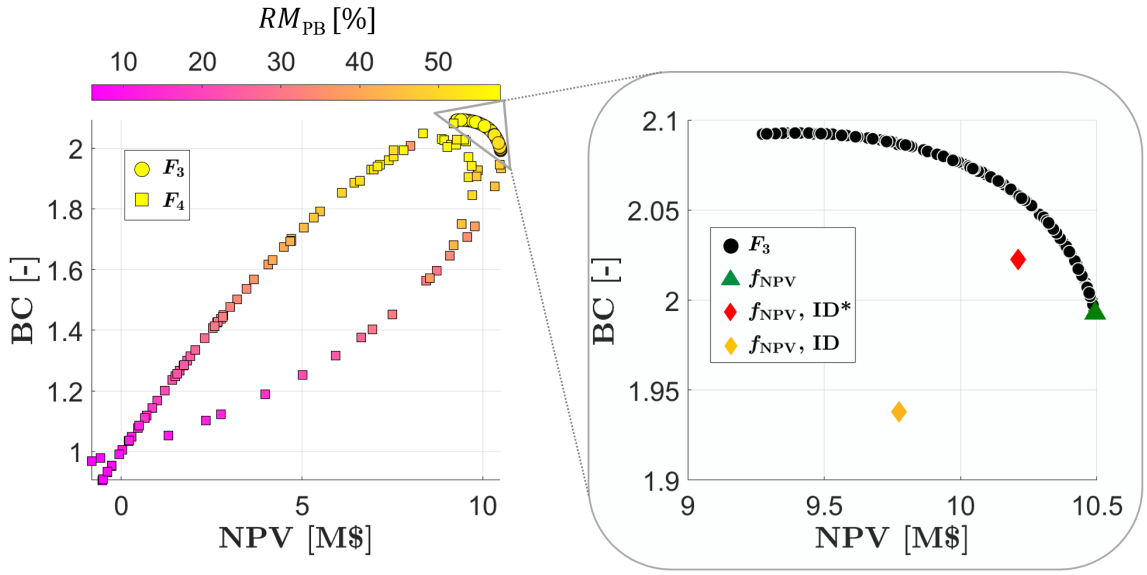

Figure 4.6: *Left panel: two-dimensional NPV and BC objective space where the alternatives of F_3 formulation (circles) are compared against the F_4 formulation (squares). Each solution colored by its robustness measure, RM_{PB}. Right panel: the alternatives of the F_3 formulation (black circles) and identical turbine solution (orange diamond) and identical turbine solution with discount (red diamond) and best NPV solution (green triangle) based on single NPV optimization.*

to the fact that greater generation capacity necessitates a larger, and thus more expensive, design. The two robustness measures clearly provide comparable evaluations of alternative designs. When contrasting robustness of a design with its NPV, designs with the highest NPVs show less robustness to both climate change (and associated drying) and to evolving financial conditions than smaller design alternatives with less installed capacity. Interestingly, RM_{NPV} is also lower for the best NPV alternative than for solutions with smaller NPV but higher cost-benefit ratio. Besides, the best BC and MR alternatives have comparable design characteristics and superior f_{BC} values that contribute to being robust to uncertain futures. On the other hand, robustness of identical turbine alternative (ID) even with less expensive design (ID) noticeably lower than all of the two objective alternatives.

To further analyse why designs with smaller installed capacity and turbine design flows seem to be more financially robust across a set of plausible futures featuring drier and more

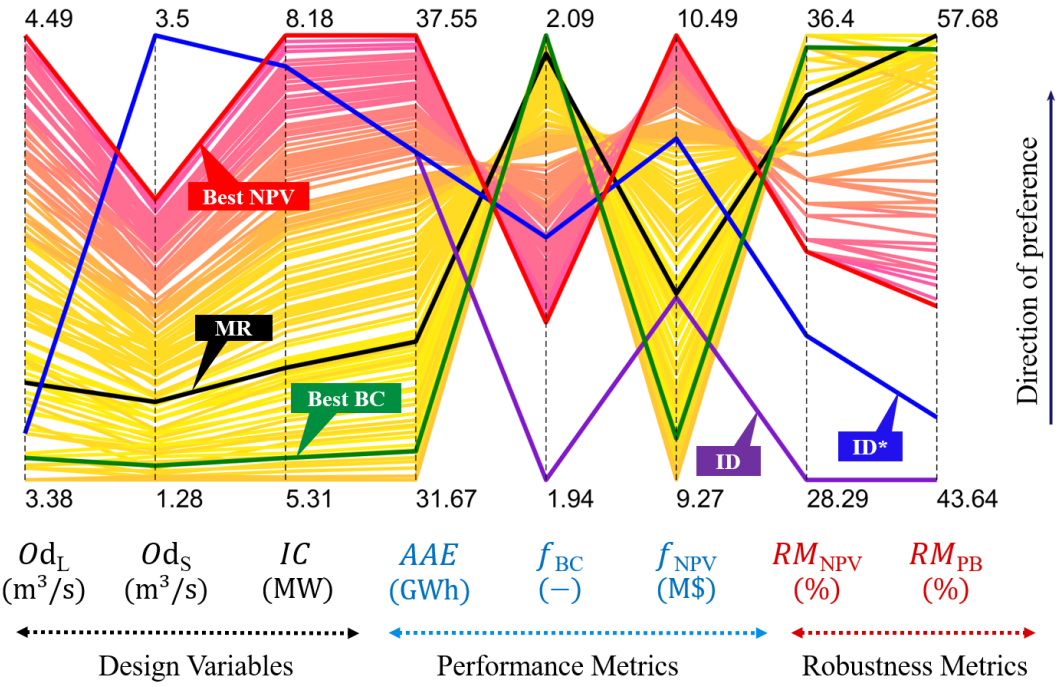

Figure 4.7: *The parallel plot of (1) design parameters of alternatives:large turbine design flow, O_{dS} (m^3/s), small turbine design flow O_{dL} (m^3/s), installed capacity IC (MW), average annual energy AAE (GWh), (2) two objective functions: f_{BC} (-), f_{NPV} (M$), and (3) their respective robustness measures value RM_{NPV}, RM_{PB} (%). Colour coding in lines is used for classification of results based on RM_{PB} value.*

variable conditions, we display in Figure 4.8 the operational performance of each selected alternative from Figure 4.7 under a moderately dry future (top panel) which is also highlighted (orange colour) in Figure 4.5. For each alternative (recall that ID and ID* are identical designs), the top, thicker horizontal bar represents overall plant efficiency whereas the thinner bars display the respective efficiencies of the large and small turbines. Both MR and Best BC alternatives have similar performance and they generate energy most of the time. Whereas the larger turbine of both MR and Best BC alternatives can only operate up to 50 % of the time, the small turbine is able to function and retain high efficiency even with low flows. In contrast, plant efficiency of the best NPV design is lower than 0.3 most of the time (60 %) and it has to be shut down almost a third of the time. What is more, the large turbine of

best NPV alternative shuts down more than three quarters of the time. Since it is even less flexible than the best NPV alternative, the ID alternative has the longest period without operation (about 40% of the time) and the lowest overall capacity factor among the selected alternatives.

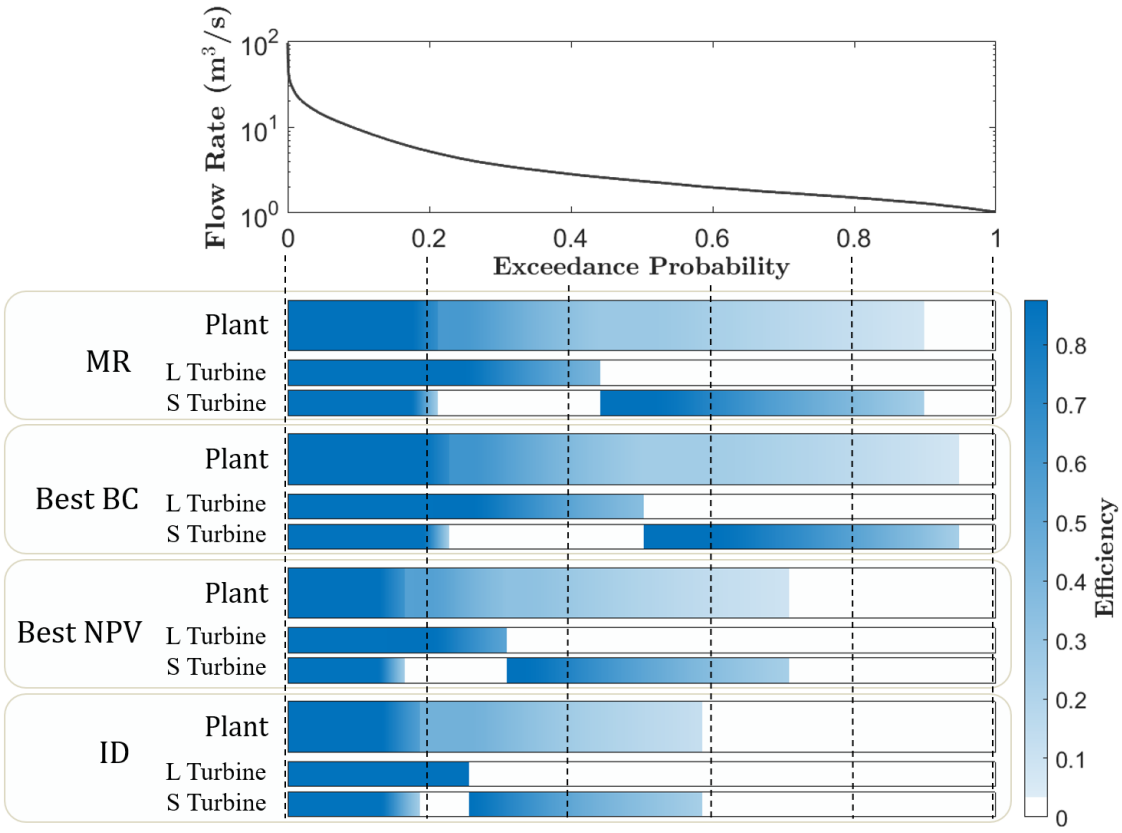

Figure 4.8: *Operational plant efficiency (labeled as plant) and turbine efficiencies (Large turbine and Small turbine) of each selected alternatives under a the future highlighted with the orange line in Figure 4.5. Recall that the ID and ID* designs are identical. The vertical dashed lines represent the scale of probabilities.*

Note that the selected future (see orange line in Figure 4.5) does not represent a very dry future. It is clear that the operational performance of a smaller, more flexible design with a higher benefit-to-cost ratio (BC) will be much better than that of a more traditional design under futures where we could observe increased frequencies of both high flows and low flows.

4.5.2 Single-site vulnerability analysis

In this section, we analyse how the deeply uncertain hydrologic and economic factors influence the performance of the five alternatives highlighted in Figures 4.7 and 4.8. First, we compute the Sobol' global sensitivity indices, with the total-order sensitivity S_{T} shown in Figure 4.9. This sensitivity metric accounts for the total contribution of each factor to the variance of each robustness metric – both by itself and in interaction with other factors (Saltelli et al., 2010). When the robustness metric is RM_{PB} (top panel on Figure 4.9), the most sensitive factors are the cost overrun C_{or} and median streamflow $\tilde{m}$ scaling factors, and this is true for all the selected alternatives. Note their relative importance changes: the NPV-maximisation designs (NPV, ID and ID*) are more sensitive to decreasing median flows because they are less flexible designs aimed at capturing high-flow conditions better. Conversely, cost overruns are key to the payback in smaller, more flexible designs BC and MR. Since interest rates do not enter in payback calculations (see Section 4.4.3, this metric is insensitive to changes in r. Additionally, we explore the Sobol' S_1 index, which assesses the variance contribution of each factor independently. Notably, the cost overrun and median flow emerge as the most sensitive factors for the MR solution. Moreover, when considering second-order sensitivity indices to evaluate the fractional contribution of parameter interactions to output variance, we find that the combinations of C_{or}-$\tilde{m}$, C_{or} - $P_{1\mathrm{st}}$, and C_{or}-CV are the most critical factors. Unsurprisingly, interest rates and energy prices exhibit minimal influence on the outcomes. Because the robustness metric primarily centers on 15-year revenue, and the range of energy prices is well-defined, with a considerably smaller range compared to other factors, its influence on the overall sensitivity analysis is limited. Contrary to this, Sobol' identifies the most sensitive factor as the interest rate for all the selected alternatives when the robustness metric is RM_{NPV} (bottom panel on Figure 4.9). This sensitivity to the interest rate is not surprising given the definition of NPV, but the difference between the two financial robustness metrics is striking given the fact that they provide similar rankings of alternatives (see Figures 4.7). However, similar to RM_{PB}, RM_{NPV} is also sensitive to C_{or} and $\tilde{m}$, with similar relative importances of these two factors across designs. The impact of energy price is insignificant for both financial robustness metrics as the range of energy price, especially for the first 10 years, is well defined that has a narrower range than any other

factors. Similarly, both of the robustness metrics are insensitive to flow variability, CV, and low flows, P_{1st}, confirming that both high and low flows are less influential to RoR energy production when compared to the central tendency. Moving on to scenario discovery, Figure

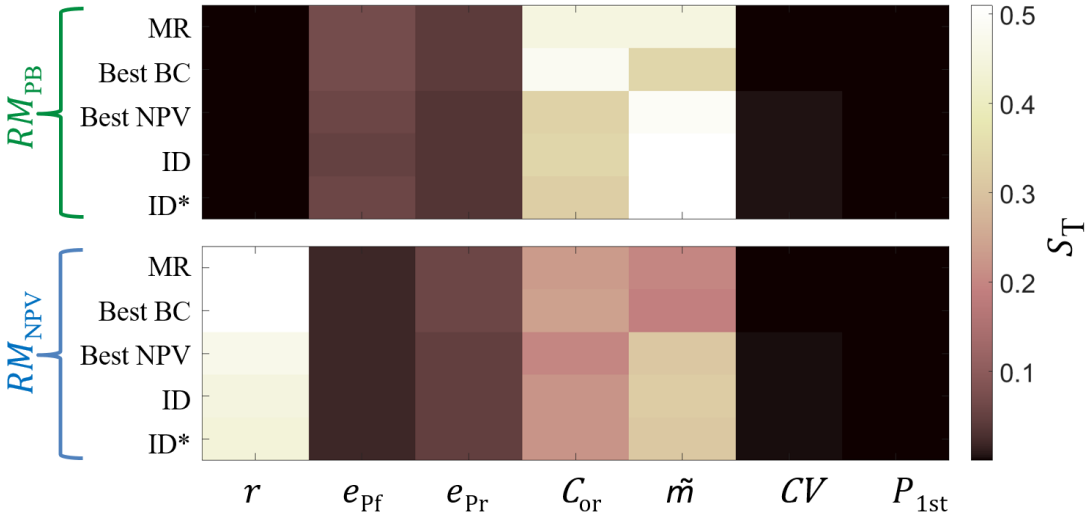

Figure 4.9: *The effect of the uncertain factors (x-axis) is quantified with the total-order S_T, sensitivity index (y-axis) based on robustness metric, RM_{PB} (first row) and RM_{NPV} (second row) and where dark gray is insensitive and white is sensitive.*

4.10 assesses where, in the space of uncertain factors, the solution labelled MR solution (most robust for RM_{PB}) fails to meet the performance requirements for each financial robustness metrics. Each panel plot contains a pair of two-dimensional projections of the 7-dimensional uncertainty space, with each point representing one of the 456 distinct feasible SOWs. A logistic regression model is then fitted to estimate the probability of failure as a function of selected two parameters to define success and failure regions. Not surprisingly, wetter worlds (higher median) decrease the probability of failure for both metrics. Clearly, any increase in cost overrun and decrease in median and energy price results in movement to the failure region, indicating high sensitivity of even the most robust solution to each of these factors when robustness metric is RM_{PB}. If a decrease in cost overrun is accompanied by increases in the energy price, the MR solution can tolerate greater decreases in the flow conditions. On

the other hand, when the robustness metric is RM_{NPV}, any increase in interest rate and cost overrun and decrease in median and energy price results in movement towards the failure region, confirming high sensitivity of even the most robust solution to each of these factors . The MR solution can tolerate greater increases in the interest rate, and the energy price for if the wetter worlds are accompanied by decreases in cost overrun. Figure 4.10 emphasises the importance of considering multiple uncertainties in combination.

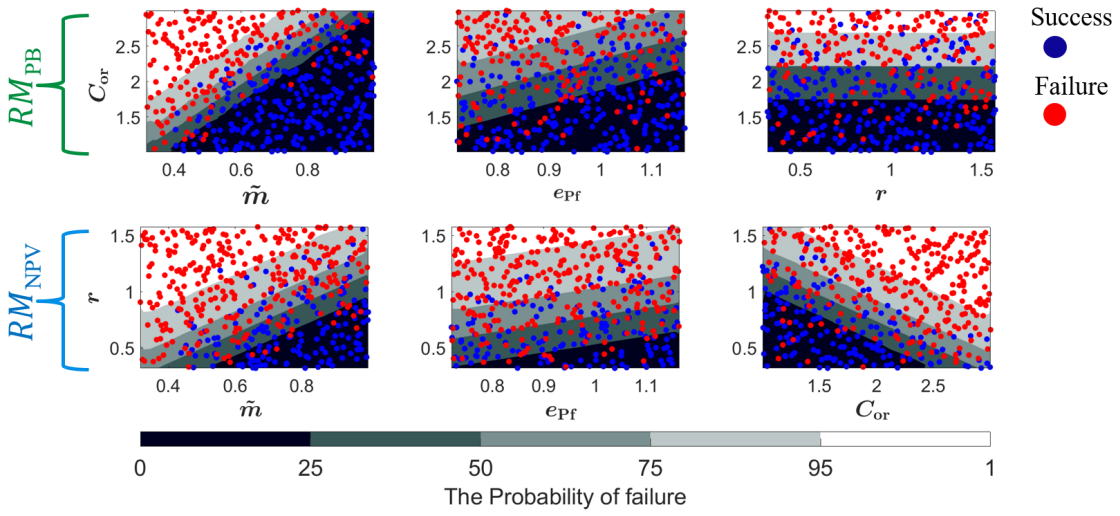

Figure 4.10: *SOWs in which the MR solution fails to meet the defined performance requirement in the two dimensional projection defined by the scaling factors on each uncertain factor. Panel plots at the first row shows analysis results of RM_{PB} and second row shows for RM_{NPV}. Blue points indicate states of the world where the MR solution satisfy to meet the performance criteria, and red points indicate states of the world where solution fails. The probability of failure as a function of these three factors is also shaded for each panel.*

To further visualise which climatic futures foster success or failures for different alternatives, in Figure 4.11, we plotted future FDCs (thin grey lines) and highlighted specific successful (orange lines) FDCs where the highest BC alternative meets the RM_{PB} robustness threshold, i.e., has 75% chance of having a payback period under 15 years, whereas another solution does not (left panel: NPV maximisation solution; right panel: ID solution). The

best BC alternative is robust in 39 additional SOWs (11.7%) compared to the best NPV design, and in 62 additional SOWs compared to the ID design. It is clear that Best BC alternative can tolerate greater decreases in future streamflow values than best NPV and ID alternatives. What is more, identical turbine configuration is significantly more vulnerable to climate change due to a lower flexibility across the range of plausible flows. Dependent on socio-economic factors, it can even fail with a FDC at the higher end of the range.

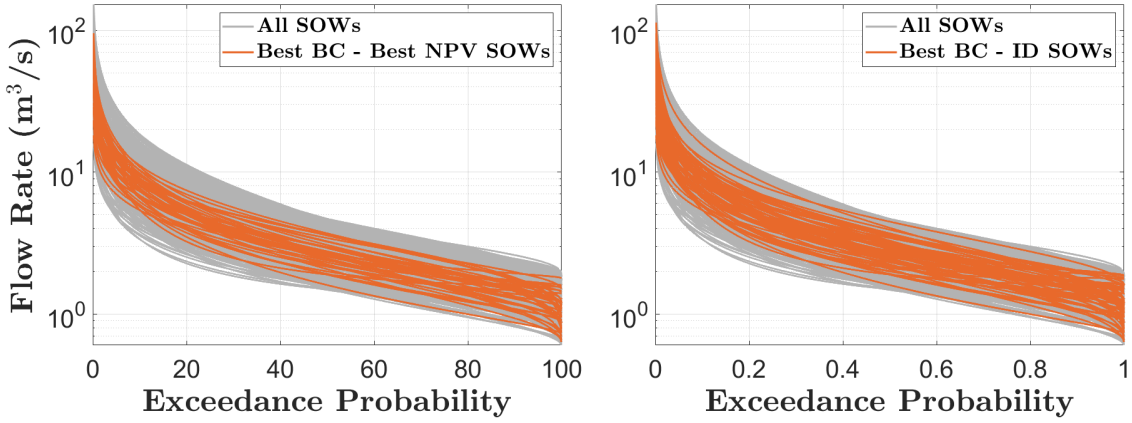

Figure 4.11: *The plots of FDC in which the highest BC alternative meet the performance criteria whereas the highest NPV alternative fails(left panel), and the ID alternative fails (right panel). Orange coloured lines shows successful SOWs, gray lines represents all the SOWs.The flow rate displayed on the y-axis is presented on a logarithmic scale.*

4.5.3 Comparison of all cases

This section gives the results of the analysis across all study sites listed in Section 4.2. The design characteristics, financial and energy performance metrics and the financial robustness metrics for the same five alternatives as in the Besik case, namely most robust according to RM_{PB} (MR), maximum NPV, maximum BC, identical turbine with a 10 % discount applied to the cost of electro-mechanical equipment (ID*) and without the discount (ID) for each of case-studies listed in Table 4.4. Buyukdere and Kaplan projects feature a significant head drop and a relatively low flow rate, making the Pelton turbine the only viable option, with a number of turbines (two) suitable for the sites' flow variability (see Figure 4.1). At the

Karacay site, both Pelton and Kaplan turbines are viable options. However, the presence of significant flow variability makes the Pelton turbine a better alternative. For all three sites, the costs of a third Pelton turbine outweigh the added flexibility. Conversely, at the Tepe site, the high CV makes a third turbine valuable, whereas the high flow rate and small gross head makes Francis the sole feasible choice. It is worth noting that for all sites, all the design alternatives recorded in Table 4.4 have the same turbine number and type. Yet, there is no indication this finding would generalize to other plants.

Besides the robustness metrics themselves, Table 4.4 also shows robustness for favorable socio-economic futures. For RM_{PB} this corresponds to a cost overrunsscaling factor smaller than 2, whereas forRM_{NPV} these futures feature a cost overrun scaling factor lower than 2 and an interest rate scaling factor lower than 1. The difference between robustness metrics across all futures and in favorable futures only underlines that financial robustness is well below 40% across sites and designs in unfavorable futures. Among the alternatives, BC solutions have smaller design characteristics resulting in lower design cost and an average annual energy output in all cases. Furthermore, BC solutions generally exhibit superior robustness performance than NPV solutions with higher design costs and yearly energy output, even though this advantage tends to disappear under favorable socio-economic futures. Besides, the ID solutions with higher initial cost has the lowest RM_{PB} and RM_{NPV} due to less operational flexibility. This indicates that high sensitivity to the reduction in cash flow caused by drier conditions.

In Figure 4.12, we further examine favourable socio-economic futures for RM_{PB}. Payback-based robustness is quantified by considering all climates (full bars) and dry climates whose mean discharge values is lower than 75 % of the long term mean observed flow (hollow bars). It is evident that if robustness is quantified by only considering dry futures where the additional cost increase is limited the performance of identical turbine configuration decreases drastically in all cases. What is more, the advantages of smaller designs become increasingly apparent across all locations, as BC solutions become more robust than even MR solutions – and recall that MR solutions are the most robust for RM_{PB}. Poor performance of NPV alternative is also observed when compared to the MR and BC solutions. Similarly, in Figure 4.13, we focus on robustness metric RM_{NPV} and futures with low cost overruns (scaling factor lower than

Table 4.4: Design characteristics, performance metrics and robustness of the most robust (MR) alternative and the alternative with highest NPV and BC, identical turbine alternatives (ID, ID*) of given five case studies.

Case Study Alternatives	**Turbine Configuration**	***IC*** [MW]	***AAE*** [GWh]	f_{NPV} [M$]	f_{BC} [-]	RM_{PB} [%]	RM_{PB} $C_{\mathrm{or}} < 2$ [%]	RM_{NPV} [%]	RM_{NPV} $C_{\mathrm{or}} < 2$ & $r < 1$ [%]
Besik, MR	Dual Francis	6.03	33.5	9.78	2.08	57.6	79.7	35.3	76.2
Besik, BC	Dual Francis	5.45	32.05	9.38	2.09	57.2	81.5	36.1	80.3
Besik, NPV	Dual Francis	8.18	37.55	10.49	1.99	49.1	68.7	32.4	70.4
Besik, ID	Dual Francis	7.98	36.01	9.77	1.92	43.6	62.9	28.2	64.7
Besik, ID*	Dual Francis	7.98	36.01	10.21	2.02	45.6	64.3	30.9	69.6
Buyukdere, MR	Dual Pelton	7.49	29.65	8.33	2	65.8	86.8	41.2	83.8
Buyukdere, BC	Dual Pelton	5.22	24.41	7.11	2.08	61.8	86.8	39.4	84.5
Buyukdere, NPV	Dual Pelton	9.96	34.10	8.81	1.85	63	83.6	39.4	80.8
Buyukdere, ID	Dual Pelton	9.43	32.81	8.51	1.86	60.2	82	37.4	79.4
Buyukdere, ID*	Dual Pelton	9.43	32.81	8.90	1.93	62.6	82.8	40.2	81.6
Tepe, MR	Triple Francis	3.78	14.75	3.09	1.60	56.2	82.4	31.2	75.7
Tepe, BC	Triple Francis	2.86	12.59	2.72	1.62	52.6	82.4	31	77.9
Tepe, NPV	Triple Francis	4.37	15.85	3.18	1.55	54.4	78.4	31.4	74.2
Tepe, ID	Triple Francis	3.97	14.72	2.91	1.54	49.6	75.2	32.2	71.3
Tepe, ID*	Triple Francis	3.97	14.72	3.19	1.63	55	81.6	28.8	76.4
Karacay, MR	Dual Pelton	2.43	7.59	1.38	1.48	43.4	74.8	27	72
Karacay, BC	Dual Pelton	2.17	7.02	1.28	1.48	42.4	74.8	26.8	72.7
Karacay, NPV	Dual Pelton	3.1	8.8	1.5	1.43	40.8	70.4	26.4	69.1
Karacay, ID	Dual Pelton	2.94	8.39	1.4	1.42	38.8	67.6	24	66.1
Karacay, ID*	Dual Pelton	2.94	8.39	1.52	1.47	42.6	72.4	27.8	71.3
Kaplan, MR	Dual Pelton	3.33	11.58	2.64	1.69	42.2	72	29.6	74.2
Kaplan, BC	Dual Pelton	2.6	10.35	2.43	1.72	39.0	70.4	27.8	73.5
Kaplan, NPV	Dual Pelton	3.62	11.98	2.67	1.66	42	70.8	30.2	74.2
Kaplan, ID	Dual Pelton	3.61	11.78	2.58	1.64	39.8	68.4	29	72.7
Kaplan, ID*	Dual Pelton	3.61	11.78	2.71	1.69	41.8	70.8	30.8	75

2). Robustness is quantified by considering all climates (full bars), dry climates whose mean discharge values is lower than 75 % of the long term mean observed flow (hollow bars) and risky futures whose interest rate values is bigger than the current rate (black dots). Similar to what happens for RM_{PB}, the BC alternative outperforms other alternatives in dry futures. In fact, it maintains a performance level above 60 % across all five sites assuming cost overruns are limited. Yet, when a drier future also features high interest rates (over 9.5% per year),

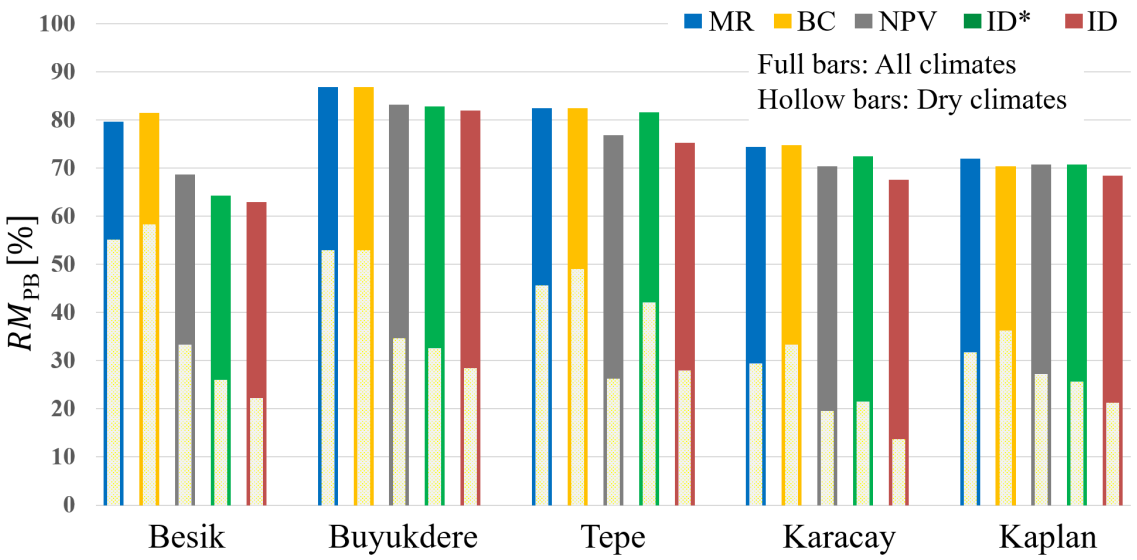

Figure 4.12: *Robustness of the most robust (MR) alternative and the alternative with highest NPV and BC, identical turbine alternative with (ID*) and without discount (ID) of each case study where cost overrun scaling factor < 2, with full bars (all climates) and hollow bars (mean flow < 75% of historical conditions).*

success rates fall across design alternatives and sites. This highlights that dry, economically unstable futures might be a bleak environment for RoR hydropower investments regardless of the other climatic and socio-economic factors.

4.6 Discussion

This discussion focuses on several important aspects from the preceding section where we demonstrated analysis results of the HYPER-MORDM framework using five different case studies. The findings highlight that RoR based traditional hydropower design which typically rely on optimizing the net present value (NPV) and employing identical turbine configurations exhibit less robustness to both climate change (and associated drying) and to uncertain socio-economic conditions than smaller design alternatives with less installed capacity. This emphasizes the need to update traditional RoR hydropower planning methods to promote the financial robustness of hydropower investments. The rest of this discussion presents several

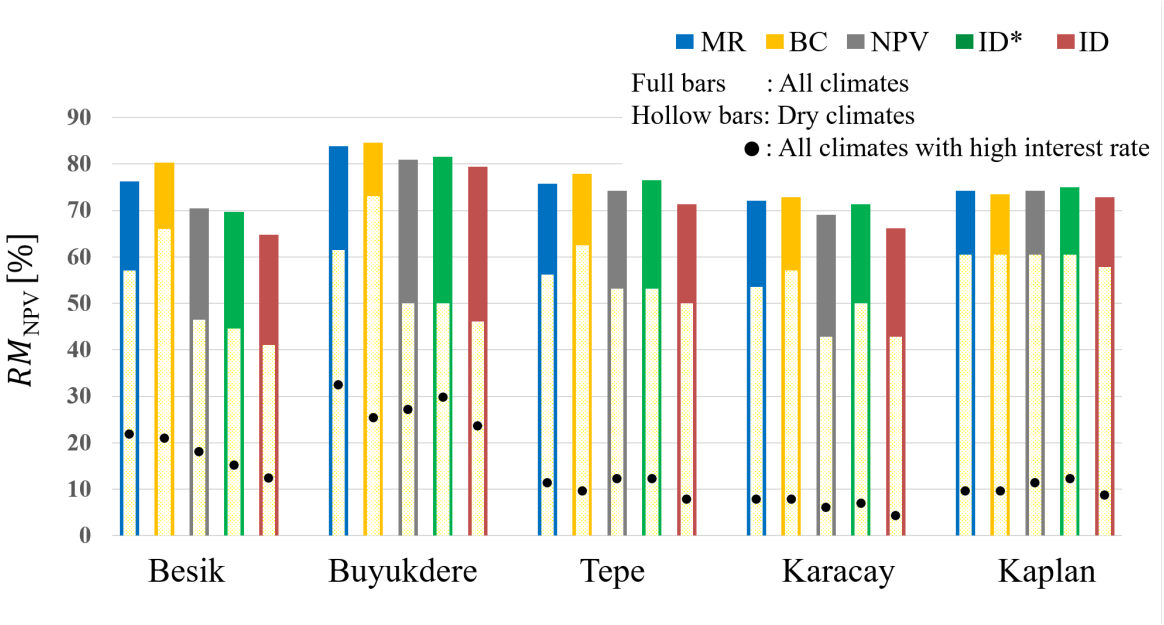

Figure 4.13: *Robustness of the most robust (MR) alternative and the alternative with highest NPV and BC, identical turbine alternative with (ID*) and without discount (ID) of each case study where cost overrun scaling factor < 2, with full bars (all climates), hollow bars (mean flow < 75% of historical conditions) and black dots (interest rate scaling factor > 1).*

key insights derived from the results, in particular for research and practice of hydropower design.

Before that, a key limitation of our work needs to be discussed. Indeed, even though the HYPER-MORDM framework is of general applicability for RoR hydropower design, the numerical results illustrated in the results section refer to only five cases proposed to be built in the same country. This is sufficient to expose the limitations of traditional design practices, but does not grant general applicability to results. Turkey boasts abundant topography – making it favorable for hydropower – and varied climates, yet the insights we got from these five cases would need to be applied to other RoR plants to gain generality. Indeed, projects in different regions face not only distinct climate, socio-economic and regulatory environments, but also very different uncertainties – recall that many uncertain factors and their ranges were context specific. An obstacle here is that both optimization and robustness analysis require a considerable amount of computing time and resources, necessitating the

use of High performance computing (HPC). This remark is general to exploratory studies of multi-objective trade-offs and robustness studies in water resource systems (e.g., Schmitt et al., 2018; Quinn et al., 2018). In this work, the computational time required to conduct optimization and analyse robustness for the experimental setup discussed in the previous section (optimisation: 1,000 years of synthetic daily discharge data using 100,000 function evaluations, robustness across S = 500 SOWs) for a single case is around 120 hours. Note this is just the final version of our study, it follows several runs featuring a similar computational effort for each site. Extension to hundreds of potential RoR sites thus necessitates large amounts of computational resources. Though often key to unlocking new insights in complex water resource systems, this use of computational power contributes to the continuous growth of data center demand, which currently account for 0.3 % of global carbon emissions Jones (2018); Cao et al. (2022*b*). This proportion is expected to rise in the future Katal et al. (2022), posing an additional, significant challenge to global climate change mitigation efforts. Workarounds to drastically reduce the computational costs for both optimization and robustness analysis of these plants would facilitate the application of the approach to a greater number of plants and lead to more general conclusions, while limiting the need for high-performance computing.

Small sample size aside, our analysis suggest that turbine configurations significantly impact the overall robustness of a project (see in particular Table 4.4). This is because larger installed capacities aimed at making the most of above-average flow conditions are more expensive while lacking the flexibility to capture low flows – at demonstrated in Figure 4.8. There is a need for understanding how these lessons derived for RoR plants could apply to reservoir-based (RB) plants. In RB plants, operators can control the flow but head variations are widely expected to intensify in a drought-prone world. These head variations impact the efficiency of turbines designed for a nominal head typically corresponding to a full reservoir – as mentioned for the Colorado River reservoirs in the introduction. This means there could be opportunities for designing turbines for different head conditions. Yet, the majority of the RB hydropower literature ignores turbine system efficiency during the design of the dam and hydropower plant system. Typically, the selection of the turbine configuration typically takes place after determining the installed capacity (DSI, 2012) due to the added complexity

of the turbine system design process. This lack of integration of turbine efficiency into design extends to recent research, (e.g., Ray et al., 2018; Bertoni et al., 2019, 2021), and this can lead to a mismatch between projected and actual energy production, even when operations are explicitly simulated. Adapting the HYPER-MORDM framework would facilitate the identification of robust alternatives capable of addressing the dynamic nature of these factors and effectively overcoming these challenges.

What is more, the aging hydropower infrastructure presents a significant challenge, with approximately one-fifth of installed hydropower turbines, accounting for around 154 GW, will be more than 55 years old by 2030 globally (IEA, 2021). Many of these turbines will need to be replaced to maintain high plant performance, and this will lead to opportunities to retrofit hydropower plants to improve their flexibility and meet changing and variable hydrological conditions. The need for a well-defined methodology to effectively evaluate and select the most appropriate turbine replacement or upgrade options is evident across both RoR and RB plants. To meet these needs, the approach proposed here should be expanded not only for RoR retrofit, but also to turbine system optimization for design and retrofit of RB hydropower plants. These extensions of our approach would also need to account for hydropower plant maintenance. The multipurpose nature of many reservoirs and the fact that hydrological variability and drought impact RoR and RB hydropower differently are significant challenges that this latter extension of the HYPER-MORDEM approach will need to tackle.

RoR installations, even though their environmental footprint is minimal when compared with that of reservoirs (Kosnik, 2010; Fearnside, 2014; Kishore et al., 2021; Yildiz et al., 2021), are not impact-free. In particular, cascade RoR plants on the same river have a significant compounding effect on river ecosystems, even though their storage capacity is negligible (Jaccard et al., 2011; Finer and Jenkins, 2012; Kelly-Richards et al., 2017). Environmental downsides mean that this kind of project should be approached with extreme caution if their financial robustness is not guaranteed. This uncertain financial robustness was apparent across all five of our case-studies, and could plausibly be present in other regions where the best sites for hydropower have already been developed. In particular, our findings suggest that the financial robustness of proposed hydropower projects often hinges on favorable socio-

economic conditions. If the outlook for interest rates is uncertain, or if investors are not sure of how the factors that lead to high cost overruns are managed, considering not developing the site might be a wise option given potential environmental impacts. Cost overruns are determined by underlying geology and a mix of environmental, social and management factors leading to design revisions (e.g., Ansar et al., 2014; Sovacool et al., 2014; Ray et al., 2018) – considering not developing the site might be a wise option given potential environmental impacts. In fact, environmental issues, along with site geology, have been identified as the foremost risks to hydropower projects (Kucukali, 2011). A possible extension of our framework for real-world application should integrate the environmental risk assessment into the analysis.

4.7 Conclusions

This paper introduces the HYPER-MORDM approach, which combines global optimization with multiobjective evolutionary algorithms (MOEAs) and many objective robust decision making (MORDM). This is to tackle the challenges associated with run-of-river (RoR) hydropower plant design under deep uncertainty, in order to (1) provide insights into potential trade-offs between design objectives and (2) to explore the financial robustness of alternatives. This research advances conventional RoR hydropower plant design, which typically relies on cost-benefit analysis, by incorporating recent advancements in decision-making under deep uncertainty. It is also the first study to explicitly incorporate variable turbine efficiency into the robust design of hydropower plants, including reservoir-based hydropower plants.

Applying HYPER-MORDM to five planned RoR hydropower plants planned in a range of hydro-climatic regions of Turkey led to several insights on robust RoR plant designs. Results confirm earlier findings that installation of more than one turbine in a hydropower plant enhances power production significantly by providing operational flexibility in the face of variable streamflows. This finding aligns with current industry practices, where the consideration of multiple turbines is common due to the simplicity of installation, maintenance benefits, and ensuring a minimum level of operation if economically feasible. When contrasting robustness of a design with its NPV, designs with the highest NPVs tend to focus on harnessing above-average flows, but this comes at the expense of financial robustness in the face of both

climate change (and associated drying) and to evolving financial conditions. In contrast, maximising the benefit cost ratio (BC) yields more financially robust solutions than maximising NPV, as it leads to less costly designs that generate slightly less revenue on average, but with increased flexibility to better exploit low flows. Traditional design approaches using identical turbine configuration and NPV maximisation have been shown to be significantly more vulnerable to climate change, and identical turbines can lead to inferior designs even under historical conditions. This is due in a large part to a less flexible configuration. These results hold even when applying a significant 10 % discount on the cost of electro-mechanic equipment. Another consequential finding is the importance of non-climatic factors, which can be more crucial than climatic ones in determining a design's financial robustness. High cost overruns have been found to often make a project non-viable and are often overlooked in the hydropower design literature. High cost overruns often reflect poor project management, including overlooking social and environmental constraints, and errors in screening a site's geology before the start of construction.

Last but not last, this study adds to a growing body of literature stressing the importance of considering multiple uncertainties in combination, and it demonstrates it for the financial robustness of RoR plant design. Taken together, these results suggest that applying HYPER-MORDM approach in the design of run-of-river hydropower plants provides water resource planners and decision makers a comprehensive framework to make informed decisions regarding the implementation of these projects and determining the most robust design alternative under deep future uncertainties. This work also stresses the need for considering turbine efficiency in hydropower plant design, including when they are part of a reservoir system. This is currently not the case, even in the middle of a global hydropower boom, and as many existing plants, large and small, will need to upgrade their turbine systems in the coming years.

MOEA benchmarking

Multiobjective evolutionary algorithms (MOEAs) represent a class of optimization algorithms widely acepted and valued for addressing real-world optimization challenges (Vachhani et al., 2015). These algorithms are particularly suited for tackling multiobjective optimization prob-

lems characterized by multiple conflicting objectives and a set of Pareto optimal solutions. MOEAs are able to approximate the Pareto optimal set by evolving a population of solutions (Zhou and Li, 2011). In this study, the search tasks aimed at generating alternatives were executed using the Amalgam MOEA. This MOEA introduces an innovative approach of adaptive multi-method search by simultaneously integrating four sub-algorithms within its framework: NSGA-II, adaptive Metropolis search, particle swarm optimization, and differential evolution (Vrugt and Robinson, 2007). The Amalgam MOEA is chosen for several compelling reasons. Firstly, it is widely recognized for its efficiency in solving complex optimization problems. The method is renowned for its ability to discover a well-distributed set of Pareto solutions within a single optimization run—a capability crucial for addressing multi-objective optimization challenges effectively (Vrugt, 2015). Furthermore, the Amalgam MOEA consistently demonstrates superior performance compared to other commonly used methods such as SPEA2, NSGA-II, and MOEA/D (Khan et al., 2015; Vrugt, 2015). Its track record of success and widespread adoption within the optimization community underscores its suitability for our study's objectives. We benchmarked Amalgam MOEA against Borg MOEA because the latter has been repeatedly proven to perform consistently well in solving complex multi-objective problems thanks to its self-adaptivity (Reed et al., 2013; Salazar et al., 2016; Gupta et al., 2020). Borg MOEA combines adaptive operator selection with ϵ -dominance, adaptive population sizing and time continuation (Hadka and Reed, 2013). This is why we did the benchmarking under the most complex formulation we are exploring in this work, i.e., the three-objective one given by equation (4.12). The performance of the two MOEAs was compered using the hypervolume indicator which is a set measure used in evolutionary multiobjective optimization to evaluate the performance of search algorithms and to guide the search (Auger et al., 2009). The two MOEAs were found to be statistically indifferent from each other for the proposed approach. What is more, the computational time required to reach desired hypervolume levels with the same number of functional evaluation was 30 % lower for Amalgam MOEA.

Data availability statement

All the data related to the five case studies, including the input parameters, the MATLAB scripts for multi-objective optimization, and robustness analysis, are openly accessible from the Zenodo open-access repository (Yildiz et al., 2024b) at https://doi.org/10.5281/zenodo.10627287. Additionally, presented robustness analysis data for each case study are provided in the University of Sheffield's data repository due to their large size at https://doi.org/10.5281/zenodo.10627287. The repository includes the pre-calculated robustness results, allowing researchers to review and analyze the robustness without the need to re-run the analysis.

CHAPTER 5

Computationally inexpensive robust RoR hydropower plant design

Abstract[1]

This paper introduces the HYPER-FORD toolbox for Fast Operation-optimized Robust Design of run-of-river HYdroPowER plants. Compared with existing design software, it (1) integrates optimized turbine operations into design optimization instead of following predefined operational rules, and (2) combines this with a regular sampling of the flow duration curve to significantly reduce data inputs. Our rigorous benchmarking demonstrates that (1) operation optimization improves design performance at low computational cost, whilst (2) data input reduction slashes computational costs by over 92% with minimal impact on design recommendations and key robustness analysis insights. Taken together, these innovations make integrated design and operation optimization, complete with in-depth robustness analysis, laptop-accessible. They also reinforce sustainability efforts by minimizing the need for high-performance computing and large associated embodied greenhouse gas emissions.

[1] Yildiz, V. and Brown, S. and Rougé, C., 2024. Robust and computationally efficient Design for Run-of-River Hydropower. Environmental Modelling & Software (under review)

5.1 Introduction

Small hydropower plants (SHPs) offer an environmentally friendly and cost-effective alternative to conventional dam-based plants (Tsuanyo et al., 2023). While only 36 % of their global potential is currently tapped (UNIDO, 2022), a significant global expansion is expected (Couto and Olden, 2018), including in industrial nations where the best sites for large-scale hydropower are already taken such as Europe (Kuriqi et al., 2020; Kishore et al., 2021). The majority of SHPs follow the run-of-the-river (RoR) scheme (Yildiz and Vrugt, 2019), relying on the dynamic flow of rivers for hydropower generation due to their sub-daily storage capacity. Out of over 3,000 power plants of 1 MW capacity or more, either planned or under construction, notably in emerging economies (Zarfl et al., 2015), RoR plants account for more than 75 % of the total (Bejarano et al., 2019). This momentum ensures that hydropower will remain a key electricity supply source globally in decades to come (Winemiller et al., 2016; Gernaat et al., 2017; Pokhrel et al., 2018; Moran et al., 2018). It also aligns with the seventh Sustainable Development Goal (SDG) of providing affordable, dependable, sustainable, and modern energy for all (McCollum et al., 2017; Dorber et al., 2020), whilst contributing to other SDG targets (Gielen et al., 2019).

RoRs designed today will be deployed in a world characterised by a changing climate and uncertain economic conditions. Observations from the Global Precipitation Climatology Center (Spinoni et al., 2014) and recent studies (Spinoni et al., 2018; Ault, 2020; Sreeparvathy and Srinivas, 2022; Yildiz et al., 2022; Fang et al., 2022) highlight increasing global trends in the frequency, length, and intensity of meteorological droughts. These trends could directly lead to increases in streamflow drought in the future over a wide range of climate zones in tropical and temperate regions (Cook et al., 2020; Zhang et al., 2023). RoR schemes lack the storage capacity to regulate seasonal discharge fluctuations, making them significantly more vulnerable to these changes than plants sited at the outlet of large reservoirs. Climate risks are compounded by the risks that socio-economic uncertainty also pose to the long-term viability of hydropower projects, and both should be considered simultaneously in project development (Shaktawat and Vadhera, 2021). In fact, there are documented examples of socio-economic risks being a more critical future uncertainty for the performance of a hydropower investment than climate change (Ray et al., 2018; Yildiz et al., 2024a). These

studies stress the importance of an integrated evaluation of the potential impacts of these uncertainties on the financial viability of hydropower investments as early as the planning phase.

Besides integrating uncertainty, hydropower plant design should also explicitly incorporate optimized operations. Yet, that is often not the case for RoR plant design where ad hoc operational rules are considered instead, primarily for computational simplicity (e.g., Anagnostopoulos and Papantonis, 2007; Mamo et al., 2018; Yildiz et al., 2024a). However, there is evidence that design and operation of hydropower infrastructure could be critically dependent on each other, including in situations where there is a need to address hydroclimatic variability, climate change and unintended consequences of development (Bertoni et al., 2019). To address this and achieve future-proof planning where investments remain financially resilient to perturbations, design and operations should be robust, i.e., able to withstand deviations from design conditions (Herman et al., 2015). Numerous frameworks (e.g., Lempert, 2002; Bryant and Lempert, 2010; Brown et al., 2012; Haasnoot et al., 2013; Kasprzyk et al., 2013) have been developed in recent years to integrate considerable future uncertainties and assess their impact on design, operations and adaptation in complex (water) infrastructure systems. Beside a common focus on robustness, they recognize that the multi-stakeholder, multi-purpose nature of these systems, combined with unquantifiable future uncertainty, lead to deep uncertainty (Kwakkel et al., 2016), whereby formulating the problem and its boundaries becomes a challenge in itself.

In water resource systems that include complex interactions between design variables and operation restrictions, both multi-objective optimization and robustness analysis typically demand a substantial amount of computing time and resources. These computational requirements become even more pronounced when conducting exploratory studies involving both steps (e.g., Quinn et al., 2018; Bertoni et al., 2019). They then create a need for large-scale computing solutions – High-Performance Computing (HPC) or cloud-based computing, and contributes significantly to the increasing need for large-scale computing solutions, including supercomputers and data centers (Hussain, Wahid, Shah, Akhunzada, Khan, Amin, Arshad and Ali, 2019; Lannelongue et al., 2021). In turn, this quest for enhanced processing capacity raises environmental concerns (Hernandez et al., 2018; Katal et al., 2023), because

the electricity that needs to be mobilized for the continuous use of computational facilities contributes to climate change, resource depletion, and strain on local power infrastructures (Bharany et al., 2022). Thus, scientific and large-scale technical computing presently account for 0.3 % of global carbon emissions, and this share is likely to increase in the future (Jones, 2018; Cao et al., 2022*a*; Katal et al., 2022), creating an additional, considerable challenge to global climate change mitigation measures. As the need for large-scale computing grows, finding innovative technical solutions that balance these computing demands with energy economy and environmental responsibility becomes critical. These solutions will also remove barriers to application of these methods beyond actors in industrialised nations – academia and corporations – that often lack the human and physical infrastructure to use the most largest computing facilities.

This study proposes approximations to slash the computational requirements associated with the robust design of RoR hydropower plants, without compromising accuracy and in fact, by explicitly incorporating optimised operations into design for the first time. This integrated novel approach is encapsulated in the HYPER-FORD toolbox, standing for for Fast Operation-optimized Robust Design of run-of-river HYdroPowER plants. It aims to make robust design and analysis more accessible thereby accelerating decision-making processes significantly. Moreover, it aims to reinforce sustainability efforts by reducing dependence on high-performance computing and mitigating carbon emissions from data centers.

The methodological steps employed in this paper, which also dictate its organization, are provided in Figure 5.1. In Section 5.2, we summarize the robust RoR hydropower design approach introduced in Yildiz et al. (2024a) which is our starting point for this paper. This is followed by the introduction of the case studies used to benchmark the innovations included in HYPER-FORD. Section 5.3 then introduces the HYPER-FORD toolbox and its two innovations; (3.1) HYPER$_{OP}$ module for coupled design and operation optimization and (3.2) a discretization of the flow duration curve (FDC) to strategically reduce data input and enhance computational efficiency. Following this, in Section 5.4, we detail the methodology for benchmarking our innovations. Benchmarking results in Section 5.5 then validate these innovations. Lastly, in Section 5.6, we discuss the broader implications of our results, explore opportunities for future research, and conclude this paper with a summary of our main

findings.

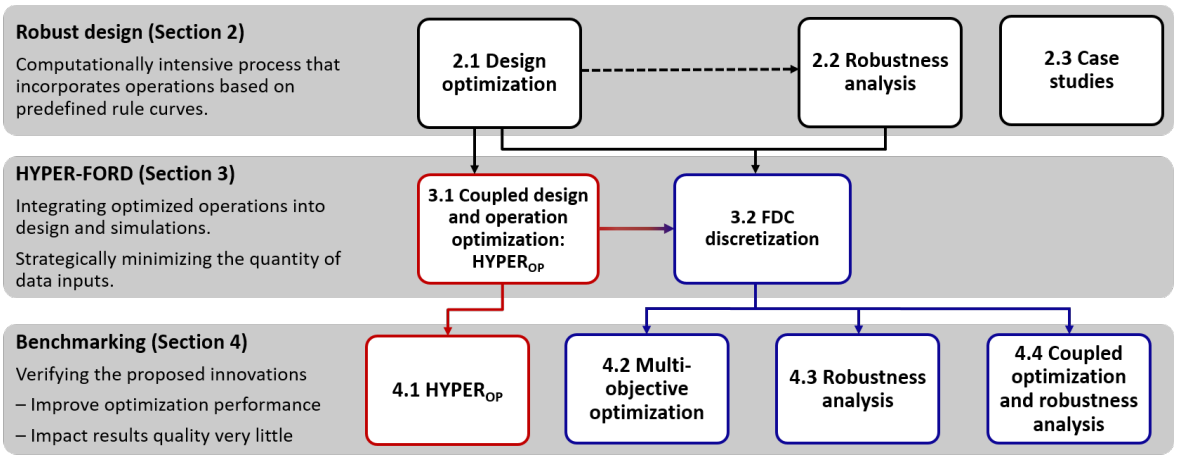

Figure 5.1: *Flowchart outlining methodological steps for developing our computationally inexpensive robust design approach.*

5.2 Robust design: HYPER-MORDM framework

From this point on, we call HYPER-MORDM the analytical framework developed in Yildiz et al. (2024a) that merges the Many Objective Robust Decision Making (MORDM) approach (Kasprzyk et al., 2013) with the versatile capabilities of the HYPER toolbox (Yildiz and Vrugt, 2019). HYPER is a state-of-the-art RoR plant design toolbox that identifies optimal design parameters for user-selected power production or financial performance metrics. As depicted in the upper grey box in Figure 5.1, the HYPER-MORDM comprises of two main steps: design optimization with multiple financial objectives (Section 5.2.1) and robustness analysis (Section 5.2.2).

A key element in both stages of HYPER-MORDM in the use of FDCs, defined as cumulative frequency curves depicting streamflow (e.g., at a planned RoR plant site) as a function of percentage of time discharge is equaled or exceeded within a specified climate state (Vogel and Fennessey, 1994). A FDC represent the full range of hydrological conditions available at a catchment's outlet (Yilmaz et al., 2008; Sadegh et al., 2016). It serves as an essential tool in the design of small hydropower systems including RoRs (Basso and Botter, 2012; Yildiz and Vrugt, 2019). FDCs are serving not only during optimization purposes, but also as a basis

for synthetically generating plausible futures for robustness analysis (Yildiz et al., 2023a). We now describe in detail the two main steps of HYPER-MORDM.

5.2.1 Design optimization

HYPER-MORDM conducts design optimization based on financial performance metrics that rely on lifetime expected net present benefits and costs. The lifetime expected net present revenues from hydropower production are given by:

$$\mathrm{R} = \sum_{y=1}^{L_s} \frac{R_y}{(1+r_y)^y} \tag{5.1}$$

where L_s is the project's lifetime, typically 50 years, and $\mathbf{R} = \{R_1 \ldots, R_{L_\mathrm{s}}\}$ and $\mathbf{r} = \{r_1, \ldots, r_{L_\mathrm{s}}\}$ are vectors of length L_s of the annual plant revenues assuming an average hydropower production throughout the year (by default in USD) and the annual interest (discount) rate in %, respectively. Similarly, the lifetime net present cost of a RoR hydropower plant design, which significantly depends on site-specific factors, can be expressed as:

$$\mathrm{C} = C_\mathrm{Tp} + \frac{C_\mathrm{Rem}}{(1+r_{HL})^{HL}} + \sum_{y=1}^{L_s} \frac{C_\mathrm{om}}{(1+r_y)^y} \tag{5.2}$$

where C_Tp is the investment cost, C_Rem is the the renovation and reconstruction cost of electro-mechanic equipment at year HL halfway through the plant's lifetime, typically at year 25, and C_om is the yearly maintenance and operation cost. Each component of benefit and cost equations is discussed in detail in Yildiz and Vrugt (2019).

Net present revenue and cost can be combined into the net present value (NPV), defined as the value of projected cash flows discounted to the present (Santolin et al., 2011):

$$f_\mathrm{NPV} = R - C \tag{5.3}$$

They can also be combined into a ratio, the benefit-cost ratio (BC):

$$f_\mathrm{BC} = \frac{R}{C} \tag{5.4}$$

Whereas NPV focuses on the expected profit, the BC focuses on the risk of the projects (Anagnostopoulos and Papantonis, 2007; Basso and Botter, 2012). Thus, maximizing the NPV leads to a design that offers the highest return, whereas maximizing the BC would

result in design with lower investment costs compared with expected revenue, and therefore diminished financial risks.

The HYPER-MORDM framework allows or both single and double objective formulation using f_{NPV} and f_{BC} as design objectives. The two objective formulation enables the user to trade-off the most commonly used traditional design objective (NPV) with another financial objective assumed to be more focused on project risks:

$$F(x) = \max[\ f_{\text{NPV}},\ f_{\text{BC}}] \tag{5.5}$$

where x is the vector of decision variables including all the key design parameters such as turbine type, turbine number, turbine's installed capacities, penstock diameter. In this approach, we employ simulation optimization to compute energy generation for each day of a multi-decadal flow record, represented by its FDC. Using daily multidecadal flow records is standard practice in simulation-optimization of water resource systems (e.g., Quinn et al., 2018; Bertoni et al., 2019).

5.2.2 Robustness analysis

The HYPER-MORDM approach involves evaluating the performance of alternatives identified during optimization across a range of plausible futures. This implies defining ranges for relevant parameters, then sampling an appropriate number of plausible climatic and socio-economic futures. In particular, sampled hydro-climatic parameters are used to derive FDCs (Yildiz et al., 2023a). In Panel A of Figure 5.2 (adapted from Yildiz et al.), the blue line represents the FDC of long-term historical observations at a possible development site in Turkey, while the gray lines depict plausible future FDCs across a range of drier and more variable futures. Each sampled FDC is disaggregated into 50 long-term time series of daily discharge values generated using the Kirsch-Nowak streamflow generator developed by Quinn et al. (2017), to model the natural variability of each climate (Panel B in Figure 5.2).

These flows are then used for robustness quantification. Each time series' duration aligns with the typical licensing duration of a RoR hydropower project in the jurisdiction where a project is being considered. The HYPER-MORDM approach focuses on financial robustness based on two key financial viability metrics, (1) the payback period (PB) and (2) NPV. The PB, is a metric that shows the length of time required to recover capital investments, is

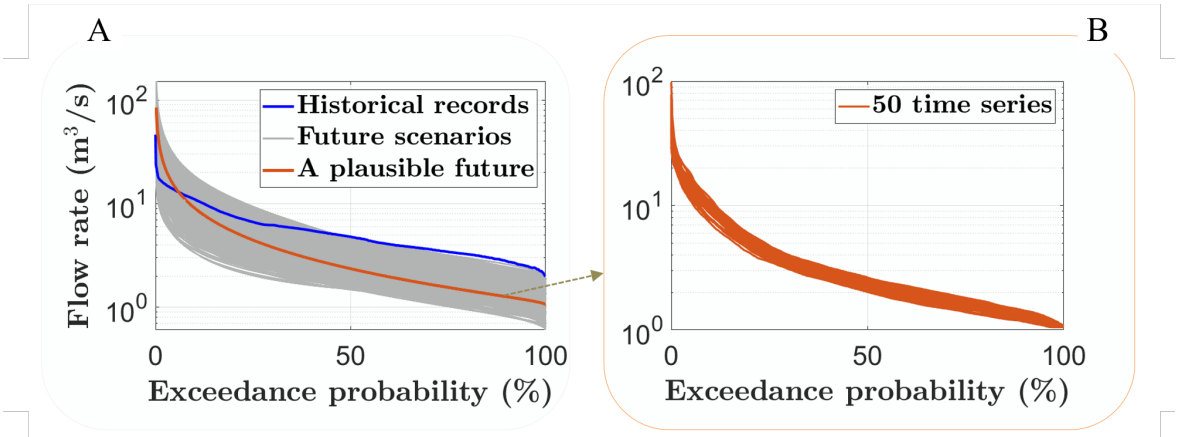

Figure 5.2: *Panel A: Plot of the flow duration curves (FDC) of of observed discharge (blue line), future flows (gray lines) and a random future (orange colour). Panel B: Desegregation of the selected future (orange colour) to 50 time series (orange lines). The X-axis denotes the exceedance probability, while the Y-axis logarithmically scales the flow rate.*

computed as;

$$PB = \frac{C_{Tp}}{\overline{R} - C_{om}} \tag{5.6}$$

where C_{Tp} it the investment cost defined in equation (5.2), and the denominator is the project's expected amount of annual net cash inflow.

Both NPV and PB metrics form the basis of robustness metrics based on satisficing criteria (Herman et al., 2015), i.e., by comparing their values to desirability thresholds. Typically, small hydropower projects are deemed viable when the PB is below 15 years (Alonso-Tristán et al., 2011; Girma, 2016; Ak et al., 2017). Consequently, for each of the 50 time series defined for each plausible future, we establish robustness using PB as a binary variable:

$$\mathrm{RM}_k = \begin{cases} 0, & \mathrm{PB} > 15; \mathrm{years} \\ 1, & \mathrm{PB} \leq 15; \mathrm{years} \end{cases} \tag{5.7}$$

Success is attributed to each plausible future if, for at least 75% of the time series (i.e., 38 or more out of 50), RM_k is confirmed to be 1. The binary variables are also aggregated across all realizations of all plausible future to create an average robustness score, denoted as RM_{PB}.

We use a similar approach to calculate the robustness metric based on NPV, RM_{NPV}. For each of the 50 time series we define robustness as a binary variable:

$$\mathrm{RM}_k = \begin{cases} 0, & \mathrm{NPV} > 0 \\ 1, & \mathrm{NPV} \leq 0 \end{cases} \tag{5.8}$$

Then, we define a future as success or failure depending on whether NPV>0 over 75% of the time. Alternatively, we aggregate over all 50 time series over all futures to compute RM_{NPV}. In-depth rationale of the determination of objective functions and derivation of robustness metrics are available in (Yildiz et al., 2024a).

5.2.3 Case studies: physical characteristics and uncertainties

This subsection introduces the case studies to which the HYPER-MORDM approach and the innovations introduced in HYPER-FORD are applied, including how climatic and socio-economic uncertainties are considered.

Case studies description

We consider five proposed RoR hydropower plants in Turkey (Yildiz et al., 2024a). The top panel of Figure 5.3 (adapted from Yildiz et al.) illustrates the diverse hydro-climatic settings of the five case studies, as indicated by the Köppen-Geiger climate classification based on four high-resolution climatic maps spanning from 1980 to 2016 (Beck et al., 2018). Besik and Kaplan RoRs have a Mediterranean-influenced humid continental climate, while Buyukdere RoR experiences a humid continental climate. Tepe RoR is situated in a humid subtropical climate area, and Karacay RoR falls under the Mediterranean climate. Table 5.1 summarises the site and streamflow characteristics of these case-studies. The coefficient of variation (CV) represents the ratio of the mean to the standard deviation of the daily streamflow time series, and different values reflect the distinct hydrological and hydro-climatic conditions across our catchments. This variability is further highlighted in Table 5.1, which presents a range from 1 to 6 in mean flows and demonstrates a threefold difference between the highest and lowest values of the coefficient of variation (CV) across the sites. Cross-catchment variations in precipitation patterns and watershed attributes such as land use, soil type, and slope contribute to distinct hydrological features, are also evident through

Table 5.1: Hydrological and site characteristics of the RoR hydropower plant case studies.

Case Study	**Mean** [m^3/s]	**Coefficient of Variation** [-]	**Environmental flow** [m^3/s]	**Gross Head** [m]	**Potential GAAE** [GWh]
Besik	5.8	0.59	0.63	117	58.31
Buyukdere	1.88	1.09	0.156	394	63.65
Tepe	6.22	1.39	0.662	56	29.93
Karacay	1.47	1.69	0.18	134	16.92
Kaplan	1.07	1.08	0.12	190	17.47

the normalized FDCs in the bottom panel of Figure 5.3. In-depth descriptions of the case studies, including climatic aspects, are available in Yildiz et al. (2024a). Table 5.1 also shows the fraction of river discharge designated for maintaining minimum environmental flow and supporting ecosystem services, as regulated by state authorities. Finally, the table shows the gross hydraulic head available at each site, and the gross potential annual average energy (GAAE) of each site, computed by taking into consideration the available gross head or water pressure, and average long-term discharge. Note that this calculation ignores frictional and minor losses, the influence of flow variability on turbine efficiency, and the fact that flows exceeding the design discharge capacity do not produce hydropower.

Most of the precipitation at Besik, Kaplan, and Buyukdere hydro sites occurs as snow during winter. The snowpack at these locations serves as a natural reservoir, ensuring a steady water supply during the drier summer months. This results in less variability in low-flow ranges compared to the other two sites. Additionally, Besik and Kaplan RoRs boast the highest potential energy, as indicated in Table 5.1. These catchments' capacity to store precipitation typically reflects in a gradual slope in the middle portion of the FDC (Yilmaz et al., 2008), with Besik exhibiting the mildest slope among the cases. Among all the sites the Besik RoR is anticipated to be the most profitable according to traditional assessments of RoR plants. Therefore, this site will be used for all benchmarking steps, whereas the other four sites will be used primarily to verify that the full HYPER-FORD methodology works as intended.

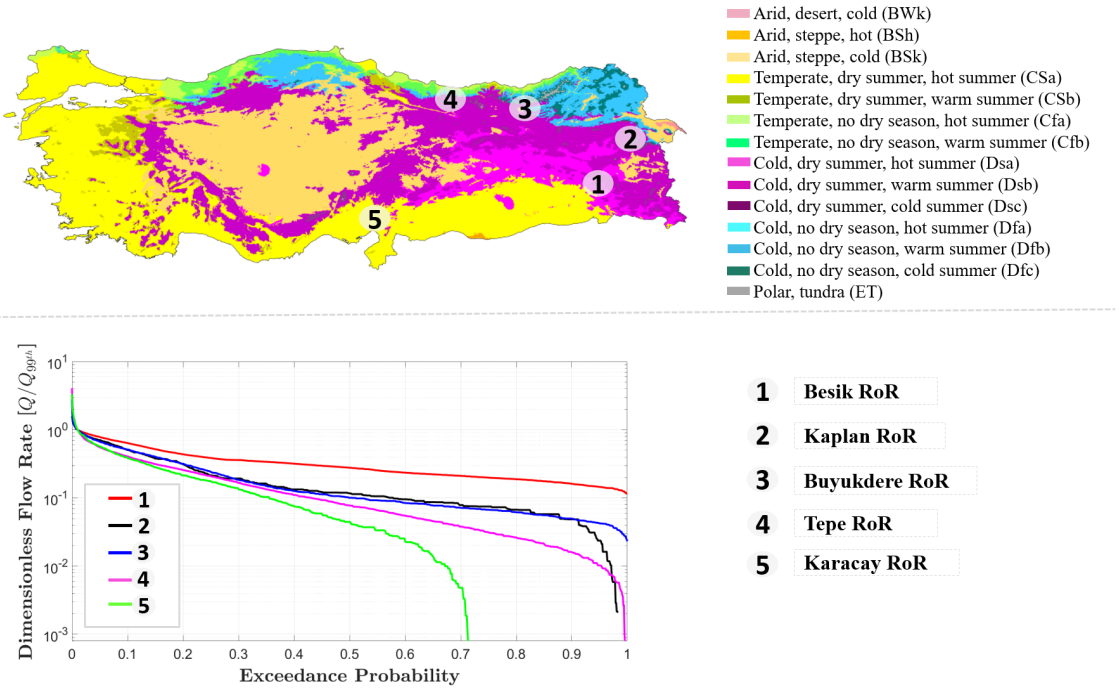

Figure 5.3: *The top panel displays the geographical locations of the five case studies on the Köppen-Geiger climate classification map of Turkey (Beck et al., 2018). In the bottom panel, Flow Duration Curves (FDC) for these case studies are shown, with normalization applied using the* 99^{th} *percentile of the flow. The flow rate values on the y-axis are presented logarithmically.*

Plausible futures

Seven uncertain factors are defined and these deeply uncertain factors are assigned sampling ranges to each, as summarized in Table 4.3 to create plausible futures. Note that multiplier ranges in this Table represent plausible rather than probable values. They provide a mechanism for understanding how wrong our baseline model assumptions can be before significant vulnerabilities to deep uncertainties occur (Herman et al., 2014). The 4 economic multipliers in this analysis are interest (discount) rate, r, cost overruns, C_{or}, during construction, and two energy prices, reflecting Turkey's energy regulations; p_{1-10} is fixed for the first 10 year by the Turkish government, including subsidies and $p_{>10}$ is the energy price for the remainder

of the project's lifetime. The 3 hydroclimatic multipliers are streamflow statistics: its median, coefficient of variation and first percentile. A comprehensive justification for all these parameters and their associated sampling ranges can be found in the supporting information for Yildiz et al. (2024a).

Once the variable ranges are set, we generate a 7-dimensional Latin Hypercube Sample of 500 plausible futures to represent the the deep uncertainties across socio-economic and hydroclimatic futures. Note that we use the three hydroclimatic parameters to parameterise a unique FDC for each plausible climate future (Yildiz et al., 2023a).

Table 5.2: Variables and sampling ranges used for robustness analysis. SF is for scaling factor, and a SF of 1 indicates baseline conditions. The initial four are economic parameters, while the three hydroclimatic parameters (highlighted in blue) pertain to streamflow statistics used in the construction of future streamflow time series.

Uncertain Factor	**Current Value**	**Lower Bound**	**Upper Bound**
Interest (discount) rate (r)	0.095	0.03	0.15
Energy price, first 10 years (p_{1-10})	5.5	5	6.5
Energy price, rest of the years ($p_{>10}$)	5.5	3	6.5
Cost overrun (C_{or}) SF	1	1	3
Median SF ($\tilde{m}$) SF	1	0.3	1
Coefficient of Variation (CV) SF	1	1	2
1st percentile (P_{1st}) SF	1	0.3	1

5.3 HYPER-FORD toolbox

We now move to the middle grey box of Figure 5.1, where we introduce the HYPER-FORD toolbox and its innovations for robust and computationally efficient optimal design. The HYPER-FORD toolbox comprises two sub-modules. In Section 5.3.1, we introduce the optimization module, HYPER$_{OP}$, tailored for joint design and operation optimization. Subsequently, in Section 5.3.2, we present the FDC approximation module build upon HYPER$_{OP}$ aimed at enhancing computational efficiency through regular sampling of the FDC.

5.3.1 Coupled design and operation optimization: HYPER$_{OP}$ module

In the earlier versions of the HYPER toolbox (Yildiz and Vrugt, 2019; Yildiz et al., 2024a), the distribution of available inflow between the different turbines was regulated by operational rules that reflect engineering practice. According to these rules, and outside of the extreme cases where turbines shut down in instances of very small or excessively large river discharge, water is allocated to the maximum number of turbines at full capacity, with any remaining flow directed to other turbines capable of operation. This approach does not explore alternative operational modes that could result in higher power production. For instance, two turbines operating efficiently at 75 % capacity may generate more power than one turbine at full capacity and another at a lower capacity, as the latter may result in reduced efficiency or even shutdowns due to technical constraints.

To address these issues, this study presents a new version of HYPER, called HYPER$_{OP}$ – where 'OP' stands for the first two letters of both words in "operation optimization". HYPER$_{OP}$ integrates optimized turbine operations into the design process, optimizing the allocation of flow to turbines during the simulation phase. This optimization ensures that the allocation of turbine flow is aligned with their unique characteristics, thereby enhancing overall efficiency. The operation optimization module (OP module), nested within the optimization algorithm, is presented in Algorithm 9 as pseudo-code. For each set of design parameters generated by the optimization algorithm, the OP module initially defines the operating range within which turbines can generate energy (minimum flow and maximum flow). It then divides this range into $I = 1000$ discrete steps. For each step, the OP module generates $J = 1000$ random samples of turbine numbers and their corresponding operation capacities to simulate energy generation. We propose $I = 1000$ and $J = 1000$ as our testing indicated it was enough to reliably provide operation optimization for designs up to 3 turbines, the maximal number of turbines considered for small (<10MW) RoR hydropower plant design. Following this process, the OP module records the optimal settings derived from these samples, thereby constructing a table of operation modes for use in subsequent simulation optimization. In cases where there are less than 1000 flows considered in the operational range of the plant, such as in FDC discretization detailed in Section 5.3.2, the OP module relies solely on these flows to determine operation modes. This study represents

Algorithm 1: Pseudocode for operation optimization algorithm

input : Turbine configuration parameters: type, number, capacities

output: Table of operation modes for each configuration

```
for Each sampled turbine configuration: type, number, capacity do
    Determine each turbine's flow range: min flow and max flow;
    Divide the flow range into I = 1000 discrete steps;
    for i = 1, ..., T do
        Draw J = 1000 random samples of turbine numbers and their operation
         capacities;
        for j = 1, ..., J do
            Simulate energy generation;
        Determine and record the sample j* that maximizes energy generation;
    Create a table of operation modes for the current turbine configuration;
```

the first instance of coupled design and operation optimization for RoR hydropower plants without any limitations on turbine configuration for up to three turbines. By contrast, traditional configurations involve identical turbine, or in three-turbine setups, one small and two large turbines.

Figure 5.4 showcases the optimized operating modes of a triple Francis turbine configuration, having one small turbine (T_1, with a design discharge of 5 m^3/s) and two large turbines (T_2, each with a design discharge of 10 m^3/s). The operational range (top panel) is finely divided into 1000 increments spanning from the minimum flow rate of 2 m^3/s (equivalent to 40 % of T_1's design discharge) to the maximum flow rate (design discharge) of 25 m^3/s. In the bottom panel, the operational modes of the turbines and their respective operating capacity are provided based on the incremental steps outlined in the top panel. Notably, turbines are programmed to shut down when the flow rate falls below their technical minimum flow rate. Subsequently, only the small turbine operates until the flow rate reaches a level efficient for the activation of the second and third turbines. All three turbines operate at full capacity when the flow rate surpasses the design discharge. This visualization offers comprehensive insights into the optimized operational dynamics of the turbine system across varying flow

conditions.

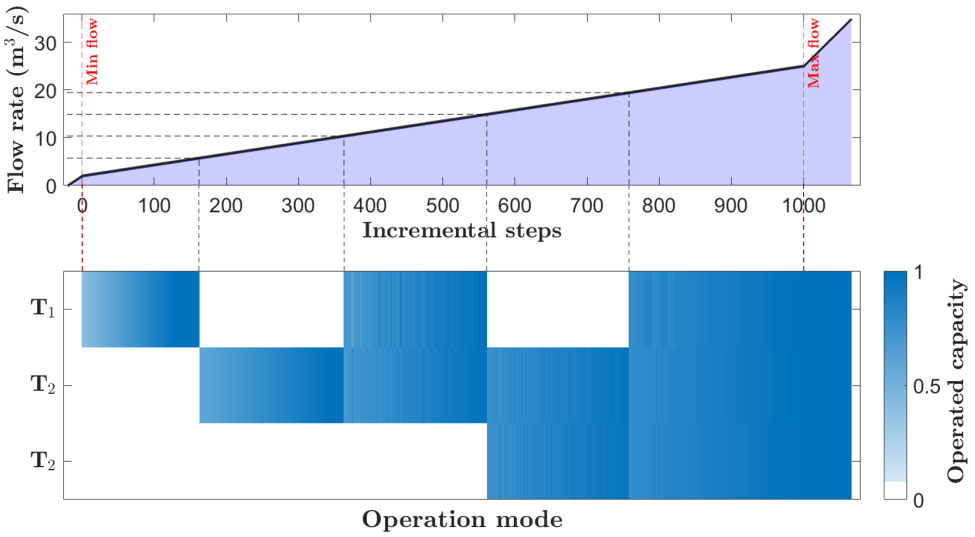

Figure 5.4: *Top panel: The operational range of a triple Francis turbine setup featuring one small turbine (T_1, design discharge: 5 m^3/s) and two large turbines (T_2, 10 m^3/s each). The range is discretized into 1000 increments between the minimum (2 m^3/s, corresponding to 40 % of T_1's design discharge) and maximum (25 m^3/s) flow rates. Vertical black dashed lines delineate transitions between turbine operating modes. Bottom panel: Representation of the respective operational modes of the turbine(s) with their operated flows depicted based on the incremental steps outlined in the top panel. The color bar indicates turbine operation capacity, with white representing no operation and darker blue indicating higher capacity.*

5.3.2 Flow duration curve discretization: approximation module

A multi-year daily FDC can be approximated by a small number of values, regularly spaced on the x-axis. Figure 5.5 illustrates this, and features 27 years of the daily flows for the Besik case study, resulting in 9860 daily discharge values. It also shows a sampling using N = 50 discharge values (depicted as black dots). It is evident that this regular sampling, in lieu of several decades of daily flows significantly reduces the computational costs associated to the performance evaluation of each design, both during simulation optimization and during robustness analysis. This is particularly notable since each flow value is repeatedly used

in each iteration: for calculating hydraulic losses, for water allocation to the turbines, to evaluate the efficiency of the turbines, and to determine energy generation.

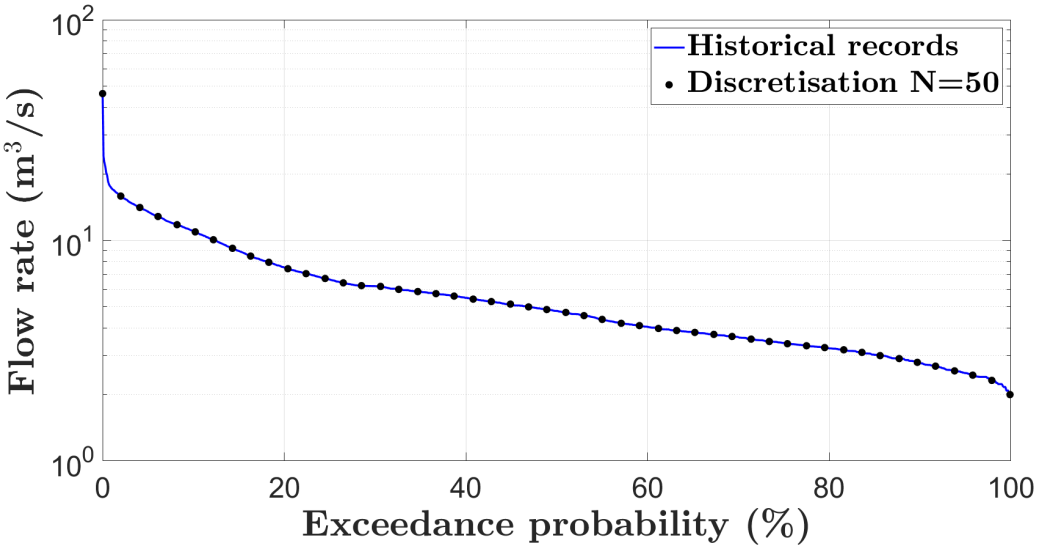

Figure 5.5: *Plot of the flow duration curves (FDC) of 27 years daily discharge record comprising 9860 data points (blue line) and $N = 50$ sampled flow rates (black dots).*

In the optimization process, we sample N evenly distributed points from the historical time series (black dots on Figure 5.5). Likewise, we apply this discretization to each of the 50 time series used to evaluate each plausible future during the subsequent robustness analysis. For both of these approximation steps, at each sampled point n ($1 \leq n \leq N$), we rely on the optimized operations provided by HYPER$_{OP}$ to yield the flow rate $q_k(n)$ at each turbine k of the K-turbine hydropower plant ($K \in \{1, 2, 3\}$). Then, the average annual power generation AAE that a K-turbine hydropower plant ($K \in \{1, 2, 3\}$) can produce over a year is given by:

$$AAE = Y_{\text{hr}}\ \rho\ g \sum_{n=1}^{N} \sum_{k=1}^{K} \eta_k(q_k(n))\ q_k(n)\ H_{\text{net}}(q_k(n)) \tag{5.9}$$

where Y_{hr} is the number of hours in 365 days, ρ is the volumetric mass density of water, g is the gravitational acceleration constant, H_{net} is the hydraulic head, and η_j is turbine efficiency. Note that both H_{net} and η_j are time dependent and vary as function of turbine inflow, penstock diameter and/or design flow, respectively. We can then approximate the

annual plant revenue as follows:

$$\text{Revenue in year } y, R_y = AAE * p_y \tag{5.10}$$

where p_y is the energy price during year y. This time dependence of energy price enables to incorporate regulatory price incentives, among other considerations. Consequently, it is being treated as constant to account for these incentives, thereby disregarding annual price fluctuations or intra-annual and intra-day variability in electricity prices. Computation of this revenue approximation enables that of both financial objectives (NPV and BC) and robustness metrics (RM_{PB} and RM_{NPV}).

5.4 Benchmarking the modifications to HYPER-MORDM

In this section, we describe the benchmarking experiments outlined in the bottom grey box of Figure 5.1. First, Section 5.4.1 details the methodology applied to benchmark of HYPER$_{OP}$. Sections 5.4.2, 5.4.3, and 5.4.4 explain the benchmarking methodology for using an approximation of the FDC, respectively in the optimization step, the robustness analysis step and when integrating both steps in a unified workflow. THe first three benchmarking steps only use the Besik RoR hydropower plant, as this is a typical candidate location for such a plant: this case study is anticipated to be the most profitable according to traditional assessments of RoR plants. The other four sites are used as an additional check on the quality of the full workflow of the HYPER-FORD toolbox in Section 5.4.4. Both design optimization and robustness analysis are performed using MATLAB on a computer equipped with an Intel(R) Core(TM) i7-10700 CPU operating at 2.9 GHz, supported by 16 GB RAM, and running the Windows 10 operating system. The analytical outcomes of all four benchmarking processes will then be presented in Section 5.5.

5.4.1 Benchmarking of HYPER$_{OP}$

The benchmarking of HYPER$_{OP}$ – joint optimization of design and operations – aims at comparing it with the original HYPER toolbox. In order to obtain the Pareto optimal set of alternatives, both HYPER and HYPER$_{OP}$ are integrated into a simulation-optimization setup with the Amalgam MOEA introduced by Vrugt and Robinson (2007) – the performance

of this MOEA was benchmarked in Yildiz et al. (2024a). All MOEA searches throughout this paper are conducted using a population size of $I = 100$ individuals and running Amalgam for $J = 1000$ generation, with an explicit two objective formulation (equation 5.5). We chose the two-objective formulation of equation (5.5) to benchmark the new toolbox, in order to provide a thorough analysis of HYPER$_{OP}$ increases solution quality of diverse solutions along the Pareto front.

In this benchmarking process, we assess HYPER$_{OP}$ in two distinct ways. Initially, for the problem, we carry out a HYPER optimization and a HYPER$_{OP}$ optimization to generate two distinct Pareto sets of alternatives. By comparing these Pareto sets, we aim to discern differences in the objective values of the alternatives, evaluating the HYPER$_{OP}$'s ability to produce designs with improved objective values and novel solutions. Subsequently, we take the set of design alternatives proposed by the original HYPER toolbox, and use them in HYPER$_{OP}$ in simulation mode to quantify how optimized operations increase the energy generation of each alternative. This step allows us to verify that HYPER$_{OP}$ functions as intended.

5.4.2 Benchmarking of FDC approximation during multi objective optimization

To benchmark multi objective optimization through the FDC approximation, we explore alternative designs (Pareto sets) generated using the HYPER$_{OP}$, still focusing on the Besik RoR hydropower plant. Initially, we generate a reference Pareto set with the long-term discharge record. Subsequently, we generate Pareto sets based on regular samplings of this discharge record, with sample sizes $N = 10, 25, 50, 100, 200,$ and 500. During optimization, the performance of solutions is evaluated using equations 5.9 and 5.10, with consideration given to the approximated revenue.

Our analysis assesses the performance of FDC approxomations by using classic key performance measures (Reed et al., 2013): hypervolume, generational distance, additive $\epsilon-$indicator, and run time. Hypervolume quantifies the volume of the objective space that is dominated by the provided set of solutions with respect to a reference point, ensuring this measure combines proximity and diversity (Hadka and Reed, 2012). Hypervolume computa-

tion requires defining an easily interpretable 0-1 scale, with 0 defined by an appropriate origin point. In our analysis, we begin by normalizing the objective functions and by placing the origin point as being 10 % worse than the worst value of each objective in the reference Pareto set (Ishibuchi et al., 2018), computed with the long-term discharge record. We consider the hypervolume of the reference Pareto set as 1. These choices enable a rigorous quantification of how far results using the FDC approximation are from those using the actual flow record. Hypervolume is complemented by generational distance (Van Veldhuizen, 1999), which calculates the average Euclidean distance between the solutions of the approximation set and the nearest member of the reference set. This metric primarily assesses convergence, yet it does not offer information regarding the diversity of the solution set (Blank and Deb, 2020). The additive $\epsilon-$indicator (Zitzler et al., 2003) evaluates the maximum distance needed to move an approximation set solution in order to dominate its nearest neighbor in the reference set. This metric is particularly sensitive to the presence of gaps and the overall diversity within the approximation set rather than convergence (Reed et al., 2013).

We also examine the optimization runtime for the long term record and each sample size, aiming to understand the relationship between sample size and run time, key to finding a good compromise between computational gains and solution quality.

Additionally, we further our analysis using an alternative metric, defined as the count of efficient solutions within the Pareto set. Alternatives generated from each FDC approximation are reevaluated with the long-term record to reveal their "true" objective values. Some solutions in the resulting set may be dominated – in the Pareto sense – by others. Our new metric evaluates the ability of approximations to generate solutions that would still be Pareto efficient with the full historical data at our disposal. These metrics, taken together, are intended to provide a comprehensive assessment of solution quality and trade-offs in our analysis, between improving run time and improving solution quality.

5.4.3 Benchmarking of FDC approximation during robustness analysis

Continuing from the previous section, we employ the Besik RoR to evaluate the effectiveness of the introduced sampling methodology in approximating robustness. For this, we compare robustness evaluations for solutions given by HYPER$_{OP}$ and obtained with the full historical

record. We proceed to evaluate the robustness of these same alternatives using the same sample of plausible futures. For each sampled future, we replace the 50 synthetically generated multi-decadal daily time series with sampling of these time-series with with varying sample sizes $N = 10, 25, 50, 100, 200, \text{and}; 500$. Similar to what happens in the optimization step, the methodology described in Section 5.3.2 is used to approximate hydropower production in benefits for each sampled FDC.

Compared with long-term future flow FDCs, we investigate the extent to which the relative ranking of alternatives based on their robustness is affected by FDC sampling . Said otherwise, we are examining whether an alternative that initially ranks high (or low) in robustness based on long-term future flows maintains that ranking when robustness is computed based on a small number of sampled point for each plausible future FDC. We specifically focus on alternatives having the highest objective values, such as the best NPV and best BC, as well as the most robust alternative. Additionally, we evaluate the runtime for each sample size to gain insights into how computational efficiency correlates with sample size and the quality of robustness results. Ultimately, our goal is to determine the sample size that offers a sufficiently accurate approximation of long-term futures in terms of robustness. This analysis is performed separately for the two defined robustness metrics.

5.4.4 Benchmarking of FDC approximation across the whole analysis

After benchmarking the impact of FDC approximations on optimization and robustness separately, we now aim at assessing the combined impact across the full workflow, both on run time and solution performance. We focus on how similar or different the design recommendations are, depending on whether we use the full historical record or a regularly spaced sample of it. For this, we use all five case studies presented in Section 5.2.3 to ensure that the approximation maintains performance across a range of site and climate characteristics. Initially, we generate design alternatives using the HYPER$_{OP}$ toolbox with long-term discharge records, with the same optimization setup as in Section 5.4.2. Subsequently, we assess their robustness across our sample of 500 plausible futures. Next, we generate design alternatives using the same experimental setup, but with the sample size of discharge records set to a value of N. We choose that value based on benchmarking results for the use of FDC approx-

imations in both optimization and robustness analysis steps. Following this, we quantify the robustness of alternatives across the sampled futures.

By comparing design alternatives and their robustness from long-term futures flows with those derived from selected sampled points, we aim to evaluate whether the overall approximated methodology produces similar robust designs. Our analysis of the design parameters specifically focus on key alternatives such as the most robust alternative, and alternatives with the highest NPV or BC value.After benchmarking the impact of FDC approximations on optimization and robustness separately, we now aim at assessing the combined impact across the full workflow, both on run time and solution performance. We focus on how similar or different the design recommendations are, depending on whether we use the full historical record or a regularly spaced sample of it. For this, we use all five case studies presented in Section 5.2.3 to ensure that the approximation maintains performance across a range of site and climate characteristics. Initially, we generate design alternatives using the HYPER$_{OP}$ toolbox with long-term discharge records, with the same optimization setup as in Section 5.4.2. Subsequently, we assess their robustness across our sample of 500 plausible futures. Next, we generate design alternatives using the same experimental setup, but with the sample size of discharge records set to a value of N. We choose that value based on benchmarking results for the use of FDC approximations in both optimization and robustness analysis steps. Following this, we quantify the robustness of alternatives across the sampled futures.

By comparing design alternatives and their robustness from long-term futures flows with those derived from selected sampled points, we aim to evaluate whether the overall approximated methodology produces similar robust designs. Our analysis of the design parameters specifically focus on key alternatives such as the most robust alternative, and alternatives with the highest NPV or BC value.

5.5 Results

In this section, we present results for the benchmarking exercises in the same order as they are presented in Section 5.4. We initially investigate the performance analysis and validation of optimization module of the HYPER-FORD toolbox, HYPER$_{OP}$ (Section 5.5.1). Our focus then shifts to HYPER-FORD toolbox combining HYPER$_{OP}$ with the FDC approximation analysis within the context of multiobjective optimization (Section 5.5.2), robustness (Section 5.5.3), and both steps combined (Section 5.5.4).

5.5.1 HYPER$_{OP}$ validation and performance

The performance analysis of the HYPER$_{OP}$ is depicted in Figure 5.6, with a comparison with the HYPER toolbox across the NPV (x-axis) and BC (y-axis) objective space. The design alternatives generated by optimization with HYPER (white dots) and HYPER$_{OP}$ (red dots) are compared in the panel A. Thanks to inbuilt operation optimization, HYPER$_{OP}$ clearly yields a diverse Pareto optimal set with higher objective values, offering a selection of design alternatives that effectively balance multiple objectives. This robust performance underscores its efficient optimization capability. It is interesting to observe a gap in the Pareto front of design alternatives generated through the HYPER toolbox, while no such gap exists in the Pareto front of design alternatives generated through HYPER$_{OP}$. This discrepancy emerges because HYPER solely depends on fixed operating conditions (rule curves), introducing technical constraints and limitations. On the other hand, HYPER$_{OP}$ benefits from built-in operation optimization, allowing flows to be efficiently allocated to the turbines to derive alternatives. Consequently, it can explore a more continuous and comprehensive range of design alternatives.

Upon reevaluating HYPER alternatives (white dots in panel A) using HYPER$_{OP}$ in simulation mode, we observe an increase in the objective values for all alternatives, as denoted by the blue triangles. We also observe a close correlation between optimal solutions yielded by HYPER$_{OP}$, and HYPER solutions reevaluated with HYPER$_{OP}$. This suggests that the improvement in objective values brought about by HYPER$_{OP}$ is mostly due to the operation optimization, and the increase in energy generation this leads to. Panel B, which presents a

comparison of energy generation performance between the two toolboxes for the same Pareto solution set (white dots in panel A), quantifies this increase. There is an approximate 2 % increase in energy generation for all the alternatives.

Together with the findings from the left panel, these results indicate that HYPER$_{OP}$ outperforms HYPER, primarily because it optimizes the operation that better captures streamflow variability instead of relying on operational rules for energy generation. This being said, the magnitude of the improvement is small, underscoring why operation optimization has been a low priority in design procedures in the past.

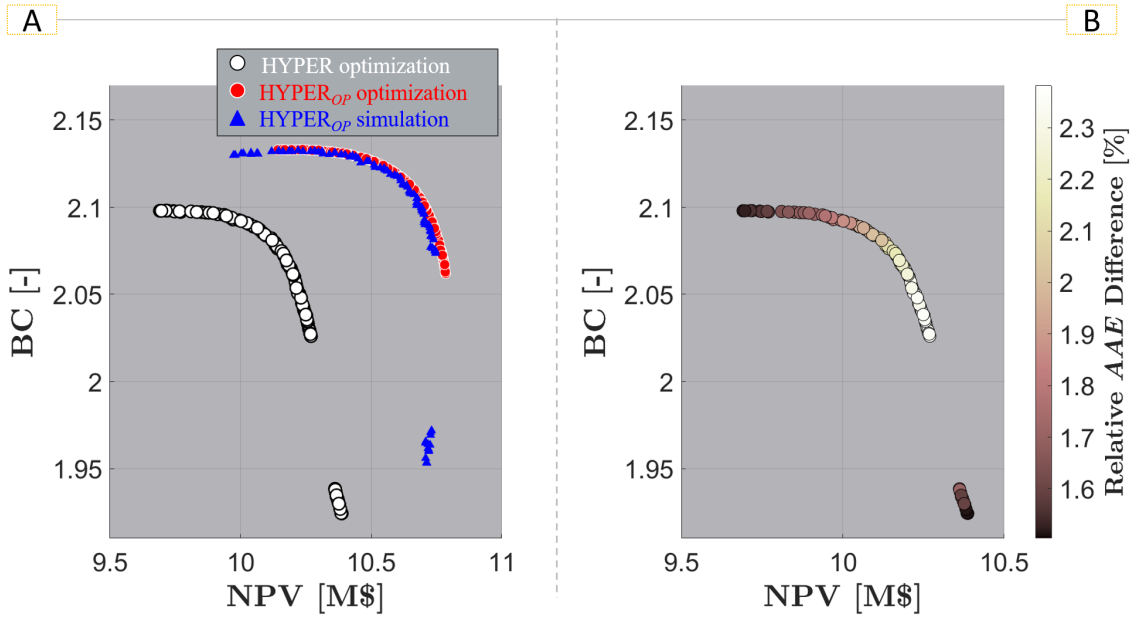

Figure 5.6: *Panel A: Pareto sets derived by HYPER (white dots) and HYPER$_{OP}$ (red dots) on the two-dimensional Benefit-Cost Ratio (BC) and Net Present Value (NPV, in million dollars) objective space. Blue triangles indicate HYPER solutions within the context of HYPER$_{OP}$. Panel B: Performance comparison of HYPER and HYPER$_{OP}$ for the same Pareto solution set. The color bar illustrates the relative annual average energy (AAE) difference between the two toolboxes, with light colors indicating higher relative differences (HYPER$_{OP}$ outperforming HYPER).*

5.5.2 FDC sampling impact on multi-objective optimization

In this section, we compare the results obtained from analyzing the design alternatives generated through FDC approximation with those derived from long-term records for the Besik case study. Table 5.3 provides a comparison of various performance metrics for optimization results using long-term records, vs. optimization results using N sample points, for different values of N. Additionally, it includes the run time required for robustness analysis, which will be discussed in the following section. Notably, the computational time required for generating alternatives is over 3.6 hours when using long-term records, whereas it is under 11 minutes for a sample sizes of $N = 100$ points, a factor of 20. The runtime's scaling with sample size is not linear, primarily due to the algorithm used for operation optimization (see Algorithm 9). Indeed, for long-term records, the OP module handles optimization tasks for a maximum of 1000 incremental flow rates, which somewhat limits gains from sampling. When sampling the FDC, the OP module only uses sampled points of the FDC that are within the flow range, which means that it handles only a subset of the N sampled points, resulting in non-linear scaling. Still in Table 5.3, the hypervolume performance for sample sizes of $N >= 50$ points is in close proximity to the Reference Pareto Front (RPF), indicating that the solution set exhibits both convergence and diversity. The generational distance for sample sizes of $N >= 100$ points closely approach the values from the reference Pareto front (RPF from now on). This indicates that the solutions have converged effectively, demonstrating the overall quality of the obtained solution set. Likewise, the $\epsilon-$Indicator for sample sizes of $N > 50$ points closely aligns with the RPF values, signifying the overall diversity within the approximation set is robust. As the sample size decreases below $N = 100$, the proportion of efficient solutions also decreases. In comparison, when $N >= 50$ points are considered, a substantial 80 % of the solutions fall within the Pareto set. Figure 5.7 provides a comparison between design alternatives obtained from $N = 10$ sampled points (blue dots, left panel) and $N = 100$ sampled points (red dots, right panel) with design alternatives derived from the RPF. The alternatives generated from sampled points (blue dots and red dots) are subsequently reevaluated using the long-term record to unveil their "true" objective values. Alternatives marked with triangles represent Pareto frontiers on both panels, indicating that these solutions dominate all other points within the set. It is evident that with a smaller

Table 5.3: Performance metrics for multi-Objective optimization and robustness analysis of long term discharge data and of different sample sizes ($N = 10$, 25, 50, 100, 200, and 500).

Number of Points	**Optimization Run Time (minutes)**	**Hypervolume**	**Generational Distance**	**Additive $\epsilon-$Indicator**	**Percentage of Efficient Solutions [0-100]**	**Robustness analysis Run Time (hours)**
10	1.37	0.94	$8.84\ 10^{-4}$	0.0064	53	0.81
25	3.05	0.97	$5.07\ 10^{-4}$	0.0053	72	1.45
50	5.24	0.98	$3.34\ 10^{-4}$	0.0104	77	1.61
100	10.28	0.98	$9.41\ 10^{-5}$	0.0032	85	1.69
200	31.72	0.98	$9.95\ 10^{-5}$	0.0.031	83	1.81
500	82.53	0.99	$9.86\ 10^{-5}$	0.0021	90	2.10
Long Term	216.96	1	0	0	100	26.32

sample size ($N = 10$), a large amount of solutions deviate from the RPF. However, for $N = 100$, it is clear that the re-evaluated Pareto front is very close to the RPF, and what is more, it comprises most design alternatives. This coincides with the metrics from Table 5.3, and illustrates the accuracy and reliability of optimization outcomes when regularly sampling $N = 100$ FDC points.

5.5.3 FDC sampling impact on robustness analysis

In this section, we provide a detailed examination of the robustness of the design alternatives forming the RPF used in the previous section, and the impact of FDC approximation on robustness results. In Figure 5.8, the parallel plot showcases various design alternatives. The top panel represents robustness metric RM_{PB}, while the bottom panel showcases RM_{NPV}, and both plots are organized in the exact same way. Each line represents one alternative and presents (i) the values of the f_{BC} and f_{NPV} design objectives, as well as (ii) the two financial robustness measures based on the dataset size (long term and sampled size). To better interpret the robustness analysis results in both plots, alternatives are clustered based on their installed capacities using the k-means clustering algorithm. K-means is an unsupervised machine learning technique designed to partition data points into a predetermined number of clusters (Fahim, 2021). In this context, using n = 10 clusters provides a sufficient representation of the data's structure, allowing to analyse and interpret the robustness of the alternatives effectively. The robustness measures along the vertical axis at the "Long Term"

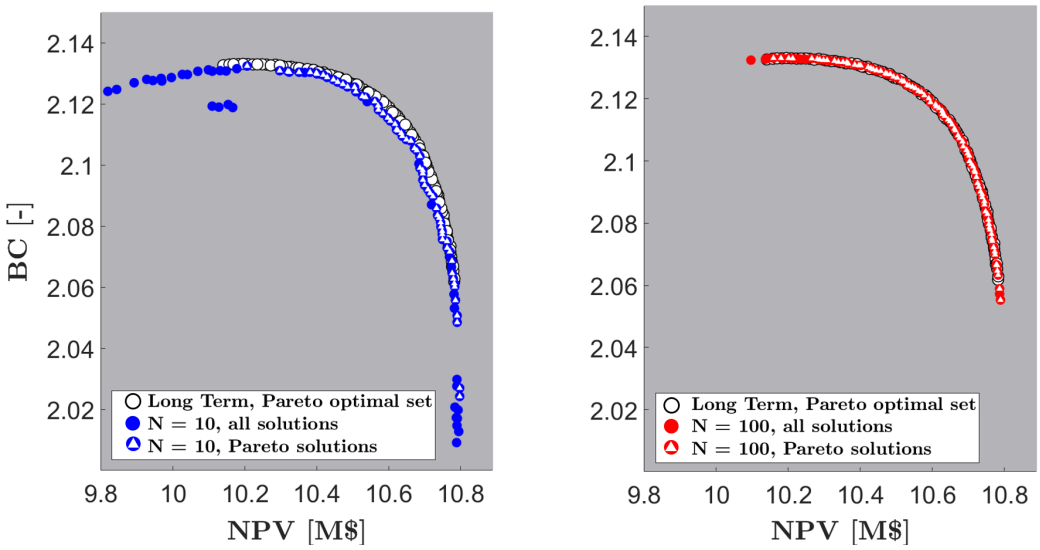

Figure 5.7: *Performance comparison of the reference Pareto front (RPF) obtained with optimization using the long-term FDC, with solutions obtained with optimization using the sampled FDC, and whose performance is re-evaluated using the long-term record. For $N = 10$ (left panel) and $N = 100$ sampled points (right panel), solutions that are non-dominated in the re-evaluated set are figured with white triangles.*

section serve as reference values since they are derived from long-term records, and compared with the robustness of the same design evaluated using different FDC approximations. The color of each line in both panels corresponds to its BC value, with yellow indicating a high BC and magenta indicating a low BC. This Figure also emphasizes the alternative with the highest NPV value (red line), the alternative with the highest BC value (green line), and the most robust alternative as identified with approximation-free robustness evaluation (black line). Clearly, there is a noticeable positive correlation between both robustness metrics and f_{BC}, and a negative correlation with f_{NPV}. This is because alternatives with higher f_{BC} values tend to be smaller in design, resulting in lower costs, making them better suited for a drought-prone world (Yildiz et al., 2024a).

This setup enables exploring the impact of FDC approximations and sample size N. Even though the robustness metric values are slightly higher for the sampled points in both panels, the overall pattern of the reference robustness metric values closely resembles that of the

sampled points. This indicates that the ranking of robust solutions remains largely consistent. For example, in both panels, the best NPV alternative exhibits the lowest robustness metric with long term record, a trend that holds true for the sampled points as well. The MR alternative, identified based on long-term flows, consistently emerges as one of the most robust solutions for RM_{NPV} across all sample sizes, and for RM_{PB} when the sample size $N >= 25$. Likewise, the best BC alternative demonstrates a similar robustness metric to the MR alternative in both panels, a consistency observed across different sampling sizes. However, notable deviations occur in the results for RM_{PB} when the sample size is small, $N <= 50$. This is where lines begin to intersect, and the differences between solutions get smaller, indicating a loss of reliability of the robustness metric. Similarly, there is a substantial divergence in the results for RM_{NPV} when the sample size $N < 50$.

The computational time for robustness analysis across various sample sizes is summarized in the rightmost column of Table 5.3. Significantly, the runtime exceeds 26 hours when utilizing long-term records, while it remains under 2 hours for sample sizes of $N \leq 100$ points, representing a reduction factor of 15. These results, when taken together, suggest that sampling futures with $N >= 50$ for robustness analysis provides a reliable and efficient approximation. Therefore, to align with the optimization analysis results, we selected $N = 100$ to conduct the robustness analysis with other case studies as discussed in the next section.

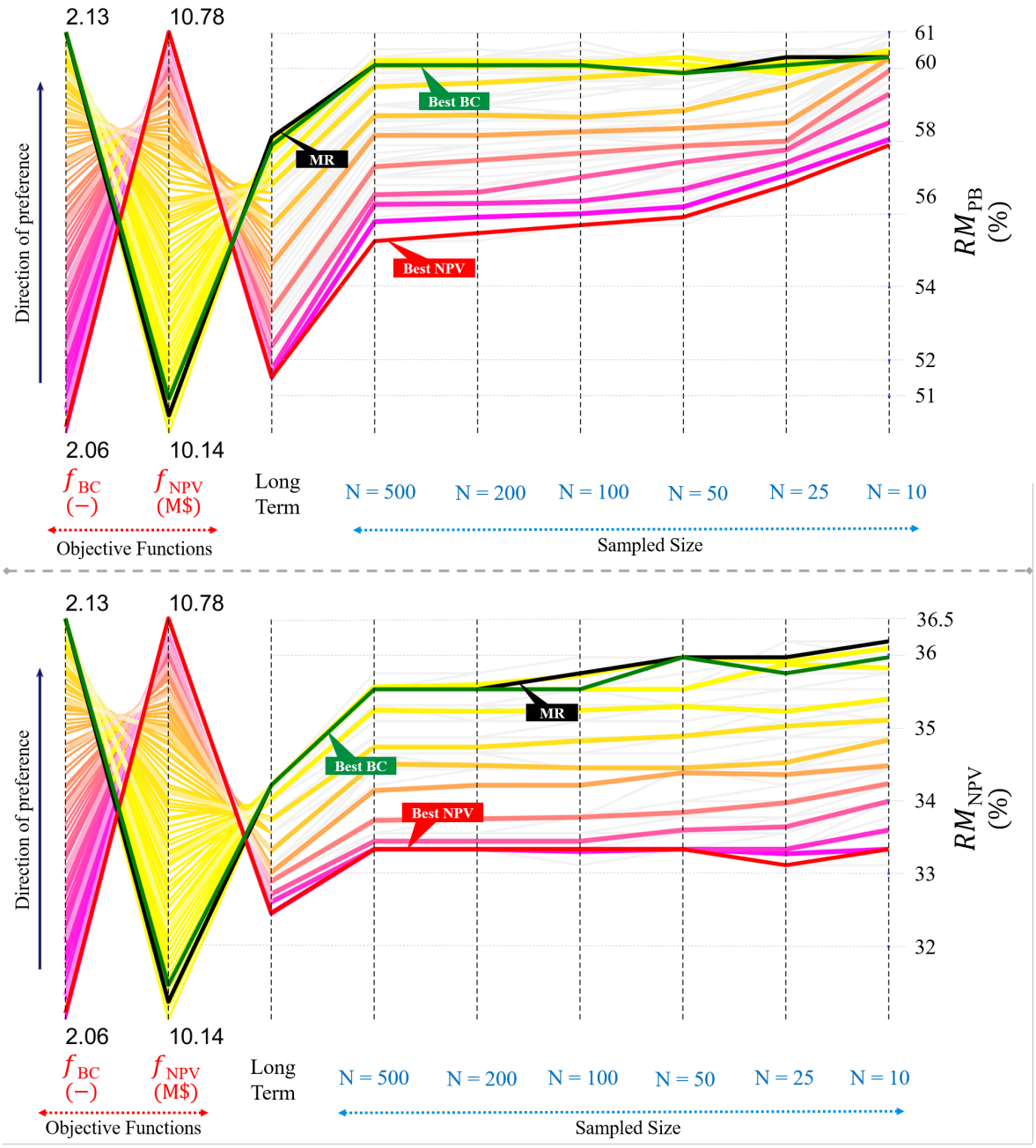

Figure 5.8: *The parallel plot of two objective functions: f_{BC} (-), f_{NPV} (M$), along with their respective robustness measures, for different sample sizes ($N = 10,\ 25,\ 50,\ 100,\ 200,$ and 500). In the top panel, the robustness measure is represented by RM_{PB}, while in the bottom panel, it is denoted as RM_{NPV}. Color coding on the lines is utilized to classify the results based on the value of f_{BC}.*

5.5.4 Whole-workflow impact of FDC sampling

In this section, we present the outcomes of our analysis across all study sites listed in Section 5.2.3. Our primary focus lies in comparing the coupled optimization and robustness analysis as well as runtime for three selected alternatives: the solution with the best NPV, the solution with the best BC, as well as the solution with the highest RM_{PB} value, identified as the Most Robust (MR). Table 5.4 presents the design characteristics, financial and energy performance metrics, and robustness metrics for these selected alternatives of each case. The data is displayed for two scenarios: long-term records (white background) and based on a sample size of $N = 100$ (gray background). It is evident that while the financial and robustness metrics of Best NPV and Best BC obtained through long-term discharge record and N = 100 sampled points are slightly different from each other, their design characteristics including turbine type, number and their respective capacities remain remarkably consistent across all the cases, regardless of FDC sampling. While sampling only $N = 100$ discharge values may lead to some loss of discharge information that affects these financial metrics, the impact on their design optimization is relatively minimal. This underscores the robustness of the approach across different scenarios, highlighting its reliability in diverse cases.

Notably, in each case-study the MR alternatives derived using FDC sampling exhibit similar design characteristics as those derived using long-term data – including turbine configuration and their respective capacities. An exception is observed in the Tepe case, where the most robust alternative features a different turbine setup. However, another robust alternative, with very similar robustness metric score, closely mirrors the design parameters observed in the long term record. This is particularly significant since these alternatives are selected through robustness analysis. The fact that sampling the future scenarios considerably decreases computational costs and resources while still yielding similar MR alternatives shows the consistency and dependability of the proposed approach in assessing the robustness of RoR designs. It is also interesting to note that the Tepe RoR case's optimal NPV alternatives on both scenarios include a triple turbine configuration consisting of two small and one large turbine. Traditionally, three-turbine systems for RoR hydropower plants employ one small and two large (identical turbines). The novel turbine operation optimization module included in HYPER$_{OP}$ model has led to the identification of this new alternative with higher

performance metrics. This demonstrates the capability of our toolbox to explore optimal solutions beyond conventional engineering norms.

The runtime for optimization, involving 20-30 years of daily discharge data with 100,000 function evaluations is substantially reduced by over 91% for $N = 100$ sampled points and by over 97% for $N = 50$ sampled points in each case study as shown in Table 5.5. Likewise, the runtime for robustness analysis across 500 plausible scenarios shows a significant decrease of over 92% for $N = 100$ sampled points and over 93% for $N = 50$ sampled points in each case study. The runtime for optimization and assessing robustness, varies between 26 and 35 hours for a single case. Note this represents the final version of our study, following several runs with a comparable computational effort for each site. However, when using $N = 100$ sampled points, the runtime is significantly reduced to less than 2.5 hours in all the cases. In other words, the computational cost is reduced by more than 92 % in each case.

Table 5.4: Design characteristics, performance metrics and robustness of the most robust (MR) alternative and the alternative with highest NPV and BC of given five case studies.

Case Study	**Methodology Alternatives**	**Turbine Configuration**	**Design Discharge** [m^3/s]	***IC*** [MW]	***AAE*** [GWh]	f_{NPV} [M$]	f_{BC} [-]	RM_{PB} [%]	RM_{NPV} [%]
Besik	Long Term, **MR**	Dual Francis	2.00 - 3.27	5.99	34.13	10.17	2.13	58.11	34.21
Besik	Long Term, **BC**	Dual Francis	2.03 - 3.28	6.03	34.22	10.19	2.13	57.80	34.21
Besik	Long Term, **NPV**	Dual Francis	2.70 - 3.98	7.60	37.34	10.78	2.06	51.53	32.45
Besik	$N = 100$, **MR**	Dual Francis	2.10 - 3.40	6.26	34.83	10.36	2.13	60.74	35.53
Besik	$N = 100$, **BC**	Dual Francis	2.03 - 3.28	6.03	34.22	10.19	2.13	60.08	35.53
Besik	$N = 100$, **NPV**	Dual Francis	2.70 - 3.97	7.60	37.33	10.78	2.06	55.70	33.11
Buyukdere	Long Term, **MR**	Dual Pelton	0.72 - 1.50	7.41	29.68	8.41	2.02	65.8	39.4
Buyukdere	Long Term, **BC**	Dual Pelton	0.54 - 0.96	4.85	23.68	6.97	2.10	60.6	37.8
Buyukdere	Long Term, **NPV**	Dual Pelton	0.91 - 1.96	9.84	34.15	8.94	1.88	63.0	37.0
Buyukdere	$N = 100$, **MR**	Dual Pelton	0.75 - 1.63	7.99	30.81	8.60	1.99	68.2	39.8
Buyukdere	$N = 100$, **BC**	Dual Pelton	0.54 - 0.98	4.94	23.95	7.05	2.10	63.6	38.4
Buyukdere	$N = 100$, **NPV**	Dual Pelton	0.93 - 2.06	10.24	34.78	8.97	1.85	66	38
Tepe	Long Term, **MR**	Dual Francis	1.84 - 4.63	3.54	14.05	2.94	1.59	54.0	28.0
Tepe	Long Term, **BC**	Dual Francis	1.46 - 3.46	2.68	12.10	2.61	1.62	51.0	27.4
Tepe	Long Term, **NPV**	Triple Francis	1.47 - 1.47 - 4.50	4.06	15.28	3.15	1.58	53.2	27.0
Tepe	$N = 100$, **MR**	Triple Francis	1.20 - 2.71 - 2.71	3.62	14.43	3.08	1.61	56	28.0
Tepe	$N = 100$, **MR***	Dual Francis	1.79 - 4.66	3.52	14.02	2.93	1.59	55.2	28.0
Tepe	$N = 100$, **BC**	Dual Francis	1.47 - 3.42	2.67	12.07	2.60	1.62	51.6	27.2
Tepe	$N = 100$, **NPV**	Triple Francis	1.41 - 1.41 - 4.61	4.06	15.34	2.90	1.50	53.8	27.4
Karacay	Long Term, **MR**	Dual Pelton	0.60 - 1.60	2.52	7.67	1.35	1.46	44.4	25.4
Karacay	Long Term, **BC**	Dual Pelton	0.52 - 1.35	2.10	6.83	1.24	1.47	42.0	25.4
Karacay	Long Term, **NPV**	Dual Pelton	0.67 - 1.77	2.82	8.19	1.39	1.43	43.4	24.6
Karacay	$N = 100$, **MR**	Dual Pelton	0.64 - 1.71	2.71	8.01	1.38	1.44	47.0	27
Karacay	$N = 100$, **BC**	Dual Pelton	0.53 - 1.34	2.10	6.84	1.24	1.47	45.6	26.6
Karacay	$N = 100$, **NPV**	Dual Pelton	0.68 - 1.79	2.87	8.28	1.39	1.42	46.6	26.2
Kaplan	Long Term, **MR**	Dual Pelton	0.62 - 1.23	3.33	11.53	2.62	1.68	42.6	28.8
Kaplan	Long Term, **BC**	Dual Pelton	0.47 - 0.85	2.33	9.91	2.34	1.72	37.4	25.4
Kaplan	Long Term, **NPV**	Dual Pelton	0.66 - 1.34	3.61	11.93	2.66	1.65	42.6	29
Kaplan	$N = 100$, **MR**	Dual Pelton	0.64 - 1.22	3.33	11.53	2.63	1.68	49.6	29.4
Kaplan	$N = 100$, **BC**	Dual Pelton	0.46 - 0.86	2.37	9.98	2.36	1.73	41.2	25.8
Kaplan	$N = 100$, **NPV**	Dual Pelton	0.66 - 1.33	3.60	11.91	2.66	1.66	49.0	29.6

Table 5.5: Optimization and robustness analysis run times for long term discharge records, $N = 100$ and $N = 50$ sampling points.

Case Study	**Long Term**	$\boldsymbol{N = 100}$	$\boldsymbol{N = 50}$
Besik, optimization [minutes]	216.9	10.2	5.2
Buyukdere, optimization [minutes]	360.5	27.2	9.2
Tepe, optimization [minutes]	384.1	29.4	9.8
Karacay, optimization [minutes]	186.2	15.5	5.5
Kaplan, optimization [minutes]	191.3	9.5	5.5
Besik, robustness analysis [hours]	26.32	1.69	1.43
Buyukdere, robustness analysis [hours]	28.29	1.82	1.78
Tepe, robustness analysis [hours]	24.65	1.94	1.83
Karacay, robustness analysis [hours]	24.52	1.83	1.71
Kaplan, robustness analysis [hours]	25.45	1.81	1.72

5.6 Summary and conclusion

In this study, we introduced the HYPER-FORD toolbox comprising two innovations in RoR plant design. First, the HYPER$_{OP}$ module builds operational tables that integrate optimized operations to design. Second, our approximation of the FDC with a regular sampling of the FDC builds upon HYPER$_{OP}$ to enhance computational efficiency through strategic reduction of data inputs. Our findings show HYPER$_{OP}$ is able to increase electricity generation by about 2% compared with traditional operational rules. Our results also demonstrate the capability of the HYPER$_{OP}$ to find design solutions not traditionally considered in engineering design of RoR hydropower plants, showing how optimized operations can expand design options.

The performance of using the FDC approximation instead of long-term daily data during optimization (of coupled design and operations) increases at very low sample sizes but stabilizes at around 100 sampled points. Beyond that, the proposed method yields a similar performance and diversity of design solutions as when using the long-term daily FDC as input. What is more, over 80% of these solutions remain Pareto optimal when re-evaluated using the long term record. This demonstrates the performance of the approach, which also slashes computational costs by 95 %. Additionally, the robustness analysis indicates that modelling plausible futures using FDC approximations with 50 sampled points or more provides a reliable approximation across the entire range of design alternatives for both robustness metrics, in the sense that robustness values are close and crucially, the relative ranking of the design alternatives is well-preserved by the sampling approximation. In the coupled design optimization and robustness analysis using 100-point FDC approximations in both steps, findings demonstrate that despite the potential loss of discharge information affecting financial and robustness metrics, the impact on the generation and evaluation of key robust design alternatives is almost non-existent. Indeed, the design characteristics, such as turbine configuration (type and number), and the total installed capacity, remain consistent across the best NPV, best BC and MR alternatives for all the presented cases. In addition, while the runtime for optimization and assessing robustness, based on using long-term records, varies between 26 and 35 hours for a single case, this duration significantly decreases when using FDC sampling. Specifically, the runtime is reduced to less than 2.5 hours for N=100 sampled

points in all cases. This represents a remarkable reduction in computational cost by more than 92 % across each case.

Overall, our method strategically reduces data inputs on FDCs while preserving the gains made thanks to operations optimization. The resulting toolbox, HYPER-FORD facilitates rapid analysis, optimization, and assessment of potential designs. In other words, it makes robust design and analysis more accessible. This empowers engineers and decision-makers to make informed choices, leading to the design and operation of RoR hydropower plants that are technically optimal and robust to uncertain futures. Additionally, HYPER-FORD makes the computation more sustainable by minimizing the need for high-performance computing, and by reducing carbon emissions from data centers.

Yet, while the cost-effective approach introduced here is versatile and applicable to various hydro sites, the numerical results presented in the preceding sections are limited to just five proposed cases within the same country. Although Turkey offers favorable topography for hydropower development, and experiences diverse climates, the effectiveness of this methodology should be demonstrated on other RoR hydropower plants located in regions with different topographical and hydrological characteristics to establish its general applicability. It is fitting then that HYPER-FORD makes the application of optimization and robustness analysis to a large number of cases computationally affordable. Hydropower projects are typically designed using traditional assessments that rely on historical flows by ignoring the impacts of future uncertainties (Bertoni et al., 2019). Under these conditions, optimization of these plants is based on cost-benefit analysis, generally maximizing NPV (Yildiz and Vrugt, 2019), aiming to identify the optimal solution rather than robust alternatives capable of performing well under a range of uncertain conditions. Additionally, the design and operation of these plants are often treated separately , overlooking the integration of turbine system design (e.g., Taner et al., 2017; Ray et al., 2018; Bertoni et al., 2019; Hurford et al., 2020; Bertoni et al., 2021). which is governed by site hydrology and financial constraints. Future studies, thus, should apply this methodology to hundreds of existing and potential RoR sites across wide regions, to more accurately assess the potential of small hydropower in an uncertain world.

In the optimization process, N evenly distributed points from the historical time series are extracted, as indicated by the black dots on Figure 5.5. Similarly, this discretization

method is employed across each of the 50-time series utilized to assess the robustness of potential future scenarios in subsequent analyses. it's conceivable to implement irregular sampling techniques instead of uniformly sampling the entire Flow Duration Curve (FDC). For instance, fewer points could be sampled from the tails of the FDC, while more points are concentrated around the central portion, providing a more nuanced representation of the flow distribution. Future studies would explore the efficacy and benefits of such irregular sampling techniques in enhancing the accuracy of optimization processes and robustness analyses.

This study, along with Yildiz et al. (2024a), underscores the importance of considering turbine efficiency in hydropower plant design. By 2030, around one-fifth of the installed hydropower turbines, totaling approximately 154 GW globally (IEA, 2021), will exceed 55 years in age. Many of these turbines requiring replacement to maintain high plant performance, and this will lead to opportunities to retrofit hydropower plants to improve their flexibility and to adapt to changing and variable hydrological conditions. The necessity for a well-defined methodology to effectively evaluate and select the most appropriate turbine replacement or upgrade options is evident across both RoR and reservoir-based hydropower plants. To address these needs, the HYPER-FORD toolbox proposed here could be utilized for RoR retrofit effectively and expanded to encompass turbine system optimization for the design and retrofit of reservoir-based hydropower plants. The multipurpose nature of many reservoirs and their ability to buffer hydrological variability and drought – at the expense of varying hydraulic heads – present significant challenges that this latter extension of the HYPER-FORD toolbox approach will need to address.

Data Availability Statement

The HYPER-FORD toolbox outlined here, along with all pertinent data concerning the five case studies, such as site and flow characteristics, are openly accessible from the the University of Sheffield's data repository at `https://doi.org/10.15131/shef.data.25676967.v1`.

CHAPTER 6

Conclusions and future research

6.1 Summary and conclusions

Conventional assessments of hydropower plants, including RoR projects, typically rely solely on historical flow data and fixed operating conditions (rule curves), neglecting not only the potential impacts of climate change, but also socio-economic uncertainties such as fluctuating electricity prices, interest rates, and possible cost overruns. Consequently, plant optimization is often based on cost-benefit analysis, prioritizing the identification of optimal solutions rather than robust alternatives which perform well under a range of uncertain conditions. Moreover, the design and operation of these plants are traditionally treated separately, without integrating turbine system design. This integration is hindered by the computational demands of holistic design optimization and robustness analysis methods. The environmental benefits of hydropower as a renewable energy source are further compromised by the emissions associated with large computing costs.

Given the challenges identified, the primary objective of this thesis was to develop innovative methods and integrated frameworks to overcome these shortcomings, contributing to scientific and technical advancements in hydropower plant design. The main outcomes of each contribution presented in this thesis, extensively discussed at the conclusion of each dedicated chapter, are summarized here to derive overarching conclusions and key takeaways.

First and foremost, a practical and innovative approach based on parameterisation of flow duration curves (FDCs) to statistically generating climate-informed streamflow futures is introduced. This method is then applied to generate future streamflow projections for a proposed run-of-river hydropower plant site in Turkey to evaluate the project's financial

viability under changing conditions. The ensemble of these projections demonstrates the method's ability to produce a wide range of climate-modified catchment responses, including increased frequency of both high flows and low flows that mimic the future projections for the region (i.e. more arid conditions with increased trend of extreme hydrological events). The method exhibits favorable performance when compared to conventional approaches that uniformly modify streamflow statistics using multipliers throughout a time series. The ease of application of the method illustrates its wide applicability in support of infrastructure robustness assessments in river basins where bespoke high-performance hydrological models are lacking, and streamflow variability impacts performance.

Next, a framework integrates the HYPER toolbox with multiobjective evolutionary algorithms and the Many Objective Robust Decision Making (MORDM) approach, widely used for Decision Making Under Deep Uncertainty, is presented. The application of HYPER-MORDM to proposed five RoR hydropower plants situated in diverse hydro-climatic regions of Turkey challenges fundamental design assumptions, notably the use of net present value (NPV) as a design objective and the installation of identical turbines. Instead, maximising the benefit-cost ratio (BC) yields plants with better financial viability over a range of plausible futures. They tend to have less costly designs that generate slightly less revenue on average, yet offer increased flexibility to harness low flows more effectively. The findings further underscore the significance of integrating turbine system design into the optimization process. Additionally, they highlight avoiding common but less effective designs with identical turbines for RoR hydropower plants. Another key insight is that socio-economic uncertainties can have as much or even greater impact on robustness than climate conditions. In fact, these uncertainties have the potential to make many small hydropower projects financially too risky to build.

The HYPER-MORDM approach effectively identifies robust design alternatives but demands substantial computational resources. To address this, the HYPER-FORD toolbox is introduced. This toolbox comprises two key innovations. Firstly, the HYPER$_{OP}$ module integrates optimized operations into the design process by constructing operational tables for the first time. Secondly, it enhances computational efficiency by approximating the Flow Duration Curve (FDC) through regular sampling, building upon the capabilities of

HYPER$_{OP}$. The toolbox is rigorously benchmarked on diverse case studies. Findings show that HYPER$_{OP}$ module is able to increase hydropower generation by about 2% compared with traditional operational rules. This enhancement is primarily attributed to HYPER$_{OP}$'s optimization of operations, effectively capturing streamflow variability. Moreover, for a sample size exceeding 100 points, it produces a sufficient number of design solutions demonstrating both convergence and diversity. Additionally, robustness analysis indicates that sampling futures with a sample size of 50 or greater offers a reliable approximation across the entire spectrum of design alternatives for both robustness metrics. While sampling datasets may lead to some loss of discharge information impacting financial and robustness metrics, the influence on design optimization and robustness analysis remains minimal, with computational costs reduced by over 92 % in each case. This approach is making robust design and analysis more accessible and reinforces sustainability efforts by minimizing the need for high-performance computing and reducing carbon emissions from data centers.

Taken together, these findings suggest that applying HYPER-MORDM approach in the design of RoR hydropower plants provides water resource planners and decision makers with a comprehensive framework to make informed decisions regarding the implementation of RoR hydropower projects and determining the most robust design alternative under deep future uncertainties. This work also stresses the need for considering turbine efficiency in hydropower plant design. This is currently not the case, even in the middle of a global hydropower boom, and as a result, many existing plants, large and small, might need to upgrade their turbine systems in the coming years. What is more, while the HYPER-MORDM approach proves effective in defining robust alternatives, its computational demands are significant. The HYPER-FORD toolbox addresses this challenge by streamlining the process through strategically reducing data inputs on FDCs while preserving nearly equal outcomes. This not only enhances computational efficiency but also removes barriers to the application of these methods beyond actors in industrialized nations, such as academia and corporations, which often lack the human and physical infrastructure to use the most largest computing facilities. These contributions aim to directly inform and benefit real-world decision-making processes, thereby facilitating more effective and sustainable water resource development and management practices.

6.2 Future research

Drawing from the key findings of this thesis, future research should prioritize the following areas of investigation, as outlined in the subsequent paragraphs.

6.2.1 Statistical generation of FDCs with temporal dynamics

The method proposed in Chapter 3 shifts the FDC, but does not say anything about the changing frequency or duration of droughts, or about the shifting seasonality of streamflow, e.g., with earlier snowmelt (Rauscher et al., 2008; Zhang et al., 2019). Yet, mounting evidence suggests that climate change will lead to hydrological intensification, i.e., dry periods will become longer and more severe, while wet periods will become more intense (Ficklin et al., 2022). While the timing of flows doesn't influence the design of Run-of-River hydropower plants due to the absence of storage, it holds significant implications for storage-based plants, affecting their operation. Information on hydrological intensification scenarios comes from outputs from large-scale climate models, and integrating that information requires turning the climate information into streamflow. One way to do it without the help of a rainfall-runoff model is to control the parameters of a daily streamflow model with a monthly climate model (Stagge and Moglen, 2013). The generation of a FDC for every climate the daily streamflow model simulates could then be used to improve results, e.g., by providing a quantile-by-quantile adjustment of the synthetic streamflow generator outputs. A similar procedure could combine hydrological model simulations with statistical generation of FDCs. The latter could correct outputs from the former, if they were obtained with a calibration that reflects historical conditions. Alternatively, plausible future drought risk scenarios with an altered FDC could be achieved by combining the methodology I proposed with synthetic hydro-climatic drought generators (Herman et al., 2016; Zaniolo et al., 2024). As for capturing the shifting seasonality of flows in a changing climate, this can be effectively achieved by integrating this approach with methods like log-space rescaling of stationary flows (Quinn et al., 2018) or reconstructing annual flow hydrographs (Nazemi et al., 2013).

6.2.2 Integrated robust design and operation of large hydropower plants

The application of the HYPER-MORDM approach to various RoR hydropower case studies reveals that turbine setup plays a crucial role in determining the overall robustness of a project. This is particularly evident due to the significant impact of larger installed capacities, which are designed to maximize performance during above-average flow conditions but often prove to be costly and lack the flexibility required to capture low flows effectively. There is a need for understanding how these lessons derived for RoR plants could apply to reservoir-based (RB) plants. In RB plants, dam operators have the ability to regulate flow, but head variations are widely expected to mirror hydrological intensification. These fluctuations in head levels significantly affect the efficiency of turbines, typically designed for a nominal head corresponding to a full reservoir. Hence, there exists a potential opportunity for the design of turbines tailored to different head conditions. However, the majority of literature on reservoir-based hydropower overlooks considerations of turbine system efficiency during the design phase of the dam and hydropower plant system. Typically, the selection of the turbine configuration takes place after determining the installed capacity (DSI, 2012) due to the added complexity of the turbine system design process. This lack of integration of turbine efficiency into design extends to recent research, (e.g., Ray et al., 2018; Bertoni et al., 2019, 2021), and this can lead to a mismatch between projected and actual energy production, even when operations are explicitly simulated. Adapting the HYPER-MORDM framework would facilitate the identification of robust alternatives capable of addressing the dynamic nature of these factors and effectively overcoming these challenges.

6.2.3 Optimizing turbine replacement and upgrades in hydropower

By 2030, approximately one-fifth of the installed hydropower turbines worldwide, totaling around 154 GW, will surpass the 55-year age mark (IEA, 2021). With this aging infrastructure, the need for replacement becomes crucial to maintain high plant performance. This necessity for replacement also presents an opportunity to retrofit hydropower plants, enhancing their flexibility to adapt to evolving and variable hydrological conditions. The need for a well-defined methodology to effectively evaluate and select the most appropriate turbine replacement or upgrade options is evident across both RoR and RB plants. To meet

these needs, the approaches proposed here should be expanded not only for RoR retrofit, but also to turbine system optimization for design and retrofit of RB hydropower plants. The multipurpose nature of many reservoirs and the fact that hydrological variability and drought impact RoR and RB hydropower differently are significant challenges that this latter extension of the HYPER-FORD approach will need to tackle. These insights highlight the potential for integrating the developed toolboxes into a flexible planning approach for adaptation pathways.

6.2.4 Enhancing accuracy in global hydropower potential assessment

Assessing hydropower potential across global, regional, and local scales is imperative for strategically shaping both future energy infrastructure and policy decisions. Currently, this assessment heavily relies on factors such as GIS-based elevation data and large-scale hydrological models or available runoff information (Zhou et al., 2015; Hoes et al., 2017). However, these methodologies often yield rough and inconsistent estimations due to simplifying assumptions in the representation of hydropower (e.g., Gernaat et al., 2017; Hoes et al., 2017; Tefera and Kasiviswanathan, 2022). Such simplifications mainly stem from the complexities of design and associated computational costs. Consequently, the resulting potential capacities may be overstated, posing a significant challenge in accurately predicting the true potential of hydropower resources. This limitation hampers effective planning and allocation of resources for energy infrastructure development. To address this challenge, there is a need to enhance assessment methodologies to ensure more precise and reliable evaluations of hydropower potential. Integrating technical design elements into current methodologies would elevate the accuracy of estimations. Tools like HYPER-FORD, introduced in this study, hold promise in overcoming these challenges effectively and enhancing the accuracy of hydropower potential assessments. In effect, HYPER-FORD opens the door for large-scale assessment of RoR hydropower by computing the design and robustness of RoR power plants with a high level of engineering realism.

6.2.5 Basin wide assessment of hydropower infrastructure

Robust design and operations of multipurpose hydropower systems, including RoR plants and RBs, and time-varying power prices poses significant challenges. These challenges stem from conflicting objectives, the interactions between the power plant facilities and with other water users, the need for representing flows and hydropower production accurately through at an hourly time step or less, and the uncertain nature of several factors including water inflows or power demands. The location, operational capacities, and water travel time between these facilities are crucial factors. For example, when an upstream dam releases water to enhance energy revenue, and it reaches a downstream RoR power plant during off-peak hours, the absence of storage can lead to low revenues for the downstream plant. The interconnected nature of hydropower systems in a basin necessitates a nuanced examination of their mutual influence, crucial for a comprehensive understanding of robust design and operation. Hence, a promising avenue for future research involves strategically integrating DMDU approaches with state-of-the-art toolboxes that I have developed, implemented on a basin-wide scale to address the highlighted issues. This integration is aimed to yield detailed insights, enabling stakeholders to make informed decisions in the face of uncertainty simply to assess the positive and negative impacts of a building a new hydraulic structure on a river basin. Moreover, this integrated approach seeks to (i) to optimize the operation of multipurpose hydropower systems and (ii) to test their robustness with respect to a range of climate scenarios by considering a whole basin. What is more, integrating the developed toolboxes into a flexible planning approach for adaptation pathways on a basin-wide scale would allow for ongoing adjustments and increased resilience to unforeseen changes, making it highly beneficial in the context of climate change. However, while flexible pathways offer adaptability, they may also require higher ongoing management costs and complexity. In contrast, robust solutions are designed to perform well across various scenarios, providing a straightforward and potentially less complex approach, but they may not be as adaptable to unexpected changes and could involve higher initial costs. Achieving a balance between the benefits of flexibility and the reliability of robustness is essential in developing efficient hydropower strategies. This balance could be further explored in future studies.

6.2.6 Integrating Sustainability and Efficiency: Advancing Hydropower with LCA and EROI Metrics

Life Cycle Assessment (LCA) and Energy Return on Investment (EROI) are two important metrics used in evaluating the environmental and energy performance of hydropower plants respectively. LCA offers a comprehensive analysis of the environmental impacts associated with the entire life cycle of a hydropower plant, from construction and operation to decommissioning, considering factors such as resource use and greenhouse gas (GHG) emissions, and providing valuable insights for comparison with other energy sources (Weisser, 2007; Raadal et al., 2011). The primary sources of GHG emissions include engineering work, such as the construction of dams or weirs, tunnels, and powerhouses, as well as the decay of biomass in areas flooded by reservoirs (Gagnon and van de Vate, 1997). Indeed, emissions from reservoir-based hydropower exhibit significant variability, driven by reservoir-related factors (Turconi et al., 2013). Variables such as the reservoir's volume, age, location, and the presence of organic matter can cause these emissions to contribute up to 90 % of the total emissions, especially for hydropower in tropical regions (Gemechu and Kumar, 2022). In contrast, life cycle GHG emissions are primarily influenced by the energy and materials used during the construction in RoR systems since it does not require a reservoir and dam. However, while RoR projects require lower energy and material requirements for engineering works, their life cycle impacts, (g CO2-eq/kWh), are usually higher compared to reservoir-based projects (Gemechu and Kumar, 2022). On the other hand, EROI measures the ratio of energy output to energy input throughout operational time of a hydropower project, offering insights into its energy efficiency and overall effectiveness as an energy source (Atlason and Unnthorsson, 2014). In general, hydropower plants have high EROI values due to their long operational lifetimes compared to other technologies (Hall et al., 2014). Gagnon et al. (2002) demonstrate that, over a 100-year period, reservoir-based hydropower plants in Quebec can achieve an EROI of 205, while run-of-river (RoR) plants can reach an EROI of 267. By evaluating both the environmental and energy performance of hydropower plants, LCA and EROI play a crucial role in informed decision-making. These assessments promote the development and operation of hydropower projects that are both environmentally sound and energy-efficient, guiding decision-making towards more sustainable practices. Future work can consider these

metrics to provide an even more comprehensive evaluation, ensuring that hydropower projects meet the highest standards of sustainability and efficiency.

Bibliography

Abera, F. F., Asfaw, D. H., Engida, A. N. and Melesse, A. M. (2018), 'Optimal operation of hydropower reservoirs under climate change: The case of tekeze reservoir, eastern nile', *Water* **10**(3), 273.

Ak, M., Kentel, E. and Kucukali, S. (2017), 'A fuzzy logic tool to evaluate low-head hydropower technologies at the outlet of wastewater treatment plants', *Renewable and Sustainable Energy Reviews* **68**, 727–737.

Alizamir, S., de Véricourt, F. and Sun, P. (2016), 'Efficient feed-in-tariff policies for renewable energy technologies', *Operations Research* **64**(1), 52–66.

Alonso-Tristán, C., González-Peña, D., Díez-Mediavilla, M., Rodríguez-Amigo, M. and García-Calderón, T. (2011), 'Small hydropower plants in spain: A case study', *Renewable and Sustainable Energy Reviews* **15**(6), 2729–2735.

AlZohbi, G. (2018), 'The cost of electromechanical equipment in a small hydro power storage plant', *Journal of Energy Systems* **2**(4), 238–259.

Amougou, C. B., Tsuanyo, D., Fioriti, D., Kenfack, J., Aziz, A. and Elé Abiama, P. (2022), 'Lcoe-based optimization for the design of small run-of-river hydropower plants', *Energies* **15**(20), 7507.

Anagnostopoulos, J. S. and Papantonis, D. E. (2007), 'Optimal sizing of a run-of-river small hydropower plant', *Energy conversion and management* **48**(10), 2663–2670.

Anderson, E. P., Jenkins, C. N., Heilpern, S., Maldonado-Ocampo, J. A., Carvajal-Vallejos, F. M., Encalada, A. C., Rivadeneira, J. F., Hidalgo, M., Cañas, C. M., Ortega, H. et al. (2018), 'Fragmentation of andes-to-amazon connectivity by hydropower dams', *Science advances* **4**(1), eaao1642.

Ansar, A., Flyvbjerg, B., Budzier, A. and Lunn, D. (2014), 'Should we build more large dams? the actual costs of hydropower megaproject development', *Energy policy* **69**, 43–56.

Arnold, W., Giuliani, M. and Castelletti, A. (2024), 'Floating photovoltaics may reduce the risk of hydro-dominated energy development in africa', *Nature Energy* pp. 1–10.

Atlason, R. S. and Unnthorsson, R. (2014), 'Energy return on investment of hydroelectric power generation calculated using a standardised methodology', *Renewable energy* **66**, 364–370.

Auger, A., Bader, J., Brockhoff, D. and Zitzler, E. (2009), Theory of the hypervolume indicator: optimal μ-distributions and the choice of the reference point, *in* 'Proceedings of the tenth ACM SIGEVO workshop on Foundations of genetic algorithms', pp. 87–102.

Ault, T. R. (2020), 'On the essentials of drought in a changing climate', *Science* **368**(6488), 256–260.

Azam, T., Jiang, W. S., Malik, S. A., Malik, S. Y., Nilofar, M., Abbas, Z. and Ullah, I. (2020), 'An analysis of causes of delay and cost overrun in construction of hydropower project', *Journal of Public Affairs* p. e2285.

Basso, S. and Botter, G. (2012), 'Streamflow variability and optimal capacity of run-of-river hydropower plants', *Water Resources Research* **48**(10).

Beck, H. E., Zimmermann, N. E., McVicar, T. R., Vergopolan, N., Berg, A. and Wood, E. F. (2018), 'Present and future köppen-geiger climate classification maps at 1-km resolution', *Scientific data* **5**(1), 1–12.

Bejarano, M. D., Sordo-Ward, A., Gabriel-Martin, I. and Garrote, L. (2019), 'Tradeoff between economic and environmental costs and benefits of hydropower production at run-of-river-diversion schemes under different environmental flows scenarios', *Journal of Hydrology* **572**, 790–804.

Berga, L. (2016), 'The role of hydropower in climate change mitigation and adaptation: a review', *Engineering* **2**(3), 313–318.

Bertoni, F., Castelletti, A., Giuliani, M. and Reed, P. (2019), 'Discovering dependencies, trade-offs, and robustness in joint dam design and operation: An ex-post assessment of the kariba dam', *Earth's Future* **7**(12), 1367–1390.

Bertoni, F., Giuliani, M. and Castelletti, A. (2020), 'Integrated design of dam size and operations via reinforcement learning', *Journal of Water Resources Planning and Management* **146**(4), 04020010.

Bertoni, F., Giuliani, M., Castelletti, A. and Reed, P. (2021), 'Designing with information feedbacks: Forecast informed reservoir sizing and operation', *Water Resources Research* **57**(3), e2020WR028112.

Bhaduri, A., Bogardi, J., Siddiqi, A., Voigt, H., Vörösmarty, C., Pahl-Wostl, C., Bunn, S., Shrivastava, P., Lawford, R., Foster, S. et al. (2015), 'Sustainable development goals: A water perspective. summary report and extended recommendations of the bonn conference 2015: Indicators, interlinkages and implementation'.

Bharany, S., Sharma, S., Khalaf, O. I., Abdulsahib, G. M., Al Humaimeedy, A. S., Aldhyani, T. H., Maashi, M. and Alkahtani, H. (2022), 'A systematic survey on energy-efficient techniques in sustainable cloud computing', *Sustainability* **14**(10), 6256.

Blank, J. and Deb, K. (2020), 'Pymoo: Multi-objective optimization in python', *Ieee access* **8**, 89497–89509.

Blöschl, G., Sivapalan, M., Wagener, T., Savenije, H. and Viglione, A. (2013), *Runoff prediction in ungauged basins: synthesis across processes, places and scales*, Cambridge University Press.
URL: *https://doi.org/10.1017/CBO9781139235761*

Bøckman, T., Fleten, S.-E., Juliussen, E., Langhammer, H. J. and Revdal, I. (2008), 'Investment timing and optimal capacity choice for small hydropower projects', *European Journal of Operational Research* **190**(1), 255–267.

Boretti, A. and Rosa, L. (2019), 'Reassessing the projections of the world water development report', *NPJ Clean Water* **2**(1), 1–6.

Boscarello, L., Ravazzani, G., Cislaghi, A. and Mancini, M. (2016), 'Regionalization of flow-duration curves through catchment classification with streamflow signatures and physiographic–climate indices', *Journal of Hydrologic Engineering* **21**(3), 05015027.
URL: *https://doi.org/10.1061/(ASCE)HE.1943-5584.0001307*

Botelho, A., Ferreira, P., Lima, F., Pinto, L. M. C. and Sousa, S. (2017), 'Assessment of the environmental impacts associated with hydropower', *Renewable and Sustainable Energy Reviews* **70**, 896–904.

Brown, A. E., Western, A. W., McMahon, T. A. and Zhang, L. (2013), 'Impact of forest cover changes on annual streamflow and flow duration curves', *Journal of Hydrology* **483**, 39–50.
URL: *https://doi.org/10.1016/j.jhydrol.2012.12.031*

Brown, C. (2011), 'Decision-scaling for robust planning and policy under climate uncertainty', *World Resources Report Uncertainty Series* **14**.

Brown, C., Ghile, Y., Laverty, M. and Li, K. (2012), 'Decision scaling: Linking bottom-up vulnerability analysis with climate projections in the water sector', *Water Resources Research* **48**(9).
URL: *https://doi.org/10.1029/2011WR011212*

Bryant, B. P. and Lempert, R. J. (2010), 'Thinking inside the box: A participatory, computer-assisted approach to scenario discovery', *Technological Forecasting and Social Change* **77**(1), 34–49.

Callegari, C., Szklo, A. and Schaeffer, R. (2018), 'Cost overruns and delays in energy megaprojects: How big is big enough?', *Energy Policy* **114**, 211–220.
URL: *https://www.sciencedirect.com/science/article/pii/S0301421517308042*

Cao, Z., Zhou, X., Hu, H., Wang, Z. and Wen, Y. (2022*a*), 'Toward a systematic survey for carbon neutral data centers', *IEEE Communications Surveys & Tutorials* **24**(2), 895–936.

Cao, Z., Zhou, X., Hu, H., Wang, Z. and Wen, Y. (2022*b*), 'Towards a systematic survey for carbon neutral data centers', *IEEE Communications Surveys & Tutorials* .

Carlino, A., Wildemeersch, M., Chawanda, C. J., Giuliani, M., Sterl, S., Thiery, W., Van Griensven, A. and Castelletti, A. (2023), 'Declining cost of renewables and climate change curb the need for african hydropower expansion', *Science* **381**(6658), eadf5848.

Carvajal, P. E., Li, F. G., Soria, R., Cronin, J., Anandarajah, G. and Mulugetta, Y. (2019), 'Large hydropower, decarbonisation and climate change uncertainty: Modelling power sector pathways for ecuador', *Energy Strategy Reviews* **23**, 86–99.

Castellarin, A., Botter, G., Hughes, D., Liu, S., Ouarda, T., Parajka, J., Post, D., Sivapalan, M., Spence, C., Viglione, A. and Vogel, R. M. (2013), 'Prediction of flow duration curves in ungauged basins', *Runoff prediction in ungauged basins: Synthesis across processes, places and scales* pp. 135–162. [accessed 04-07-2023].

Ceran, B., Jurasz, J., Wróblewski, R., Guderski, A., Złotecka, D. and Kaźmierczak, Ł. (2020), 'Impact of the minimum head on low-head hydropower plants energy production and profitability', *Energies* **13**(24), 6728.

Ceseña, E. M., Panteli, M., Mutale, J., Mancarella, P., Tomlinson, J. and Harou, J. J. (2019), Integrated energy-water model for interdependent storage, run-of-river and pump hydropower, *in* '2019 IEEE Milan PowerTech', IEEE, pp. 1–6.

Chen, C., Kalra, A. and Ahmad, S. (2019), 'Hydrologic responses to climate change using downscaled gcm data on a watershed scale', *Journal of Water and Climate Change* **10**(1), 63–77.
URL: *https://doi.org/10.2166/wcc.2018.147*

Chen, S., Chen, B. and Fath, B. D. (2015), 'Assessing the cumulative environmental impact of hydropower construction on river systems based on energy network model', *Renewable and Sustainable Energy Reviews* **42**, 78–92.

Cheng, L., AghaKouchak, A., Gilleland, E. and Katz, R. W. (2014), 'Non-stationary extreme value analysis in a changing climate', *Climatic change* **127**(2), 353–369.

Cheng, Q., Ming, B., Liu, P., Huang, K., Gong, Y., Li, X. and Zheng, Y. (2021), 'Solving hydro unit commitment problems with multiple hydraulic heads based on a two-layer nested optimization method', *Renewable Energy* **172**, 317–326.

Cook, B. I., Mankin, J. S., Marvel, K., Williams, A. P., Smerdon, J. E. and Anchukaitis, K. J. (2020), 'Twenty-first century drought projections in the cmip6 forcing scenarios', *Earth's Future* **8**(6), e2019EF001461.

Cosgrove, W. J. and Loucks, D. P. (2015), 'Water management: Current and future challenges and research directions', *Water Resources Research* **51**(6), 4823–4839.

Couto, T. B. and Olden, J. D. (2018), 'Global proliferation of small hydropower plants–science and policy', *Frontiers in Ecology and the Environment* **16**(2), 91–100.

Couture, T. and Gagnon, Y. (2010), 'An analysis of feed-in tariff remuneration models: Implications for renewable energy investment', *Energy policy* **38**(2), 955–965.

Dai, A. (2011), 'Drought under global warming: a review', *Wiley Interdisciplinary Reviews: Climate Change* **2**(1), 45–65.

Demircan, M., Gürkan, H., Eskioğlu, O., Arabacı, H. and Coşkun, M. (2017), 'Climate change projections for turkey: three models and two scenarios', *Türkiye Su Bilimleri ve Yönetimi Dergisi* **1**(1), 22–43.
URL: *https://doi.org/10.31807/tjwsm.297183*

Deyou, L., Heng, L. and Krēmere, W. X. E. (2019), 'World small hydropower development report'.

Diaz, F. J., Contreras, J., Muñoz, J. I. and Pozo, D. (2010), 'Optimal scheduling of a price-taker cascaded reservoir system in a pool-based electricity market', *IEEE Transactions on Power Systems* **26**(2), 604–615.

Dorber, M., Arvesen, A., Gernaat, D. and Verones, F. (2020), 'Controlling biodiversity impacts of future global hydropower reservoirs by strategic site selection', *Scientific reports* **10**(1), 1–13.

Doyle, M. W., Stanley, E. H., Harbor, J. M. and Grant, G. S. (2003), 'Dam removal in the united states: emerging needs for science and policy', *Eos, Transactions American Geophysical Union* **84**(4), 29–33.

DSI (2012), *Dams and Hydropower Plants Hydromechanical and Electromechanical Design Guide (in Turkish)*, General Directorate of State Hydraulic Works (DSI).

Duan, Q., Schaake, J., Andréassian, V., Franks, S., Goteti, G., Gupta, H., Gusev, Y., Habets, F., Hall, A., Hay, L., Hogue, T., Huang, M., Leavesley, G., Liang, X., Nasonova, O., Noilhan, J., Oudin, L., Sorooshian, S., Wagener, T. and Wood, E. (2006), 'Model parameter estimation experiment (mopex): An overview of science strategy and major results from the second and third workshops', *Journal of Hydrology* **320**(1), 3–17. The model parameter estimation experiment.
URL: *https://www.sciencedirect.com/science/article/pii/S002216940500329X*

Egré, D. and Milewski, J. C. (2002), 'The diversity of hydropower projects', *Energy Policy* **30**(14), 1225–1230.

EMRA (2022), 'Energy market regulatory authority, renewable energy support mechanisms', https://www.epdk.gov.tr/yekdem.

EXIST (2022), *Electricity Market Summary Information Report*, Energy Exchange Istanbul (EXIST).

Fahim, A. (2021), 'K and starting means for k-means algorithm', *Journal of Computational Science* **55**, 101445.

Fang, Z., Zhang, W., Brandt, M., Abdi, A. M. and Fensholt, R. (2022), 'Globally increasing atmospheric aridity over the 21st century', *Earth's Future* **10**(10), e2022EF003019.

Fearnside, P. M. (2014), 'Impacts of brazil's madeira river dams: Unlearned lessons for hydroelectric development in amazonia', *Environmental Science & Policy* **38**, 164–172.

Feng, J. and Shen, W. Z. (2017), 'Design optimization of offshore wind farms with multiple types of wind turbines', *Applied energy* **205**, 1283–1297.

Ficklin, D. L., Null, S. E., Abatzoglou, J. T., Novick, K. A. and Myers, D. T. (2022), 'Hydrological intensification will increase the complexity of water resource management', *Earth's Future* **10**(3), e2021EF002487. e2021EF002487 2021EF002487.
URL: *https://agupubs.onlinelibrary.wiley.com/doi/abs/10.1029/2021EF002487*

Field, C. B., Barros, V., Stocker, T. F. and Dahe, Q. (2012), *Managing the risks of extreme events and disasters to advance climate change adaptation: special report of the intergovernmental panel on climate change*, Cambridge University Press.

Finer, M. and Jenkins, C. N. (2012), 'Proliferation of hydroelectric dams in the andean amazon and implications for andes-amazon connectivity', *Plos one* **7**(4), e35126.

Forouzbakhsh, F., Hosseini, S. and Vakilian, M. (2007), 'An approach to the investment analysis of small and medium hydro-power plants', *Energy Policy* **35**(2), 1013–1024.

Fowler, K., Knoben, W., Peel, M., Peterson, T., Ryu, D., Saft, M., Seo, K.-W. and Western, A. (2020), 'Many commonly used rainfall-runoff models lack long, slow dynamics: Implications for runoff projections', *Water Resources Research* **56**(5), e2019WR025286.

Gagnon, L., Belanger, C. and Uchiyama, Y. (2002), 'Life-cycle assessment of electricity generation options: The status of research in year 2001', *Energy policy* **30**(14), 1267–1278.

Gagnon, L. and van de Vate, J. F. (1997), 'Greenhouse gas emissions from hydropower: the state of research in 1996', *Energy Policy* **25**(1), 7–13.

Gaudard, L., Gabbi, J., Bauder, A. and Romerio, F. (2016), 'Long-term uncertainty of hydropower revenue due to climate change and electricity prices', *Water Resources Management* **30**(4), 1325–1343.

Gemechu, E. and Kumar, A. (2022), 'A review of how life cycle assessment has been used to assess the environmental impacts of hydropower energy', *Renewable and Sustainable Energy Reviews* **167**, 112684.

Génevaux, C. (2018), 'The sustainable development goals for water and sanitation services interpreting the targets and indicators', *PROGRAMME SOLIDARITÉ EAU pp* pp. 1–55.

Gernaat, D. E., Bogaart, P. W., van Vuuren, D. P., Biemans, H. and Niessink, R. (2017), 'High-resolution assessment of global technical and economic hydropower potential', *Nature Energy* **2**(10), 821–828.

Gielen, D., Boshell, F., Saygin, D., Bazilian, M. D., Wagner, N. and Gorini, R. (2019), 'The role of renewable energy in the global energy transformation', *Energy Strategy Reviews* **24**, 38–50.

Giorgi, F. and Lionello, P. (2008), 'Climate change projections for the mediterranean region', *Global and planetary change* **63**(2-3), 90–104.

Girma, Z. (2016), 'Techno-economic feasibility of small scale hydropower in ethiopia: The case of the kulfo river, in southern ethiopia', *Journal of Renewable Energy* **2016**.

Giuliani, M. and Castelletti, A. (2016), 'Is robustness really robust? how different definitions of robustness impact decision-making under climate change', *Climatic Change* **135**(3-4), 409–424.

Giuliani, M., Herman, J. D., Castelletti, A. and Reed, P. (2014), 'Many-objective reservoir policy identification and refinement to reduce policy inertia and myopia in water management', *Water resources research* **50**(4), 3355–3377.

Giuliani, M., Quinn, J. D., Herman, J. D., Castelletti, A. and Reed, P. M. (2017), 'Scalable multiobjective control for large-scale water resources systems under uncertainty', *IEEE Transactions on Control Systems Technology* **26**(4), 1492–1499.

González, J. S., Rodríguez, A. G., Mora, J. C., Payán, M. B. and Santos, J. R. (2011), 'Overall design optimization of wind farms', *Renewable Energy* **36**(7), 1973–1982.

Gupta, R. S., Hamilton, A. L., Reed, P. M. and Characklis, G. W. (2020), 'Can modern multiobjective evolutionary algorithms discover high-dimensional financial risk portfolio tradeoffs for snow-dominated water-energy systems?', *Advances in water resources* **145**, 103718.

Haasnoot, M., Kwakkel, J. H., Walker, W. E. and ter Maat, J. (2013), 'Dynamic adaptive policy pathways: A method for crafting robust decisions for a deeply uncertain world', *Global environmental change* **23**(2), 485–498.
URL: *https://doi.org/10.1016/j.gloenvcha.2012.12.006*

Hadka, D., Herman, J., Reed, P. and Keller, K. (2015), 'An open source framework for many-

objective robust decision making', *Environmental Modelling & Software* **74**, 114–129.
URL: *https://www.sciencedirect.com/science/article/pii/S1364815215300190*

Hadka, D. and Reed, P. (2012), 'Diagnostic assessment of search controls and failure modes in many-objective evolutionary optimization', *Evolutionary computation* **20**(3), 423–452.

Hadka, D. and Reed, P. (2013), 'Borg: An Auto-Adaptive Many-Objective Evolutionary Computing Framework', *Evolutionary Computation* **21**(2), 231–259.
URL: *https://doi.org/10.1162/EVCO_a_00075*

Hall, C. A., Lambert, J. G. and Balogh, S. B. (2014), 'Eroi of different fuels and the implications for society', *Energy policy* **64**, 141–152.

Hamarat, C., Kwakkel, J. H. and Pruyt, E. (2013), 'Adaptive robust design under deep uncertainty', *Technological Forecasting and Social Change* **80**(3), 408–418.

Hamududu, B. and Killingtveit, A. (2012), 'Assessing climate change impacts on global hydropower', *Energies* **5**(2), 305–322.

Hase, B. and Seidel, C. (2021), 'Balancing services by run-of-river-hydropower at low reservoir amplitudes: Potentials, revenues and emission impacts', *Applied Energy* **294**, 116988.

Hassan, Q., Algburi, S., Sameen, A. Z., Salman, H. M. and Jaszczur, M. (2023), 'A review of hybrid renewable energy systems: Solar and wind-powered solutions: Challenges, opportunities, and policy implications', *Results in Engineering* p. 101621.

Hassan, Q., Viktor, P., Al-Musawi, T. J., Ali, B. M., Algburi, S., Alzoubi, H. M., Al-Jiboory, A. K., Sameen, A. Z., Salman, H. M. and Jaszczur, M. (2024), 'The renewable energy role in the global energy transformations', *Renewable Energy Focus* **48**, 100545.

Hennig, T. and Harlan, T. (2018), 'Shades of green energy: geographies of small hydropower in yunnan, china and the challenges of over-development', *Global Environmental Change* **49**, 116–128.

Herbert-Acero, J. F., Probst, O., Réthoré, P.-E., Larsen, G. C. and Castillo-Villar, K. K. (2014), 'A review of methodological approaches for the design and optimization of wind farms', *Energies* **7**(11), 6930–7016.

Herman, J. D., Reed, P. M., Zeff, H. B. and Characklis, G. W. (2015), 'How should robustness be defined for water systems planning under change?', *Journal of Water Resources Planning and Management* **141**(10), 04015012.
URL: *https://doi.org/10.1061/(ASCE)WR.1943-5452.0000509*

Herman, J. D., Zeff, H. B., Lamontagne, J. R., Reed, P. M. and Characklis, G. W. (2016), 'Synthetic drought scenario generation to support bottom-up water supply vulnerability assessments', *Journal of Water Resources Planning and Management* **142**(11), 04016050.

Herman, J. D., Zeff, H. B., Reed, P. M. and Characklis, G. W. (2014), 'Beyond optimality: Multistakeholder robustness tradeoffs for regional water portfolio planning under deep uncertainty', *Water Resources Research* **50**(10), 7692–7713.
URL: *https://doi.org/10.1002/2014WR015338*

Hernandez, L., Jimenez, G. and Marchena, P. (2018), 'Energy efficiency metrics of university data centers', *Knowledge Engineering and Data Science* **1**(2), 64–73.

Hertwich, E., de Larderel, J. A., Arvesen, A., Bayer, P., Bergesen, J., Bouman, E., Gibon, T., Heath, G., Peña, C., Purohit, P., Ramirez, A. and Suh, S. (2016), *Green Energy Choices: The benefits, risks, and trade-offs of low-carbon technologies for electricity production*, Report of the International Resource Panel, United Nations Environment Program (UNEP).

Hipel, K. W. and Ben-Haim, Y. (1999), 'Decision making in an uncertain world: Information-gap modeling in water resources management', *IEEE Transactions on Systems, Man, and Cybernetics, Part C (Applications and Reviews)* **29**(4), 506–517.

Hoes, O. A., Meijer, L. J., Van Der Ent, R. J. and Van De Giesen, N. C. (2017), 'Systematic high-resolution assessment of global hydropower potential', *PloS one* **12**(2), e0171844.

Hosseini, S., Forouzbakhsh, F. and Rahimpoor, M. (2005), 'Determination of the optimal installation capacity of small hydro-power plants through the use of technical, economic and reliability indices', *Energy Policy* **33**(15), 1948–1956.

Hurford, A., Harou, J. J., Bonzanigo, L., Ray, P., Karki, P., Bharati, L. and Chinnasamy, P. (2020), 'Efficient and robust hydropower system design under uncertainty-a demonstration in nepal', *Renewable and Sustainable Energy Reviews* **132**, 109910.

Hussain, M. I., Muscolo, A., Farooq, M. and Ahmad, W. (2019), 'Sustainable use and management of non-conventional water resources for rehabilitation of marginal lands in arid and semiarid environments', *Agricultural Water Management* **221**, 462–476.
URL: *https://www.sciencedirect.com/science/article/pii/S0378377419304044*

Hussain, S. M., Wahid, A., Shah, M. A., Akhunzada, A., Khan, F., Amin, N. u., Arshad, S. and Ali, I. (2019), 'Seven pillars to achieve energy efficiency in high-performance computing data centers', *Recent Trends and Advances in Wireless and IoT-enabled Networks* pp. 93–105.

IEA (2021), *Hydropower Special Market Report*, International Energy Agency, Paris. [accessed 18-May-2023].

IEA (2022), *Hydroelectricity*, International Energy Agency, Paris. [accessed 05-May-2023].

IEA, I. E. A. (2023a), 'Sdg7: Data and projections'.
URL: *https://www.iea.org/reports/sdg7-data-and-projections*

IEA, International Energy Agency, I. R. E. A. (2023b), 'Tracking sdg7: The energy progress report'.

IHA (2023), 'World hydropower outlook'.

IRENA, I. G. R. (2012), *Renewable Energy Cost Analysis - Hydropower*, IRENA: Abu Dhabi, UAE.

IRENA, I. G. R. (2020), 'Energy transformation 2050', *IRENA: Abu Dhabi, UAE* .

Ishibuchi, H., Imada, R., Setoguchi, Y. and Nojima, Y. (2018), 'How to specify a reference point in hypervolume calculation for fair performance comparison', *Evolutionary computation* **26**(3), 411–440.

Jaccard, M., Melton, N. and Nyboer, J. (2011), 'Institutions and processes for scaling up renewables: Run-of-river hydropower in british columbia', *Energy Policy* **39**(7), 4042–4050.

Jamali, S., Abrishamchi, A. and Madani, K. (2013), 'Climate change and hydropower planning in the middle east: implications for iran's karkheh hydropower systems', *Journal of Energy Engineering* **139**(3), 153–160.

Jones, N. (2018), 'How to stop data centres from gobbling up the world's electricity', *Nature* **561**(7722), 163–166.

Jurasz, J., Mikulik, J., Krzywda, M., Ciapała, B. and Janowski, M. (2018), 'Integrating a wind-and solar-powered hybrid to the power system by coupling it with a hydroelectric power station with pumping installation', *Energy* **144**, 549–563.

Kaldellis, J., Vlachou, D. and Korbakis, G. (2005), 'Techno-economic evaluation of small hydro power plants in greece: a complete sensitivity analysis', *Energy Policy* **33**(15), 1969–1985.

Kao, S.-C. (2013), 'An assessment of energy potential from new stream-reach development in the united states', *Oak Ridge National Laboratory* .

Kasprzyk, J. R., Nataraj, S., Reed, P. M. and Lempert, R. J. (2013), 'Many objective robust decision making for complex environmental systems undergoing change', *Environmental Modelling & Software* **42**, 55–71.
URL: *https://doi.org/10.1016/j.envsoft.2012.12.007*

Katal, A., Dahiya, S. and Choudhury, T. (2022), 'Energy efficiency in cloud computing data centers: a survey on software technologies', *Cluster Computing* pp. 1–31.

Katal, A., Dahiya, S. and Choudhury, T. (2023), 'Energy efficiency in cloud computing data centers: a survey on software technologies', *Cluster Computing* **26**(3), 1845–1875.

Kelley, C. P., Mohtadi, S., Cane, M. A., Seager, R. and Kushnir, Y. (2015), 'Climate change in the fertile crescent and implications of the recent syrian drought', *Proceedings of the national Academy of Sciences* **112**(11), 3241–3246.

Kelly-Richards, S., Silber-Coats, N., Crootof, A., Tecklin, D. and Bauer, C. (2017), 'Governing the transition to renewable energy: A review of impacts and policy issues in the small hydropower boom', *Energy Policy* **101**, 251–264.

Khan, W., Salhi, A., Asif, M., Adeeb, R. and Sulaiman, M. (2015), 'Enhanced version of multi-algorithm genetically adaptive for multiobjective optimization', *International journal of advanced computer science and applications* **6**(12), 279–287.

Kibler, K. M., Tullos, D. D. and Kondolf, G. M. (2011), 'Learning from dam removal monitoring: challenges to selecting experimental design and establishing significance of outcomes', *River Research and Applications* **27**(8), 967–975.

Kishore, T. S., Patro, E. R., Harish, V. and Haghighi, A. T. (2021), 'A comprehensive study on the recent progress and trends in development of small hydropower projects', *Energies* **14**(10), 2882.

Klein, A. (2008), *Feed-in tariff designs: options to support electricity generation from renewable energy sources*, VDM Müller.

Klein, S. and Fox, E. (2022), 'A review of small hydropower performance and cost', *Renewable and Sustainable Energy Reviews* **169**, 112898.

Kondolf, G. M., Rubin, Z. K. and Minear, J. (2014), 'Dams on the mekong: Cumulative sediment starvation', *Water Resources Research* **50**(6), 5158–5169.

Kornis, M. S., Weidel, B. C., Powers, S. M., Diebel, M. W., Cline, T. J., Fox, J. M. and Kitchell, J. F. (2015), 'Fish community dynamics following dam removal in a fragmented agricultural stream', *Aquatic Sciences* **77**(3), 465–480.

Kosnik, L. (2010), 'The potential for small scale hydropower development in the us', *Energy Policy* **38**(10), 5512–5519.

Kosugi, K. (1994), 'Three-parameter lognormal distribution model for soil water retention', *Water Resources Research* **30**(4), 891–901.
URL: *https://doi.org/10.1029/93WR02931*

Kosugi, K. (1996), 'Lognormal distribution model for unsaturated soil hydraulic properties', *Water Resources Research* **32**(9), 2697–2703.
URL: *https://doi.org/10.1029/96WR01776*

Kucukali, S. (2011), 'Risk assessment of river-type hydropower plants using fuzzy logic approach', *Energy Policy* **39**(10), 6683–6688.

Kucukali, S. (2014), 'Finding the most suitable existing hydropower reservoirs for the development of pumped-storage schemes: An integrated approach', *Renewable and Sustainable Energy Reviews* **37**, 502–508.

Kumar, D. and Katoch, S. (2014), 'Sustainability indicators for run of the river (ror) hydropower projects in hydro rich regions of india', *Renewable and Sustainable Energy Reviews* **35**, 101–108.

Kuriqi, A., Pinheiro, A. N., Sordo-Ward, A. and Garrote, L. (2020), 'Water-energy-ecosystem nexus: Balancing competing interests at a run-of-river hydropower plant coupling a hydrologic–ecohydraulic approach', *Energy Conversion and Management* **223**, 113267.

Kwakkel, J. H., Walker, W. E. and Haasnoot, M. (2016), 'Coping with the wickedness of public policy problems: approaches for decision making under deep uncertainty'.

Kwakkel, J. H., Walker, W. E. and Marchau, V. A. (2010), 'Classifying and communicating uncertainties in model-based policy analysis', *International journal of technology, policy and management* **10**(4), 299–315.

Lannelongue, L., Grealey, J. and Inouye, M. (2021), 'Green algorithms: quantifying the carbon footprint of computation', *Advanced science* **8**(12), 2100707.

Lazzaro, G. and Botter, G. (2015), 'Run-of-river power plants in alpine regions: Whither optimal capacity?', *Water resources research* **51**(7), 5658–5676.

Lefley, F. (1996), 'The payback method of investment appraisal: A review and synthesis', *International Journal of Production Economics* **44**(3), 207–224.

Lempert, R. J. (2002), 'A new decision sciences for complex systems', *Proceedings of the National Academy of Sciences* **99**(suppl 3), 7309–7313.
URL: *https://doi.org/10.1073/pnas.082081699*

Lempert, R. J. (2003), 'Shaping the next one hundred years: new methods for quantitative, long-term policy analysis'.

Lempert, R. J. (2014), 'Embedding (some) benefit-cost concepts into decision support processes with deep uncertainty', *Journal of Benefit-Cost Analysis* **5**(3), 487–514.

Lempert, R. J., Groves, D. G., Popper, S. W. and Bankes, S. C. (2006), 'A general, analytic method for generating robust strategies and narrative scenarios', *Management science* **52**(4), 514–528.

Lempert, R. J., Popper, S. W., Groves, D. G., Kalra, N., Fischbach, J. R., Bankes, S. C., Bryant, B. P., Collins, M. T., Keller, K., Hackbarth, A. et al. (2013), 'Making good decisions without predictions: Robust decision making for planning under deep uncertainty', *RAND Corporation, Santa Monica, California. Available: rand. org/pubs/research_briefs/RB9701.(March 2016)* .

Leong, C. and Yokoo, Y. (2021), 'A step toward global-scale applicability and transferability of flow duration curve studies: A flow duration curve review (2000–2020)', *Journal of Hydrology* **603**, 126984.

Li, X., Li, T., Wei, J., Wang, G. and Yeh, W. W.-G. (2013), 'Hydro unit commitment via mixed integer linear programming: A case study of the three gorges project, china', *IEEE Transactions on Power Systems* **29**(3), 1232–1241.

Lin, H.-J. (2010), 'Why should managers like payback period?', *Available at SSRN 1688730* .

Lipp, J. (2007), 'Lessons for effective renewable electricity policy from denmark, germany and the united kingdom', *Energy policy* **35**(11), 5481–5495.

Loisel, H., Mangin, A., Vantrepotte, V., Dessailly, D., Dinh, D. N., Garnesson, P., Ouillon, S., Lefebvre, J.-P., Mériaux, X. and Phan, T. M. (2014), 'Variability of suspended particulate matter concentration in coastal waters under the mekong's influence from ocean color (meris) remote sensing over the last decade', *Remote Sensing of Environment* **150**, 218–230.

Loucks, D. P. and van Beek, E. (2017), 'Water resources planning and management: An overview', *Water Resource Systems Planning and Management* pp. 1–49.

Lund, J. R. (1992), 'Benefit-cost ratios: Failures and alternatives', *Journal of Water Resources Planning and Management* **118**(1), 94–100.

Lütkenhorst, W. and Pegels, A. (2014), 'Stable policies–turbulent markets. germany's green industrial policy: The costs and benefits of promoting solar pv and wind energy', *Lütkenhorst, Wilfried and Pegels, Anna (2014): Stable Policies–Turbulent Markets. Germany's Green Industrial Policy: The Costs and Benefits of Promoting Solar PV and Wind Energy (January 2014). International Institute for Sustainable Development Research Report. Winnipeg: IISD* .

Maier, H. R., Guillaume, J. H., van Delden, H., Riddell, G. A., Haasnoot, M. and Kwakkel, J. H. (2016), 'An uncertain future, deep uncertainty, scenarios, robustness and adaptation: How do they fit together?', *Environmental Modelling & Software* **81**, 154–164.

Mamo, G., Marence, M., Chacon-Hurtado, J. and Franca, M. (2018), 'Optimization of run-of-river hydropower plant capacity', *International Water Power and Dam Construction* .

Manzano-Agugliaro, F., Taher, M., Zapata-Sierra, A., Juaidi, A. and Montoya, F. G. (2017), 'An overview of research and energy evolution for small hydropower in europe', *Renewable and Sustainable Energy Reviews* **75**, 476–489.

Marchau, V. A., Walker, W. E., Bloemen, P. J. and Popper, S. W. (2019), *Decision making under deep uncertainty: from theory to practice*, Springer Nature.

Markannen, S. and Braeckman, P. (2019), 'Financing sustainable hydropower projects in emerging markets: an introduction to concepts and terminology', *Available at SSRN 3538207* .

McCluskey, A. and Lalkhen, A. G. (2007), 'Statistics ii: Central tendency and spread of data', *Continuing Education in Anaesthesia, Critical Care and Pain* **7**(4), 127–130.
URL: *https://doi.org/10.1093/bjaceaccp/mkm020*

McCollum, D., Gomez Echeverri, L., Riahi, K. and Parkinson, S. (2017), *Sdg7: Ensure access to affordable, reliable, sustainable and modern energy for all*, International Council for Science, Paris.

McPhail, C., Maier, H., Kwakkel, J., Giuliani, M., Castelletti, A. and Westra, S. (2018),

'Robustness metrics: How are they calculated, when should they be used and why do they give different results?', *Earth's Future* **6**(2), 169–191.

Mekonnen, M. M. and Hoekstra, A. Y. (2016), 'Four billion people facing severe water scarcity', *Science advances* **2**(2), e1500323.

Milly, P., Betancourt, J., Falkenmark, M., Hirsch, R. M., Kundzewicz, Z. W., Lettenmaier, D. P. and Stouffer, R. J. (2008), 'Stationarity is dead: Whither water management?', *Earth* **4**(20).

Mishra, S., Singal, S. and Khatod, D. (2011), 'Optimal installation of small hydropower plant—a review', *Renewable and Sustainable Energy Reviews* **15**(8), 3862–3869.

Miskat, M. I., Ahmed, A., Rahman, M. S., Chowdhury, H., Chowdhury, T., Chowdhury, P., Sait, S. M. and Park, Y.-K. (2021), 'An overview of the hydropower production potential in bangladesh to meet the energy requirements', *Environ. Eng. Res* **26**, 200514.

Moran, E. F., Lopez, M. C., Moore, N., Müller, N. and Hyndman, D. W. (2018), 'Sustainable hydropower in the 21st century', *Proceedings of the National Academy of Sciences* **115**(47), 11891–11898.

Naidu, B. (2020), 'Scenario of'small hydro'in india', *Renewable Energy-Small Hydro* p. 19.

Nazemi, A., Wheater, H. S., Chun, K. P. and Elshorbagy, A. (2013), 'A stochastic reconstruction framework for analysis of water resource system vulnerability to climate-induced changes in river flow regime', *Water Resources Research* **49**(1), 291–305.
URL: *https://doi.org/10.1029/2012WR012755*

Nedaei, M. and Walsh, P. R. (2022), 'Technical performance evaluation and optimization of a run-of-river hydropower facility', *Renewable Energy* **182**, 343–362.

O'Connor, J. E., Duda, J. J. and Grant, G. E. (2015), '1000 dams down and counting', *Science* **348**(6234), 496–497.

Okot, D. K. (2013), 'Review of small hydropower technology', *Renewable and Sustainable Energy Reviews* **26**, 515–520.

Olbertz, N. (2021), 'Sustainable hydro-power plants with focus on fish-friendly turbine design'.

Onen, M. O. (2018), *Numerical Simulation Model of Single and Multiple Reservoir Operations: Concepts, Numerical Modeling, Operational Rules, and Operation Optimization*, University of California, Irvine.

Oud, E. (2002), 'The evolving context for hydropower development', *Energy Policy* **30**(14), 1215–1223.

Owusu, P. A. and Asumadu-Sarkodie, S. (2016), 'A review of renewable energy sources, sustainability issues and climate change mitigation', *Cogent Engineering* **3**(1), 1167990.

Paish, O. (2002), 'Small hydro power: technology and current status', *Renewable and sustainable energy reviews* **6**(6), 537–556.

Peel, M. C. and Blöschl, G. (2011), 'Hydrological modelling in a changing world', *Progress in Physical Geography* **35**(2), 249–261.
URL: *https://doi.org/10.1177/0309133311402550*

Penche, C. (1998), *Layman's handbook: on how to develop a small hydro site*, European Small Hydropower Association (ESHA).

Penche, C. (2004), 'Guide on how to develop a small hydropower plant', *European Small Hydropower Association, Brussels, Belgium* .

Pendergrass, A. G., Knutti, R., Lehner, F., Deser, C. and Sanderson, B. M. (2017), 'Precipitation variability increases in a warmer climate', *Scientific reports* **7**(1), 1–9.

Pérez-Díaz, J. I., Chazarra, M., García-González, J., Cavazzini, G. and Stoppato, A. (2015), 'Trends and challenges in the operation of pumped-storage hydropower plants', *Renewable and Sustainable Energy Reviews* **44**, 767–784.

Pimentel, D., Berger, B., Filiberto, D., Newton, M., Wolfe, B., Karabinakis, E., Clark, S., Poon, E., Abbett, E. and Nandagopal, S. (2004), 'Water resources: agricultural and environmental issues', *Bioscience* **54**(10), 909–918.

Plummer Braeckman, J. and Guthrie, P. (2015), Loss of value: effects of delay on hydropower stakeholders, *in* 'Proceedings of the Institution of Civil Engineers-Engineering Sustainability', Vol. 169, Thomas Telford Ltd, pp. 253–264.

Pokhrel, Y., Burbano, M., Roush, J., Kang, H., Sridhar, V. and Hyndman, D. W. (2018), 'A review of the integrated effects of changing climate, land use, and dams on mekong river hydrology', *Water* **10**(3), 266.

Pumo, D., Caracciolo, D., Viola, F. and Noto, L. V. (2016), 'Climate change effects on the hydrological regime of small non-perennial river basins', *Science of the Total Environment* **542**, 76–92.
URL: *https://doi.org/10.1016/j.scitotenv.2015.10.109*

Pyrgou, A., Kylili, A. and Fokaides, P. A. (2016), 'The future of the feed-in tariff (fit) scheme in europe: The case of photovoltaics', *Energy Policy* **95**, 94–102.

Quinn, J. D., Reed, P. M., Giuliani, M. and Castelletti, A. (2017), 'Rival framings: A framework for discovering how problem formulation uncertainties shape risk management trade-offs in water resources systems', *Water Resources Research* **53**(8), 7208–7233.

Quinn, J. D., Reed, P. M., Giuliani, M., Castelletti, A., Oyler, J. W. and Nicholas, R. E. (2018), 'Exploring how changing monsoonal dynamics and human pressures challenge multireservoir management for flood protection, hydropower production, and agricultural water supply', *Water Resources Research* **54**(7), 4638–4662.
URL: *https://doi.org/10.1029/2018WR022743*

Raadal, H. L., Gagnon, L., Modahl, I. S. and Hanssen, O. J. (2011), 'Life cycle greenhouse gas (ghg) emissions from the generation of wind and hydro power', *Renewable and Sustainable Energy Reviews* **15**(7), 3417–3422.

Rauscher, S. A., Pal, J. S., Diffenbaugh, N. S. and Benedetti, M. M. (2008), 'Future changes in snowmelt-driven runoff timing over the western us', *Geophysical Research Letters* **35**(16).

Ray, P. A., Bonzanigo, L., Wi, S., Yang, Y.-C. E., Karki, P., Garcia, L. E., Rodriguez, D. J. and Brown, C. M. (2018), 'Multidimensional stress test for hydropower investments facing

climate, geophysical and financial uncertainty', *Global Environmental Change* **48**, 168–181. **URL:** *https://doi.org/10.1016/j.gloenvcha.2017.11.013*

Reed, P. M., Hadka, D., Herman, J. D., Kasprzyk, J. R. and Kollat, J. B. (2013), 'Evolutionary multiobjective optimization in water resources: The past, present, and future', *Advances in water resources* **51**, 438–456.

Rehmani, M. H., Reisslein, M., Rachedi, A., Erol-Kantarci, M. and Radenkovic, M. (2018), 'Integrating renewable energy resources into the smart grid: Recent developments in information and communication technologies', *IEEE Transactions on Industrial Informatics* **14**(7), 2814–2825.

Resch, G., Held, A., Faber, T., Panzer, C., Toro, F. and Haas, R. (2008), 'Potentials and prospects for renewable energies at global scale', *Energy policy* **36**(11), 4048–4056.

Rogeau, A., Girard, R. and Kariniotakis, G. (2017), 'A generic gis-based method for small pumped hydro energy storage (phes) potential evaluation at large scale', *Applied energy* **197**, 241–253.

Rosenberg, D. M., McCully, P. and Pringle, C. M. (2000), 'Global-scale environmental effects of hydrological alterations: introduction', *BioScience* **50**(9), 746–751.

Rougé, C. and Cai, X. (2014), 'Crossing-scale hydrological impacts of urbanization and climate variability in the greater chicago area', *Journal of Hydrology* **517**, 13–27.

Ruijsch, J., Verstegen, J. A., Sutanudjaja, E. H. and Karssenberg, D. (2021), 'Systemic change in the rhine-meuse basin: Quantifying and explaining parameters trends in the pcr-globwb global hydrological model', *Advances in Water Resources* **155**, 104013. **URL:** *https://doi.org/10.1016/j.advwatres.2021.104013*

Sadegh, M., Vrugt, J., Gupta, H. V. and Xu, C. (2016), 'The soil water characteristic as new class of closed-form parametric expressions for the flow duration curve', *Journal of Hydrology* **535**, 438–456.

Saft, M., Peel, M. C., Western, A. W., Perraud, J.-M. and Zhang, L. (2016), 'Bias in stream-

flow projections due to climate-induced shifts in catchment response', *Geophysical Research Letters* **43**(4), 1574–1581.

Salazar, J. Z., Reed, P. M., Herman, J. D., Giuliani, M. and Castelletti, A. (2016), 'A diagnostic assessment of evolutionary algorithms for multi-objective surface water reservoir control', *Advances in water resources* **92**, 172–185.

Saltelli, A., Annoni, P., Azzini, I., Campolongo, F., Ratto, M. and Tarantola, S. (2010), 'Variance based sensitivity analysis of model output. design and estimator for the total sensitivity index', *Computer physics communications* **181**(2), 259–270.

Saltelli, A., Ratto, M., Andres, T., Campolongo, F., Cariboni, J., Gatelli, D., Saisana, M. and Tarantola, S. (2008), *Global sensitivity analysis: the primer*, John Wiley & Sons.

Saługa, P. W. and Kamiński, J. (2018), 'The cost of equity in the energy sector', *Polityka Energetyczna* **21**.

Santolin, A., Cavazzini, G., Pavesi, G., Ardizzon, G. and Rossetti, A. (2011), 'Techno-economical method for the capacity sizing of a small hydropower plant', *Energy Conversion and Management* **52**(7), 2533–2541.

Schaeffer, R., Szklo, A. S., de Lucena, A. F. P., Borba, B. S. M. C., Nogueira, L. P. P., Fleming, F. P., Troccoli, A., Harrison, M. and Boulahya, M. S. (2012), 'Energy sector vulnerability to climate change: a review', *Energy* **38**(1), 1–12.

Schmitt, R. J., Bizzi, S., Castelletti, A. and Kondolf, G. (2018), 'Improved trade-offs of hydropower and sand connectivity by strategic dam planning in the mekong', *Nature Sustainability* **1**(2), 96–104.

Schmitt, R. J., Bizzi, S., Castelletti, A., Opperman, J. and Kondolf, G. M. (2019), 'Planning dam portfolios for low sediment trapping shows limits for sustainable hydropower in the mekong', *Science advances* **5**(10), eaaw2175.

Séguin, S., Fleten, S.-E., Côté, P., Pichler, A. and Audet, C. (2017), 'Stochastic short-term hydropower planning with inflow scenario trees', *European Journal of Operational Research* **259**(3), 1156–1168.

Seibert, J., van Meerveld, H. et al. (2016), 'Hydrological change modeling: challenges and opportunities.', *Hydrological Processes* **30**(26), 4966–4971.

Shaktawat, A. and Vadhera, S. (2021), 'Risk management of hydropower projects for sustainable development: a review', *Environment, Development and Sustainability* **23**(1), 45–76.

Sheffield, J., Wood, E. F., Pan, M., Beck, H., Coccia, G., Serrat-Capdevila, A. and Verbist, K. (2018), 'Satellite remote sensing for water resources management: Potential for supporting sustainable development in data-poor regions', *Water Resources Research* **54**(12), 9724–9758.

Sheikholeslami, R. and Razavi, S. (2017), 'Progressive latin hypercube sampling: An efficient approach for robust sampling-based analysis of environmental models', *Environmental modelling & software* **93**, 109–126.

Shortridge, J. E. and Guikema, S. D. (2016), 'Scenario discovery with multiple criteria: An evaluation of the robust decision-making framework for climate change adaptation', *Risk Analysis* **36**(12), 2298–2312.

Sinagra, M., Sammartano, V., Aricò, C., Collura, A. and Tucciarelli, T. (2014), 'Cross-flow turbine design for variable operating conditions', *Procedia Engineering* **70**, 1539–1548.

Singh, R., Reed, P. M. and Keller, K. (2015), 'Many-objective robust decision making for managing an ecosystem with a deeply uncertain threshold response', *Ecology and Society* **20**(3).

Singh, V. K. and Singal, S. (2017), 'Operation of hydro power plants-a review', *Renewable and Sustainable Energy Reviews* **69**, 610–619.

Singh, V. P. (2018), 'Hydrologic modeling: progress and future directions', *Geoscience letters* **5**(1), 1–18.
URL: *https://doi.org/10.1186/s40562-018-0113-z*

Siu, T. K., Nash, G. A. and Shawwash, Z. K. (2001), 'A practical hydro, dynamic unit commitment and loading model', *IEEE transactions on power systems* **16**(2), 301–306.

Sobol, I. M. (2001), 'Global sensitivity indices for nonlinear mathematical models and their monte carlo estimates', *Mathematics and computers in simulation* **55**(1-3), 271–280.

Sovacool, B. K., Gilbert, A. and Nugent, D. (2014), 'An international comparative assessment of construction cost overruns for electricity infrastructure', *Energy Research & Social Science* **3**, 152–160.

Spinoni, J., Naumann, G., Carrao, H., Barbosa, P. and Vogt, J. (2014), 'World drought frequency, duration, and severity for 1951–2010', *International Journal of Climatology* **34**(8), 2792–2804.

Spinoni, J., Vogt, J. V., Naumann, G., Barbosa, P. and Dosio, A. (2018), 'Will drought events become more frequent and severe in europe?', *International Journal of Climatology* **38**(4), 1718–1736.

Sreeparvathy, V. and Srinivas, V. (2022), 'Meteorological flash droughts risk projections based on cmip6 climate change scenarios', *npj Climate and Atmospheric Science* **5**(1), 77.

Stagge, J. H. and Moglen, G. E. (2013), 'A nonparametric stochastic method for generating daily climate-adjusted streamflows', *Water Resources Research* **49**(10), 6179–6193.
URL: *https://doi.org/10.1002/wrcr.20448*

Steffen, B. (2020), 'Estimating the cost of capital for renewable energy projects', *Energy Economics* **88**, 104783.

Steinbach, J. and Staniaszek, D. (2015), 'Discount rates in energy system analysis discussion paper', *BPIE: Berlin, Germany* .

Sternberg, R. (2010), 'Hydropower's future, the environment, and global electricity systems', *Renewable and Sustainable Energy Reviews* **14**(2), 713–723.

SYGM (2016), 'Climate change impacts on water resources, final report (in turkish)', *General Directorate Of Water Management, Ministry of Agriculture and Forestry, Turkey* . [accessed 19-February-2023].

Taktak, R. and D'Ambrosio, C. (2017), 'An overview on mathematical programming approaches for the deterministic unit commitment problem in hydro valleys', *Energy Systems* **8**(1), 57–79.

Taner, M. Ü., Ray, P. and Brown, C. (2017), 'Robustness-based evaluation of hydropower infrastructure design under climate change', *Climate Risk Management* **18**, 34–50.

Tefera, W. M. and Kasiviswanathan, K. (2022), 'A global-scale hydropower potential assessment and feasibility evaluations', *Water Resources and Economics* **38**, 100198.

Teotónio, C., Fortes, P., Roebeling, P., Rodriguez, M. and Robaina-Alves, M. (2017), 'Assessing the impacts of climate change on hydropower generation and the power sector in portugal: a partial equilibrium approach', *Renewable and Sustainable Energy Reviews* **74**, 788–799.

Thornton, G. and Pipeline, C. E. (2018), 'Renewable energy discount rate survey results–2017', *Grant Thornton and Clean Energy Pipeline Initiative, Grant Thornton UK LLP* .

Tian, X., Galelli, S. and de Neufville, R. (2018), 'Impact of operating rules on planning capacity expansion of urban water supply systems', *Urban Water Journal* **15**(7), 654–661.

Tramblay, Y., Rutkowska, A., Sauquet, E., Sefton, C., Laaha, G., Osuch, M., Albuquerque, T., Alves, M. H., Banasik, K., Beaufort, A., Brocca, L., Camici, S., Csabai, Z., Dakhlaoui, H., DeGirolamo, A. M., Dörflinger, G., Gallart, F., Gauster, T., Hanich, L., Kohnová, S., Mediero, L., Plamen, N., Parry, S., Quintana-Seguí, P., Tzoraki, O. and Datry, T. (2021), 'Trends in flow intermittence for european rivers', *Hydrological Sciences Journal* **66**(1), 37–49.
URL: *https://doi.org/10.1080/02626667.2020.1849708*

Tsuanyo, D., Amougou, B., Aziz, A., Nka Nnomo, B., Fioriti, D. and Kenfack, J. (2023), 'Design models for small run-of-river hydropower plants: a review', *Renewables: Wind, Water, and Solar* **10**(1), 3.

Tullos, D., Tilt, B., Liermann, C. R. et al. (2009), 'Understanding and linking the biophysical,

socio economic and geopolitical effects of dams.', *Journal of environmental management* **90**(Supplement 3).

Turconi, R., Boldrin, A. and Astrup, T. (2013), 'Life cycle assessment (lca) of electricity generation technologies: Overview, comparability and limitations', *Renewable and sustainable energy reviews* **28**, 555–565.

Turkes, M., Turp, M. T., An, N., Ozturk, T. and Kurnaz, M. L. (2020), *Impacts of Climate Change on Precipitation Climatology and Variability in Turkey*, Springer International Publishing, Cham.

Turner, S. W., Ng, J. Y. and Galelli, S. (2017b), 'Examining global electricity supply vulnerability to climate change using a high-fidelity hydropower dam model', *Science of the Total Environment* **590**, 663–675.

UN (2015), 'United nations: Transforming our world: The 2030 agenda for sustainable development', *UN: New York, NY, USA* .

UN (2019), 'The sustainable development goals report 2019', *New York* .

UN-Water (2023), 'Sustainable development goal 6 synthesis report on water and sanitation'.

UNDRR (2015), 'Resilience: In the 2030 agenda for sustainable development', *UNDRR: Geneva, Switzerland* .

UNIDO (2022), *World small hydropower development report*, United Nations Industrial Development Organization (UNIDO) and the International Center on Small Hydro Power (ICSHP).
URL: *https://www.unido.org/WSHPDR2022*

USBR (2011), 'Hydropower resource assessment at existing reclamation facilities'.

Vachhani, V. L., Dabhi, V. K. and Prajapati, H. B. (2015), Survey of multi objective evolutionary algorithms, *in* '2015 international conference on circuits, power and computing technologies [ICCPCT-2015]', IEEE, pp. 1–9.

Van Genuchten, M. T. (1980), 'A closed-form equation for predicting the hydraulic conductivity of unsaturated soils', *Soil science society of America journal* **44**(5), 892–898.
URL: *https://doi.org/10.2136/sssaj1980.03615995004400050002x*

Van Veldhuizen, D. A. (1999), *Multiobjective evolutionary algorithms: classifications, analyses, and new innovations*, Air Force Institute of Technology.

Van Vliet, M. T., Sheffield, J., Wiberg, D. and Wood, E. F. (2016), 'Impacts of recent drought and warm years on water resources and electricity supply worldwide', *Environmental Research Letters* **11**(12), 124021.

Vogel, R. M. and Fennessey, N. (1994), 'Flow duration curves i: new interpretation and confidence intervals', *Journal of Water Resources Planning and Management* **120**(4).

Voros, N., Kiranoudis, C. and Maroulis, Z. (2000), 'Short-cut design of small hydroelectric plants', *Renewable Energy* **19**(4), 545–563.

Vrugt, J. (2015), 'Multi-criteria optimization using the amalgam software package: theory, concepts, and matlab implementation', *Manual, Version* **1**, 1–53.

Vrugt, J. A. and Robinson, B. A. (2007), 'Improved evolutionary optimization from genetically adaptive multimethod search', *Proceedings of the National Academy of Sciences* **104**(3), 708–711.
URL: *https://www.pnas.org/content/104/3/708*

Vrugt, J. A. and Sadegh, M. (2013), 'Toward diagnostic model calibration and evaluation: Approximate bayesian computation', *Water Resources Research* **49**(7), 4335–4345.
URL: *https://doi.org/10.1002/wrcr.20354*

Walker, W. E., Lempert, R. J. and Kwakkel, J. H. (2013), *Deep Uncertainty*, Springer US, Boston, MA, pp. 395–402.
URL: *https://doi.org/10.1007/978-1-4419-1153-7*$_{1140}$

Wang, D. and Hejazi, M. (2011), 'Quantifying the relative contribution of the climate and direct human impacts on mean annual streamflow in the contiguous united states', *Water*

resources research **47**(10).
URL: *https://doi.org/10.1029/2010WR010283*

Wang, J. and Rosenberg, D. E. (2023), 'Adapting colorado river basin depletions to available water to live within our means', *Journal of Water Resources Planning and Management* **149**(7), 04023026.

Wang, X., Virguez, E., Kern, J., Chen, L., Mei, Y., Patiño-Echeverri, D. and Wang, H. (2019), 'Integrating wind, photovoltaic, and large hydropower during the reservoir refilling period', *Energy Conversion and Management* **198**, 111778.

Wasti, A., Ray, P., Wi, S., Folch, C., Ubierna, M. and Karki, P. (2022), 'Climate change and the hydropower sector: A global review', *Wiley Interdisciplinary Reviews: Climate Change* **13**(2), e757.

Weisberg, H. (1992), *Central tendency and variability*, Sage.

Weisser, D. (2007), 'A guide to life-cycle greenhouse gas (ghg) emissions from electric supply technologies', *Energy* **32**(9), 1543–1559.

Wild, T. B., Reed, P. M., Loucks, D. P., Mallen-Cooper, M. and Jensen, E. D. (2019), 'Balancing hydropower development and ecological impacts in the mekong: Tradeoffs for sambor mega dam', *Journal of Water Resources Planning and Management* **145**(2), 05018019.

Wilks, D. S. (2011), *Statistical methods in the atmospheric sciences*, Vol. 100, Academic press.

Winemiller, K. O., McIntyre, P. B., Castello, L., Fluet-Chouinard, E., Giarrizzo, T., Nam, S., Baird, I. G., Darwall, W., Lujan, N. K., Harrison, I., Stiassny, M. L. J., Silvano, R. A. M., Fitzgerald, D. B., Pelicice, F. M., Agostinho, A. A., Gomes, L. C., Albert, J. S., Baran, E., Petrere, M., Zarfl, C., Mulligan, M., Sullivan, J. P., Arantes, C. C., Sousa, L. M., Koning, A. A., Hoeinghaus, D. J., Sabaj, M., Lundberg, J. G., Armbruster, J., Thieme, M. L., Petry, P., Zuanon, J., Vilara, G. T., Snoeks, J., Ou, C., Rainboth, W., Pavanelli, C. S., Akama, A., van Soesbergen, A. and Sáenz, L. (2016), 'Balancing hydropower and biodiversity in the amazon, congo, and mekong', *Science* **351**(6269), 128–129.
URL: *https://www.science.org/doi/abs/10.1126/science.aac7082*

Yah, N. F., Oumer, A. N. and Idris, M. S. (2017), 'Small scale hydro-power as a source of renewable energy in malaysia: A review', *Renewable and Sustainable Energy Reviews* **72**, 228–239.

Yard, S. (2000), 'Developments of the payback method', *International journal of production economics* **67**(2), 155–167.

Ye, L., Gu, X., Wang, D. and Vogel, R. M. (2021), 'An unbiased estimator of coefficient of variation of streamflow', *Journal of Hydrology* **594**, 125954.
URL: *https://doi.org/10.1016/j.jhydrol.2021.125954*

Yildiz, V. (2015), *Numerical simulation model of run of river hydropower plants: Concepts, Numerical modeling, Turbine system and selection, and design optimization*, University of California, Irvine.

Yildiz, V., Brown, S. and Rougé, C. (2024a), 'Importance of variable turbine efficiency in run-of-river hydropower design under deep uncertainty', *Water Resources Research* **60**(6), e2023WR035713.

Yildiz, V., Brown, S. and Rougé, C. (2024b), 'Ror-hydropower-robust-design'.
URL: *https://doi.org/10.5281/zenodo.10627287*

Yildiz, V., Brown, S. and Rougé, C. (Under Review, 2024c), 'Making robust design computationally affordable: the case of optimised run-of-river hydropower plant design', *Environmental modelling & software* .

Yildiz, V., Hatipoglu, M. A. and Kumcu, S. Y. (2022), *Climate Change Impacts on Water Resources*, Springer International Publishing, Cham, chapter 1, pp. 17–25.

Yildiz, V., Milton, R., Brown, S. and Rougé, C. (2023a), 'Technical note: Statistical generation of climate-perturbed flow duration curves', *Hydrology and Earth System Sciences* **27**(13), 2499–2507.
URL: *https://hess.copernicus.org/articles/27/2499/2023/*

Yildiz, V., Rougé, C. and Brown, S. (2021), Application multi-objective robust decision-

making to the design of run-ofriver hydropower plants, *in* 'EGU General Assembly Conference Abstracts', pp. EGU21–12887.

Yildiz, V., Rougé, C., Milton, R. and Brown, S. (2023b), 'Climateperturbed_fdcs: V1.0.2'.
URL: *https://doi.org/10.5281/zenodo.7662679*

Yildiz, V. and Vrugt, J. A. (2019), 'A toolbox for the optimal design of run-of-river hydropower plants', *Environmental modelling & software* **111**, 134–152.
URL: *https://doi.org/10.1016/j.envsoft.2018.08.018*

Yilmaz, K. K., Gupta, H. V. and Wagener, T. (2008), 'A process-based diagnostic approach to model evaluation: Application to the nws distributed hydrologic model', *Water resources research* **44**(9).
URL: *https://doi.org/10.1029/2007WR006716*

Yüksel, I. (2010), 'Hydropower for sustainable water and energy development', *Renewable and Sustainable Energy Reviews* **14**(1), 462–469.

Zaniolo, M., Fletcher, S. and Mauter, M. (2024), 'Find: A synthetic weather generator to control drought frequency, intensity, and duration', *Environmental Modelling & Software* **172**, 105927.

Zarfl, C., Lumsdon, A. E., Berlekamp, J., Tydecks, L. and Tockner, K. (2015), 'A global boom in hydropower dam construction', *Aquatic Sciences* **77**, 161–170.

Zarrin, A. and Dadashi-Roudbari, A. (2021), 'Projection of future extreme precipitation in iran based on cmip6 multi-model ensemble', *Theoretical and Applied Climatology* **144**(1), 643–660.
URL: *https://doi.org/10.1007/s00704-021-03568-2*

Zhang, B., Xia, Y., Huning, L. S., Wei, J., Wang, G. and AghaKouchak, A. (2019), 'A framework for global multicategory and multiscalar drought characterization accounting for snow processes', *Water resources research* **55**(11), 9258–9278.

Zhang, Q., Smith, B. and Zhang, W. (2012), 'Small hydropower cost reference model',

ORNL/TM-2012/501. Oak Ridge National Laboratory. http://info. ornl. gov/sites/publications/files/pub39663. pdf .

Zhang, X., Li, H.-Y., Deng, Z. D., Ringler, C., Gao, Y., Hejazi, M. I. and Leung, L. R. (2018), 'Impacts of climate change, policy and water-energy-food nexus on hydropower development', *Renewable Energy* **116**, 827–834.

Zhang, Y., Zheng, H., Zhang, X., Leung, L. R., Liu, C., Zheng, C., Guo, Y., Chiew, F. H., Post, D., Kong, D. et al. (2023), 'Future global streamflow declines are probably more severe than previously estimated', *Nature Water* **1**(3), 261–271.

Zhou, Q. and Li, Z. (2011), 'Zhou a., qu b.-y., li h., zhao s.-z., suganthan pn, zhang q', *Multiobjective evolutionary algorithms: a survey of the state of the art, Swarm Evol. Comput* **1**(1), 32–49.

Zhou, Y., Hejazi, M., Smith, S., Edmonds, J., Li, H., Clarke, L., Calvin, K. and Thomson, A. (2015), 'A comprehensive view of global potential for hydro-generated electricity', *Energy & Environmental Science* **8**(9), 2622–2633.

Zhuang, J., Liang, Z., Lin, T. and Guzman, F. (2007), 'Theory and practice in the choice of social discount rate for cost-benefit analysis', *Asian Development Bank: Philippines* .

Zitzler, E., Thiele, L., Laumanns, M., Fonseca, C. M. and Da Fonseca, V. G. (2003), 'Performance assessment of multiobjective optimizers: An analysis and review', *IEEE Transactions on evolutionary computation* **7**(2), 117–132.

Appendices

APPENDIX A

Supplementary information to Chapter 3

This supplementary information demonstrates that for triplets (M, V, L) of streamflow statistics representing average behavior, variability, and low flows, there is unique parameterisation of the flow duration curve (FDC) according to the Kosugi model. We consider the "mean" case where $(M, V, L) = (\mu, \sigma, q_{low})$ where μ is the mean, σ is the standard deviation and q_{low} is the 1^{st} or 5^{th} percentile of flow, and the "median case" $(M, V, L) = (m, CV, q_{low})$ where m is the median and $CV = \mu/\sigma$ is the coefficient of variation. It also provides conditions on (M, V, L) for the existence of a parameterisation.

A.1 Kosugi function reminders

We model the flow duration curve (FDC) with the Kosugi equation, as proposed by Sadegh et al. (2016). The equation models streamflow q as a function of the flow quantile $u \in [0, 1]$:

$$q(u) = c + (a - c)\, z(u)^b \tag{A.1}$$

where (a, b, c) are parameters, with a and c in the same units as q, and b unitless. We need $a - c > 0$ and $b > 0$ for $z(u)$ is defined as follows, and represented in Figure S1:

$$z(u) = \exp\left[\sqrt{2}\,\mathrm{erfc}^{-1}(2u)\right] \tag{A.2}$$

This supplementary information will relate parameters (a, b, c) to triplets of streamflow statistics (M, V, L) representing average behavior, variability, and low flows. It will do so first in the "mean" case of $(M, V, L) = (\mu, \sigma, q_{low})$ in Section A.2, where μ is the mean, σ is the standard deviation and q_{low} is the 1^{st} or 5^{th} percentile of flow. Then in Section A.3

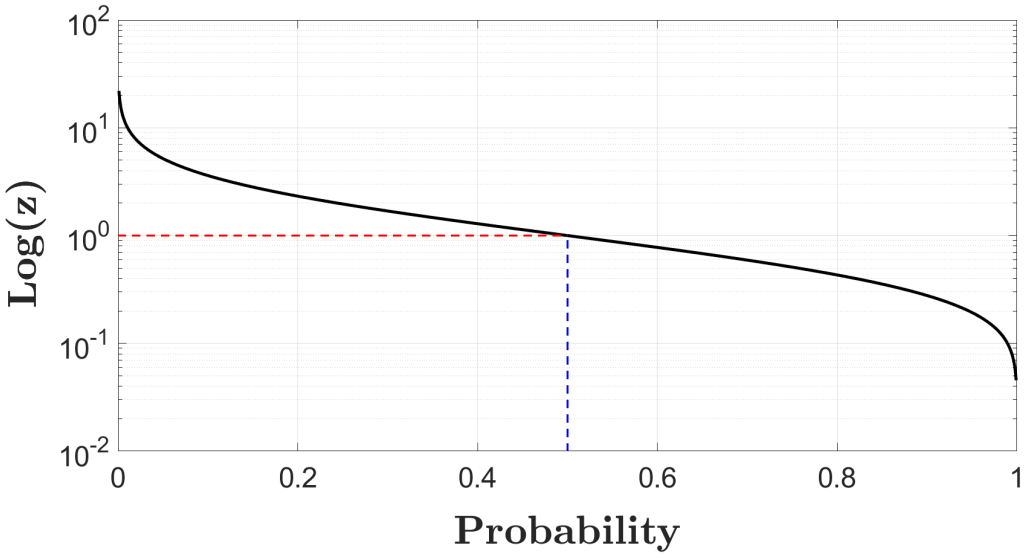

Figure S1: *The $z(e)$ function.*

we will examine the "median case" of $(M, V, L) = (m, CV, q_{low})$, where m is the median and $CV = \mu/\sigma$ is the coefficient of variation.

A.2 "Mean" case $(M, V, L) = (\mu,\, \sigma,\, q_{low})$

In this section we assume we know the streamflow mean μ, standard deviation σ and low flow percentile q_{low}. We assume we have $\mu > q_{low}$. We will prove the (a, b, c) triplet of Kosugi parameter is unique, and give a sufficient condition on (μ, σ, q_{low}) for its existence.

A.2.1 Relating parameter triplets

Writing the definition of mean, standard deviation and low flow quantile for the Kosugi FDC yields three equations. For this, let us introduce the auxiliary function f:

$$f(b) = \int_0^1 z(u)^b \, du \tag{A.3}$$

We can then write the mean μ according to its definition as the integral of $q(u)$ for $u \in [0, 1]$. Using the linearity properties of the integral yields:

$$\mu = c + (a - c) f(b) \tag{A.4}$$

Similarly, by definition of the variance, and using the definition of the mean above, we have:

$$\sigma^2 = \int_0^1 \left[c + (a-c)z(u)^b\right]^2 du - [c + (a-c)f(b)]^2 \tag{A.5}$$

Developing the squares and exploiting again the linearity of the integral enables us to simplify this into this definition of V:

$$\sigma = (a-c)\sqrt{f(2b) - f(b)^2} \tag{A.6}$$

Lastly, introducing $\varepsilon = z(q_{low})$ where $q_{low} = 0.99$ (respectively 0.95) if we are interested in the first (resp. fifth) flow percentile, we have the following relationship for q_{low}:

$$q_{low} = c + (a-c)\,\varepsilon^b \tag{A.7}$$

A.2.2 Solution strategy

Clearly, for b fixed, (a, c) is the solution of a system of two linear equations. For instance, from equations (A.4) and (A.7), we get:

$$\begin{cases} \mu = c + (a-c)f(b) \\ q_{low} = c + (a-c)\,\varepsilon^b \end{cases} \tag{A.8}$$

which is equivalent to:

$$\begin{cases} a - c = \dfrac{\mu - q_{low}}{f(b) - \varepsilon^b} \\ a = \dfrac{q_{low}\,(f(b) - 1) + \mu(1 - \varepsilon^b)}{f(b) - \varepsilon^b} \\ c = \dfrac{q_{low}\,f(b) - \mu\,\varepsilon^b}{f(b) - \varepsilon^b} \end{cases} \tag{A.9}$$

We can then relate streamflow parameters (μ, σ, q_{low}) to Kosugi parameter function of b alone, by replacing $(a - c)$ into equation (A.6):

$$\frac{\sigma}{\mu - q_{low}} = \frac{\sqrt{f(2b) - f(b)^2}}{f(b) - \varepsilon^b} = \mathcal{F}(b) \tag{A.10}$$

Thus, whether we can find a unique triplet (a, b, c) for (μ, σ, q_{low})hinges on whether $\mathcal{F}(b)$ is monotonous for $b > 0$. Then existence will depend on (1) proving that $f(b) > \varepsilon^b$ for $b > 0$ (so $\mathcal{F}(b)$ is defined and positive), and (2) establishing the lower bond for $\mathcal{F}(b)$. For all of this, it would be easier to work with a simpler expression for $f(b)$. This is the topic of the next paragraph.

A.2.3 Simplifying $f(b)$

Let us operate a variable change $x = \mathrm{erfc}^{-1}(2u)$ in the integral that defines $f(b)$. Then for $u = 0$, we have $x = +\infty$, for $u = 1$ we have $x = -\infty$. We also have $u = \mathrm{erfc}(x)/2 = (1 - \mathrm{erf}(x))/2$. Using the derivation of the error function to relate du and dx we can therefore write:

$$f(b) = \int_0^1 \exp\left[\sqrt{2}\,\mathrm{erfc}^{-1}(2u)\right]^b du = \int_{+\infty}^{-\infty} e^{\sqrt{2}bx} \frac{-e^{-x^2}}{\sqrt{\pi}} dx \tag{A.11}$$

Which directly leads to:

$$f(b) = \frac{1}{\sqrt{\pi}} \int_{-\infty}^{+\infty} \exp\left(-(x - \frac{b}{\sqrt{2}})^2\right) e^{b^2/2} dx \tag{A.12}$$

Then a further change of variable $y = x - b/\sqrt{2}$ leads to:

$$f(b) = e^{b^2/2} \left(\frac{1}{\sqrt{\pi}} \int_{-\infty}^{+\infty} e^{-y^2} dy\right) \tag{A.13}$$

and since the quantity between the parentheses is equal to 1 this simplifies into:

$$f(b) = e^{b^2/2} \tag{A.14}$$

This remarkable equation simplifies the calculations going forward. It also demonstrates that $f(b) - \varepsilon^b = \exp(b^2) - \exp(b\ln(\varepsilon))$ is positive for $b > 0$, because $\ln(\varepsilon) < 0$.

A.2.4 Unicity of the parameterisation

Using the result from equation (A.14) into equation (A.10), we can write:

$$\mathcal{F}(b) = \frac{g(b)}{h(b)} \tag{A.15}$$

with:

$$\begin{cases} g(b) = \sqrt{e^{b^2} - 1} \\ h(b) = 1 - e^{-b^2/2}\varepsilon^b \end{cases} \tag{A.16}$$

Recall that to demonstrate unicity of the Kosugi parameterisation, it is enough to show that for $b > 0$, $\mathcal{F}(b)$ grows monotonically with b. Derivation with respect to b yields:

$$\begin{cases} g'(b) = \dfrac{b\, e^{b^2}}{g(b)} \\ h'(b) = (b - \ln(\varepsilon))e^{-b^2/2}\varepsilon^b \end{cases} \tag{A.17}$$

where ln is the base e logarithm, $(\ln(e) = 1)$. Since $g(b) > 0$, we can write for $b > 0$:

$$\mathcal{F}'(b) = \frac{1}{g(b)h^2(b)} \Big(g(b)g'(b)h(b) - g^2(b)h'(b) \Big) \tag{A.18}$$

Thanks to the above equation, $\mathcal{F}'(b)$ has the same sign as $\mathcal{U} = gg'h - g^2h'$. $\mathcal{U}(b)$ is given by:

$$\mathcal{U}(b) = be^{b^2} + \varepsilon^b \left[b(e^{-b^2/2} - 2e^{b^2/2}) + \ln(\varepsilon) \left(e^{b^2/2} - e^{-b^2/2} \right) \right] \tag{A.19}$$

Figure S2 graphically shows that $\ln(\mathcal{U}(b)) > 0$ for $b > 0$, in both cases where $\varepsilon = z(0.99)$ (if q_{low} is the first percentile) or $\varepsilon = z(0.95)$ (if q_{low} is the first percentile). We also represented e^{b^2} on Figure S2, since it becomes the dominant term in $\mathcal{U}(b)$ as b grows farther from 0. It is therefore clear that $\mathcal{F}(b)$ grows with b when $b > 0$, and that therefore, there is at most a unique b solution of equation (A.10). Equation (A.9) provides unique a and c for a value of b. This enables us to conclude on the uniqueness of the Kosugi parameterisation.

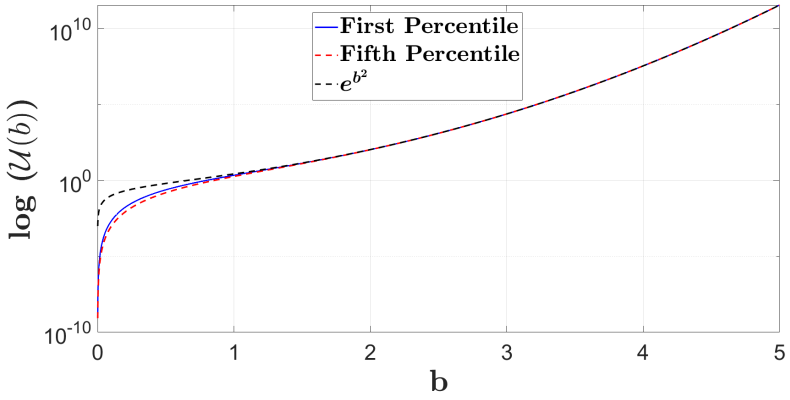

Figure S2: *Representation of* $\log(\mathcal{U}(b))$ *to establish that* $\mathcal{F}'(b) > 0$. *Blue coloured line and dashed red line represent the derivation based on first percentile and fifth percentile of flow respectively. The dashed black line signifies* e^{b^2}.

A.2.5 Condition for existence

$\mathcal{F}(b) = g(b)/h(b)$ grows monotonically with b when $b > 0$, and goes to $+\infty$ as $b \to +\infty$. Therefore, a solution exists if:

$$\frac{\sigma}{\mu - q_{low}} \lim_{b \to 0^+} h(b) > \lim_{b \to 0} g(b) \tag{A.20}$$

and these limits are defined because both g and h are continuously differentiable over $]0, +\infty)$. The respective first-order Taylor expansions of g and h at 0^+ yield:

$$\begin{cases} g(b) = b + o(b) \\ h(b) = -\ln(\varepsilon)\, b + o(b) \end{cases} \tag{A.21}$$

Since Taylor expansions are unique, the results from equation (A.21) into equation (A.20) yields the existence condition:

$$\frac{\sigma}{\mu - q_{low}} > \frac{-1}{\ln(\varepsilon)} \tag{A.22}$$

where $\varepsilon < 1$ so $\ln(\varepsilon) < 0$ and $-1/\ln(\varepsilon) \approx 0.43$ if q_{low} is the first percentile; 0.61 if q_{low} is the fifth percentile. Note this condition is sufficient: if it is met, one can find the unique b with equation (A.10), then a and c with equation (A.9).

A.3 Median, coefficient of variation and low flow quantile

In this section we assume we know the streamflow median m, coefficient of variation $CV = \sigma/\mu$, and low flow percentile q_{low}. We assume flow is not constant for large-stretches of the FDC (true for natural flows in perennial rivers) so we have $m > q_{low}$ and $CV > 0$. We will prove the (a, b, c) triplet of Kosugi parameter is unique, and exists given a condition on (μ, σ, q_{low}) that is often met in practice.

A.3.1 Relating parameter triplets

The median m corresponds to $q(0.5)$ in equation (A.1). Since for $u = 0.5$ we have $z(u) = 0$, we have:

$$M = a \tag{A.23}$$

CV is the ratio of standard deviation and mean. These two quantities are given by equations (A.6) and (A.4), respectively, so:

$$CV = \frac{(a - c)\sqrt{f(2b) - f(b)^2}}{c + (a - c)f(b)} \tag{A.24}$$

Finally, q_{low} still verifies equation (A.7).

A.3.2 Solution strategy

Finding a is immediate thanks to equation (A.23), and combined with equation (A.7), this directly leads to the following expression for c:

$$c = \frac{q_{low} - m\varepsilon^b}{1 - \varepsilon^b} \tag{A.25}$$

which means that c can be easily and uniquely computed once b is known. To find b, we use equation (A.24) and replace $f(b)$ with $e^{b^2/2}$ thanks to equation (A.14). This leads to:

$$CV = \frac{\sqrt{e^{b^2} - 1}}{e^{-b^2/2}\frac{c}{a-c} + 1} \tag{A.26}$$

Let us introduce R as the ratio of L by M:

$$R = \frac{L}{M} \tag{A.27}$$

Clearly, we have $0 < R < 1$. Equations (A.23) and (A.25) then become:

$$\frac{c}{a-c} = \frac{R - \varepsilon^b}{1 - R} \tag{A.28}$$

And finally:

$$CV = (1 - R)\frac{\sqrt{e^{b^2} - 1}}{1 - R + (R - \varepsilon^b)e^{-b^2/2}} = \mathcal{G}(b) \tag{A.29}$$

where $\mathcal{G}$ only depends on b because R is a known parameter. As was the case in Section A.2, we need to establish that there is (at most) a single $b > 0$ for a given value of V, and find the condition for existence. Then we can then deduce c. Yet, before establishing unicity and condition for existence, it is important to clarify on which range for $b > 0$ we can say that $\mathcal{G}(b)$ is defined.

A.3.3 Range of b for which the equation for CV is defined

Similar to equation (A.15), we can write:

$$\mathcal{G}(b) = (1 - R)\frac{g(b)}{k(b)} \tag{A.30}$$

with $g(b)$ (and $g'(b)$) defined as in equations (A.16) and (A.17), and $k(b)$ defined as:

$$k(b) = 1 - R + (R - \varepsilon^b)e^{-b^2/2} \tag{A.31}$$

$\mathcal{G}(b)$ is defined in the range for $b > 0$ in which $k(b) \neq 0$. Since $g(b) > 0$, it corresponds to a coefficient of variation in the range in which $k(b) > 0$. We have $k(0) = 0$ and $\lim_{b\to\infty} k(b) = 1 - R > 0$, and need to understand variations to know what happens in between. $k(b)$ is derivated as follows:

$$k'(b) = \left[-bR + (b - \ln(\varepsilon))\varepsilon^b\right] e^{-b^2/2} \tag{A.32}$$

so that $k'(b)$ has the sign of $v(b) = \left[-bR + (b - \ln(\varepsilon))\varepsilon^b\right]$. In turn we have:

$$v'(b) = -R + [1 + (b - \ln(\varepsilon))\ln(\varepsilon)]\,\varepsilon^b \tag{A.33}$$

Since $\ln(\varepsilon) < -1$, for any positive value of b, $[1 + (b - \ln(\varepsilon))\ln(\varepsilon)] < 0$. This means that v is monotonously decreasing for $b \geq 0$. We have $v(0) = -\ln(\varepsilon) > 1$, and $\lim_{b\to\infty} k(b) = -\infty$ because $-bR$ is the dominant term. Therefore, there is a b_{lim} such that $v(b_{lim}) = 0$. For $b < b_{lim}$, $k(b)$ grows strictly and monotonously to a global maximum $k(b_{lim})$, then it degrows for $b > b_{lim}$ towards its limit value $1 - R > 0$. This means that $k(b_{lim}) > 0$, and $k(b) > 0$ for $b > 0$.

A.3.4 Unicity of the parameterisation

For $b > b_{lim}$, We know that the numerator $g(b)$ always grows with $b > 0$, and for $b > b_{lim}$, the numerator decreases strictly, so $\mathcal{G}(b)$ is strictly and monotonously growing. To demonstrate this is the case for any $b > 0$ we need to prove that $\mathcal{G}'(b)$ never reaches 0. This will complete the proof that the Kosugi parameterisation is unique if it exists. The following equivalence is true:

$$\mathcal{G}'(b) = 0 \iff gg'k - g^2k' = 0 \tag{A.34}$$

This is equivalent to this linear equation in R:

$$R = \varepsilon^b + \frac{\ln(\varepsilon)\ \varepsilon^b\ (e^{b^2} - 1) + b\ e^{3b^2/2}\ (1 - \varepsilon^b)}{b\ (1 - 2\ e^{b^2} + e^{3b^2/2})} \tag{A.35}$$

The last expression is plotted in Figure S3 for both L = first percentile (blue line) and fifth percentile (dashe
Clearly, stationarity requires $R < 0$ or $R > \lim_{b\to\infty} R = 1^+$. Both of these are impossible, because $0 < R < 1$ by definition of R as the ratio of q_{low} by m. Therefore $\mathcal{G}(b)$ is monotonic and strictly growing with b. This means that there is at most one b for a given CV.

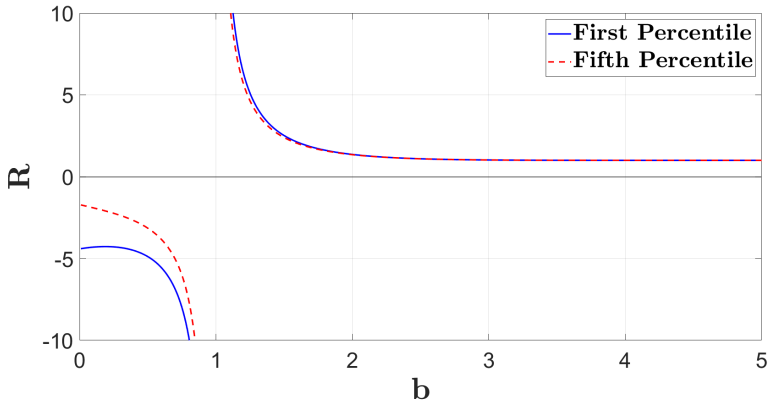

Figure S3: *Plot of the stationary point locus in $b - R$ space on which $\mathcal{G}'(b) = 0$, as given by Equation A.35. Blue coloured line and dashed red line represent the derivation based on first percentile and fifth percentile of flow respectively*

A.3.5 Condition for existence

$\mathcal{G}(b) = (1 - R)\ g(b)/k(b)$ is monotonous and grows with b when $b > 0$, and goes to $+\infty$ as $b \to +\infty$. Therefore, a solution exists if:

$$\frac{CV}{1-R} \lim_{b \to 0^+} k(b) > \lim_{b \to 0} g(b) \tag{A.36}$$

and these limits are defined because both g and k are continuously differentiable over $]0, +\infty)$. The respective first-order Taylor expansions of g at 0^+ is given in equation (A.21) and for k we have:

$$k(b) = -\ln(\varepsilon)\, b + o(b) \tag{A.37}$$

Since Taylor expansions are unique, the results from equation (A.37) into equation (A.36) yields the existence condition:

$$\frac{CV}{1-R} > \frac{-1}{\ln(\varepsilon)} \tag{A.38}$$

where $\varepsilon < 1$ so $\ln(\varepsilon) < 0$ and $-1/\ln(\varepsilon) \approx 0.43$ if q_{low} is the first percentile; 0.61 if q_{low} is the fifth percentile.

Note this condition is sufficient: if it is fulfilled, one can find the unique b with equation (A.29) then, A.23 and A.25 equations above directly lead to obtaining unique values of a and c.